CoA Note Mat. No. 10

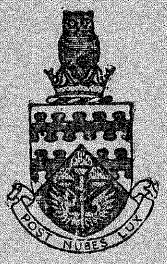

THE COLLEGE OF AERONAUTICS
CRANFIELD

A STUDY OF THE THERMAL DEGRADATION OF AN AMINE-CURED EPOXIDE RESIN AT TEMPERATURES BELOW 350°C

by

C. Patterson-Jones and D. A. Smith

CoA Note Mat. No. 10

January, 1967

THE COLLEGE OF AERONAUTICS

DEPARTMENT OF MATERIALS

A study of the thermal degradation of an amine-cured epoxide resin at temperatures below 350°C

- by -

C. Patterson-Jones, M.Sc.,

and

D.A. Smith, M.Sc., F.R.I.C., A.P.I.

SUMMARY

An epoxy resin made by the reaction of the diglycidyl ether of bis-phenol A and diaminodiphenyl methane was thermally degraded in vacuo at temperatures between 200°C and 350°C. The effect of degradation was examined by means of measurement of changes in the dielectric properties of the material and also by examination of compounds evolved by the cured resin. Definite evidence for the evolution of N-methyl aniline and N:N-dimethylaniline is advanced and added evidence for a dehydration reaction is put forward. Possible degradation mechanisms are discussed.

Acknowledgements

The authors would like to thank CIBA(ARL) Ltd., for materials with which this work was done, and Dr. B.P. Stark and Mr. S. Neumann of CIBA(ARL) Ltd., for their kind help. We would like to thank Mr. W.P. Baker (A.E.I. Ltd.) for the loan of the dielectric bridge of his design, used in the investigation, and for his advice on dielectrics. We also record our thanks to Mr. G. Pogany (Oxford University) for several helpful conversations on relaxation processes. One of us (C. Patterson-Jones) would like to thank the C.S.I.R. of South Africa for the opportunity of carrying out this research.

Contents

A: Introduction

The thermal stability of Epoxide* resins, both cured and uncured, has been studied by a wide variety of methods. Investigations have ranged from those designed to give information about the performance of cured epoxides under service conditions to basic studies intended to determine the nature of the molecular processes occurring during degradation. A complete review of all the literature available will not be attempted, firstly because it is not strictly pertinent to this report, and secondly because such a review has been made.[5]

It is necessary, however, to review briefly some of the more basic investigations.[5] Many different epoxide resins have been used in these investigations which have been concerned both with the pure resin and with resins cured with a host of different types of hardener. In most of the investigations commercial resins and hardeners of uncertain composition containing unknown impurities have been used. The resins have been degraded under various conditions - under vacuum, in air, in inert atmospheres etc. - and samples of widely varying geometries, from thin films to those of unspecified and undetermined shape, have been employed. Temperatures of degradation have ranged from 100°C to 1200°C and both isothermal and heat-pulse methods have been used. Methods of monitoring the degradation have included chromotography, infra-red spectral analyses, mass-spectrographic analyses, tagged-atom methods, differential thermal analysis, differential thermogravimetry and weight measurements.(1) (2) (3) (8) (12) (17) (20) (21) (24) (25) (26) (27) (29) (36) Some investigations have concentrated solely on the gaseous products, some on the condensible products, few on all the products and some on none of the products. Few investigations have paid any attention to the physical state of the resin during the degradation.

In general, the most useful and informative studies have been those in which attempts have been made to analyse and characterise the compounds which result from the degradation. In this connection investigations using differential thermal analysis, differential thermogravimetry and weight loss measurements, without analytical techniques to back them up, are of limited value. It appears from the literature that in many investigations, the method used has attracted more attention than the problem to which it is applied. Thus the degradation temperature used in investigations involving gas-chromotographic techniques have been dictated by the need to obtain products sufficiently volatile to pass through the chromotograph column. Anderson has reported kinetic studies of the degradation. In the author's opinion no kinetic study can be made of any

---

* Throughout this report the term 'Epoxide resin' will refer specifically to a condensation product of Bisphenol A and Epichlorhydrin unless stated otherwise.

chemical reaction until not only the starting materials but, in addition, each and every product have been characterised and quantitatively analysed for reactions under widely varying and completely specified ranges of experimental conditions. The exception to this is the isolation study of one particular chemical reaction from a complex reaction by some experimental artifice. Even this, however, presupposes a complete specification of all other variables including the concentration of all the other species present during the reaction. Thus data such as activation energies quoted by workers using techniques like differential thermal analysis alone are unlikely to be meaningful or instructive. Workers have paid little attention to the geometry of the samples which were degraded. Sample geometry could affect the nature of the degradation process.

It is important to mention the work of Neiman et al.[24] [25] [26] [27] and Lee[20] [21]. It is clear from the experimental details in the papers of Neiman et al. that these workers concentrated almost exclusively on the gaseous products of their degradations and based their mechanisms on these results. It appears to be unrealistic to base mechanisms for the whole degradation on the results for products which are minor products (some 3% of the total). Once it is understood, however, that Neiman et al.'s results refer solely to the gaseous products, there is not necessarily any discrepancy between these results and those of Lee who analysed all the condensible products.

Mechanisms proposed for the degradation of cured resins, in particular those of Neiman et al. and Lee, have often depended on results obtained for the degradation of uncured resins and have, in fact, often been extensions of mechanisms proposed for the degradation of the pure resins. It was felt that this needed some critical attention. The work of Stuart and Smith[36] and Keenan [17] emphasised the need to consider the cured resin.

There still existed an important consideration, to which hitherto no workers had paid much attention. This was the physical state of the resin during degradation and how degradation subsequently affected the physical state of resin. This is particularly important when considering results for uncured resins which are liquid or gaseous at the temperatures involved, and results for cured resins which are, at least initially, necessarily solids. Correlation of the two sets of data is difficult in view of the widely differing epoxide concentrations involved, but considerable justification would have to be made for extrapolation of results for a liquid system to those for a solid system. So far this has not been forthcoming.

In many of the previous investigations relatively high temperatures have been used for a variety of reasons. It is axiomatic that the higher the temperature the more complicated is the ensuing reaction.

The aims of this investigation were the following:

1. To obtain a cured resin whose chemical composition and physical state were well characterised.

2. To degrade the resin under specified conditions at as low a temperature as was practicable.

3. To determine what physical changes the resin molecule underwent as a result of purely thermal degradation.

4. To analyse the resin and any products evolved during degradation in order to determine what chemical changes the resin underwent.

5. On the basis of the results, to propose a mechanism for the degradation which would realistically represent the chemical and physical changes occurring during degradation.

These aims were only partially achieved. Dielectric studies were made to characterise the resin network physically and these showed conclusively that the network was degraded even at low temperatures, so that mechanisms for the degradation based on the reactions of residual epoxide groups are unrealistic. These results, however, were not susceptible to any quantitative interpretation for reasons discussed later. (Section F). Chemical analyses were made using classical methods of organic chemistry backed by infra-red analysis. These showed that phenol, N-methyl aniline and N:N-dimethyl aniline were the main condensible products of the degradation at 300°C of a resin made from a 100:28.8 w/w mixture of the diglycidyl ether of Bisphenol A and p-p' diaminodiphenyl methane. Considerable quantitites of tar[2] were produced but no gaseous products were detected. Hydrogen and water could not be detected because of inherent weaknesses in the apparatus. An attempt was made to account for the analytical and dielectric results.

B: Literature Review

B.1: Cure of Epoxy compounds with Amines

In 1956 Shechter, Wynstra and Kurkjy [34] studied the reaction between primary amines and phenyl glycidyl ether. The use of model compounds to simulate the reactions which occur during cure of an epoxide resin with an amine hardener enabled conventional chemical analyses to be made for primary, secondary and tentiary amine and epoxide. The results indicated that reaction between primary and secondary amine groups and epoxides:

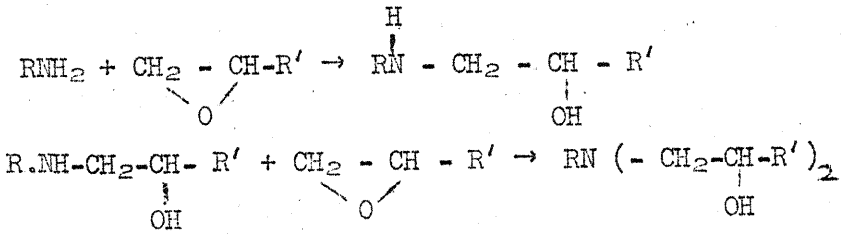

was not accompanied to an appreciable extent by etherification of the aliphatic hydrexyl:

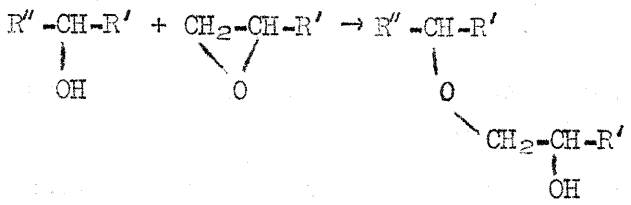

Primary and secondary amines showed no appreciable difference in reactivity towards epoxide groups. Hydroxyl groups catalysed the reaction between primary and secondary amine and epoxide groups and a mechanism was proposed to explain this effect.

O'Neill and Cole (1956)[28] used infra-red analysis and conventional chemical analyses to study the curing of epoxide resins with fatty acids and amines. Results for amine cures showed the simultaneous disappearance of epoxy groups and amine groups and the appearance of hydroxyl groups. The buildup of non-soluble material was determined by Soxhlet extraction using ethyl methyl ketone. The main buildup of insoluble material followed after the initial, most rapid reaction of epoxide groups and was accompanied by little change in epoxide concentration.

Dannenberg and Harp[11] (1956) distinguished between degree of conversion of epoxide groups and degree of cross linking during cure. The essential distinction and inter-relation between these two quantities was demonstrated by measurements on amine-cured epoxide resins. The estimation of epoxide groups was made by infra-red analysis and conventional chemical analysis of swollen samples. The degree of cross linking was estimated by a specially developed heat indentation test and measurements of equilibrium swelling.

The reaction of epoxy resins and polyamide resins was studied by Peerman, Tolberg and Floyd[31] (1957). Infra-red spectrometry was used to determine the concentration of epoxy groups and mechanical tests on the cured resins were made; the heat distortion temperature proved a sensitive monitor of cure. A discussion of the competing factors of decrease in viscosity at high temperatures and corresponding increased reaction rates during curing is given, leading to the concept of optimum cure temperature.

Smith[35] (1961) reviewed the literature on the mechanisms and kinetics of the reactions between amines and epoxides. From this review and on the basis of work of his own, Smith extended Sheckter, Wynstra and Kurkjy's mechanism involving hydrogen bonding for the reaction

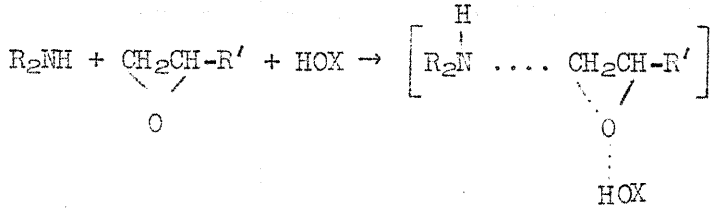

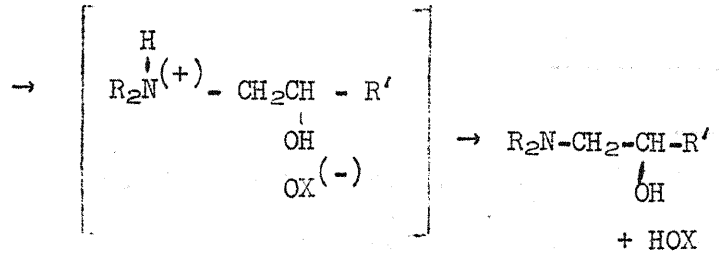

to one which did not involve an improbable termolecular collision:

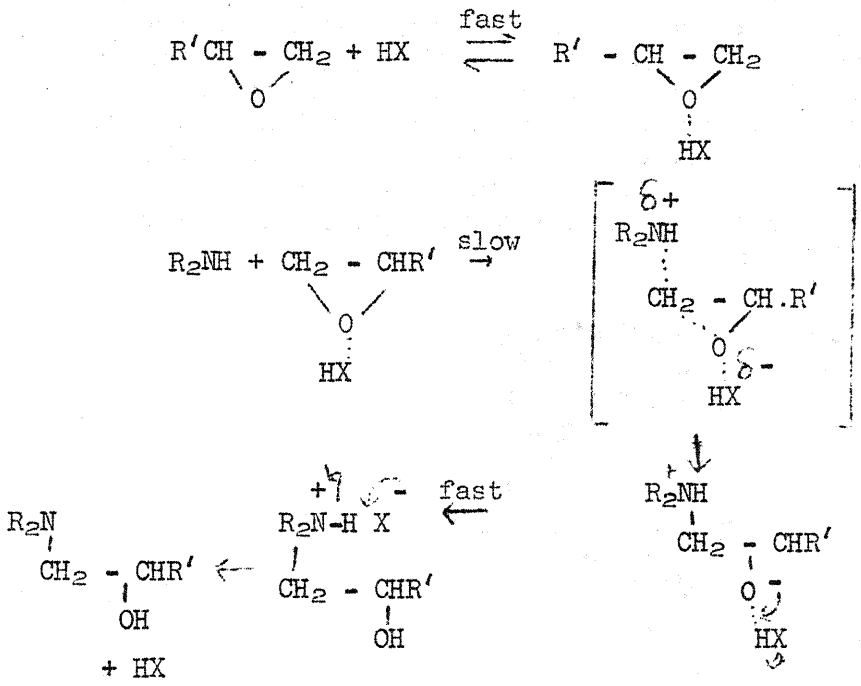

The kinetics of the reaction were analysed and data for the reaction between an epoxide resin and an alkenyl-substituted heterocyclic polyamine indicated that a termolecular hydrogen bonded transition state occurred in this reaction.

The difficulties inherent in using the conventional part of the infra-red spectrum (2-15 μ) to study the reaction between amine and epoxy groups (viz. the absorption at approximately the same frequency of hydroxyl and amine groups and the lack of an exact quantitative relation between epoxy concentration of groups and the absorbance at 10.96 μ) were circumvented by Dannenberg[10](1963), who used the new infra-red to study the reaction. Dannenberg demonstrated the existence of hydrogen bonding of hydroxyl groups in the liquid which was replaced by a different type of hydrogen bonding of hydroxyl groups upon solidification of the reaction mixture due to cooling or gelling.

B.2 Degradation of Epoxy compounds

B.2.a: Thermal Degradation

Neiman, Golubenkova, Kovarskaya, Strizkova, Leventovskaya, Akutin and Moiseev[25](1959) studied the thermal degradation of an uncured epoxide resin at temperatures from 200°C to 500°C. The samples were degraded in previously evacuated tubes and the reaction was followed by observing the pressure rise in the tubes. Chromotographic analysis of the gases produced, which formed some 2% of the products of the reaction, proved the presence of methane and carbon monoxide and traces of ethane and propane. The condensible products consisted of water and formaldehyde (some 8% of the reaction products), as shown by conventional chemical methods. Infra red analysis was used to show that appreciable distillation of the low Molecular Weight fractions in the resin occurred without their modification. An insoluble, infusible mass was left in the reaction tube. A free radical mechanism for the degradation of the resin was proposed to account for the main volatile products:

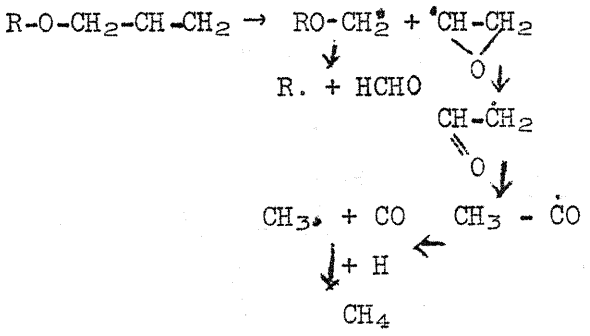

Water was supposed to have arisen from the polymerisation of the resin to form ether bridges.

Anderson[1] [2] [3](1961 and 1962) used the technique of thermogravimetry to study the degradation of cured epoxide resins.

Moiseev, Neiman, Kovarskaya, Zenova and Guryanova[24](1962) synthesised an epoxy resin from Bisphenol A with a C^{14} atom on the central carbon atom. The uncured resin was thermally degraded in a sealed, previously evacuated tube at 300°C, 500°C and 800°C. The tubes were cooled and the products volatile at room temperature frozen in trays. Tiny quantities of aldehydes were formed and carbon monoxide and methane were the main gaseous products. Gases formed a very small proportion of the total products (of the order of one percent at 400°C). The solid residue retained all but a fraction of the original activity. The activity of the carbon monoxide and methane was very low compared to that of the traces of other gases, in particular propane. This was put forward as evidence in support of Neiman et al's (1961) mechanism for

carbon monoxide and methane formation from epoxy groups. A mechanism was given for the formation of propane and other hydrocarbons from the unit:

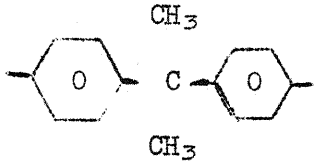

Neiman, Kovarskaya, Golubenkova, Strizhkova, Levantovskaya and Akutin[27](1962) described the degradation of both uncured resin and resin cured with maleic anhydride and polyethylene polyamine. The reaction was studied by observing the pressure rise due to evolution of gaseous products. Degradation of the cured resins commenced at higher temperatures than those for the degradation of pure resins. The gaseous products were analysed by gas-chromotography: methane, carbon monoxide and propane formed the main products of the degradation of a low molecular weight resin, both when uncured and cured with 7% polyethylene polyamine. Gaseous products only formed 2-5% of the total products. Formaldehyde, acetaldehyde and water were detected and together with the gaseous products formed not more than 15% of the total products. Liquid products, identified as low molecular weight fractions of the resin were found when the pure resin was degraded. The remainder of the products consisted of a hard infusible solid. The non-gaseous products of the degradation of the cured resins were not discussed nor were the cure histories given. The discussion of the degradation and the mechanism proposed followed that in the previous report of these workers[25]. It is not clear whether this discussion was intended to refer to the cured resins or not. Oxidative degradations was briefly mentioned and was supposed to occur via an antecatalytic free-radical reaction involving hydroperoxy radicals.

Lee[20](1965) studied the degradation of epoxide resins, uncured and cured with amine and anhydride hardeners. Commercial resins and hardeners were used and details of cure schedules were given. A variety of techniques were used to study the degradations including thermogravimetric analysis and differential thermal analysis. Vapour-phase chromatography was used to analyse volatile products of degradation on a hot filament. Mass-spectrometry was used to analyse directly the vapours evolved during pyrolysis in a Vycer flask at 350°C or 450°C. The same techniques was used to analyse products condensed in a trap during the degradation of resin in a previously evacuated tube heated to 475°C. The results showed that for the degradation at 350°C of the uncured low molecular weight epoxide resin, the major volatile products were toluene and water. At 450°C the major volatiles were toluene, methyl cyclopentadiene and water. The high boiling point products of degradation at 475°C were phenol, cresols, Ethyl substituted phenols, isopropyl phenol, isopropenyl phenol and Bis-phenol A.

The main volatile product of the degradation at 350°C of a low molecular weight epoxide resin cured with p-p' diamino diphenyl methane was water (297 mole ~%). At 450°C the major volatiles were methyl cyclopentadiene, carbon monoxide, water, carbon dioxide, acetaldehyde, methyl chloride and methane. The high boiling point products of degradation at 475°C were similar to these produced in the degradation of the uncured resin. On the basis of these results Lee concluded that the degradation mechanism for the cured resin was similar to that for the uncured resin.

Lee discussed the degradation mechanism proposed by Neiman and workers and showed that the main course of the degradation could not follow this scheme since the major products were phenolic compounds. Lee proposed several detailed degradation mechanisms to account for the products but all but one start from cleavage of ether groups formed by etherification of epoxide groups. The exception involves isomerisation of the epoxy group to an aldehyde group. These reactions may have occurred during degradation on cure of some of the resins but certainly do not occur in the case of an epoxide resin cured with p-p' diamino diphenyl methane. Lee makes no reference in his discussion to this system and it is not clear whether his degradation schemes are supposed to apply in this case.

Lee[21] (1965) extended his work on the degradation of uncured resins. An epoxy-novolac resin and a Bisphenol A type of epoxide resin were studied. Degradation was done in tubes heated to 475° and under vacuum. Condensible products were trapped and dissolved in acetone. The acetone solution was evaporated and the condensibles separated from water by extraction with methylene di Chloride Mass spectrometric measurements showed that phenol and cresols were the main condensible products, with traces of other phenolic species. Lee discussed the results and proposed mechanisms to account for the products based on the formation of Bisphenol A and its subsequent decomposition.

Stuart and Smith[36] (1965) pyrolysed a commercial epoxide resin of low molecular weight cured with two different amine hardeners as a hot filament and used gas-chromotography to analyse the products. Analysis was made by comparison of retention times of degradation products with those of simple components; in this way, product identification was described as 'highly probable, probable' etc.... Temperatures of degradations were reported as varying from 400°C to 700°C. Hydrogen carbon dioxide, benzene, toluene, phenol, xylenes and cresols were described as highly probable products; probable products were formaldehyde, acetaldehyde and phenyl glycidyl ether. Both the mechanisms of Neiman et al. and Lee were discussed. It was pointed out that in no work so far had compounds containing nitrogen been reported. Reactions were added to those given by Lee for the mechanism, to account for some of the products: hydrogen was supposed to be lost directly from both aliphatic and aromatic parts of the cured resin molecule; the formation of phenyl glycidyl ether was proposed: further reaction of this compound gave phenol, acrolein and

benzene; the formation of

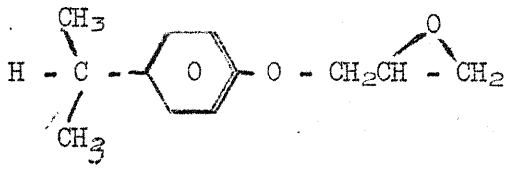

was proposed, its subsequent degradation leading to p-isopropyl phenol, p-cresol, isopropyl benzene, toluence and xylenes.

Keenan[17](1966) used the apparatus of Stuart and Smith to extend their work. The cured resin studied was made from the pure diglycidyl ether of Bisphenol A and pure p-p' diamino diphenyl methane. Keenan analysed the residue left in the pyrolysis head after degradation and products which condensed in an acetone/dry ice traps after passing through the column. Attempts were made to identify peaks on pyrograms with definite compounds, while thin layer chromatography followed by analysis by infra-red spectrometry and conventional chemical methods was used in an attempt to characterise the residues and condensible products from the gas chromatograph. Keenan discussed the strength of the chemical bonds in the cured resin and concluded that the two strongest bonds were the carbon oxygen and carbon nitrogen bonds. Degradation was thought to be initiated by scission of the weakest bonds viz. the aliphatic carbon - nitrogen bond and the

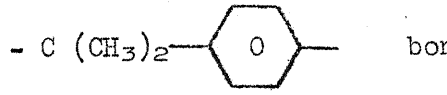 bond.

Reactions which could follow these two processes were detailed to account for some of the products reported in this and Lee's work.

B.2.b: Oxidative Degradation

Park and Blount[29](1956) studied the oxidation of acid cured epoxide resins at 180°C in the form of thin films. The effects of variables such as air dry time, post-cure treatment, film thickness, molecular weight of resin and solvent formulation on rate of oxygen uptake by the films were reported. Infra-red spectra of oxidised films showed that oxidation was accompanied by a decrease in the concentration of hydroxyl groups together with an increase in the concentrations of carbonyl groups. No evidence of the formation of carbon-carbon double bonds was found so that the mechanism

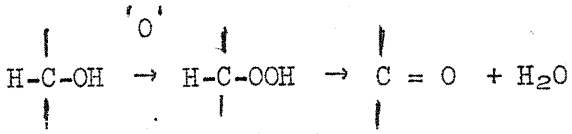

was preferred to the mechanism

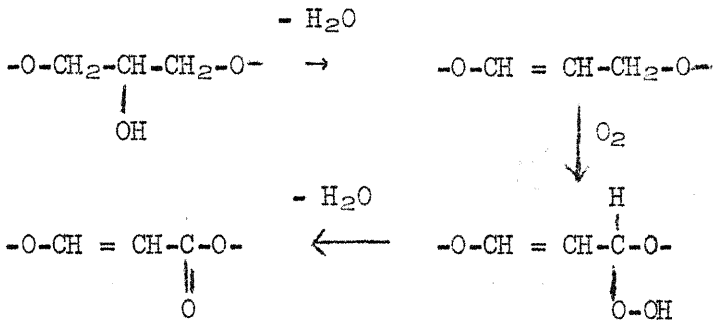

but it was realised that the former was by no means a complete description of the process.

Neiman, Kovarskaya, Yazvikova, Sidneev and Akutin[26](1961) studied the oxidation of a low molecular weight epoxide resin hardened with polyethylene polyamine and maleic anhydride at temperatures in the range 160° - 250°C. The cured resin in the form of a powder was placed in a tube connected to a vacuum apparatus such that an initial pressure of oxygen could be introduced and the subsequent pressure variation observed. At all temperatures and oxygen pressure there was no pressure change for a time followed by a decrease in oxygen pressure. This induction period was shortened by higher oxidation temperatures and by higher oxygen pressures. The reaction was supposed to be autocatylitic and to proceed by a branched free-radical chain mechanism. Hydroperoxides acted as source of free radical centres. Hydroperoxides were analysed by conventional chemical techniques.

Conley[8](1964) and Dante and Conley[12](1964) reported the results of infra-red analysis of films of cured epoxide resins cast on rock salt window during oxidation at temperatures around 225°C. Commercial resins were fractionated and individual fractions cured with m-phenylene diamine and diethylenetriamine. The oxidative degradation of a film made from a low molecular weight resin and m-phenylene diamine was accompanied by the growth of peaks at 5-8 and 6.0 pr in the infra-red spectrum, as was that of the resin cured with the aliphatic amine. Couley showed that the weak link in the resin is the curing N-C link. On the basis of the behaviour of 1.2 amino-alcohols when oxidised and the results of the investigation a mechanism was proposed for the reaction.

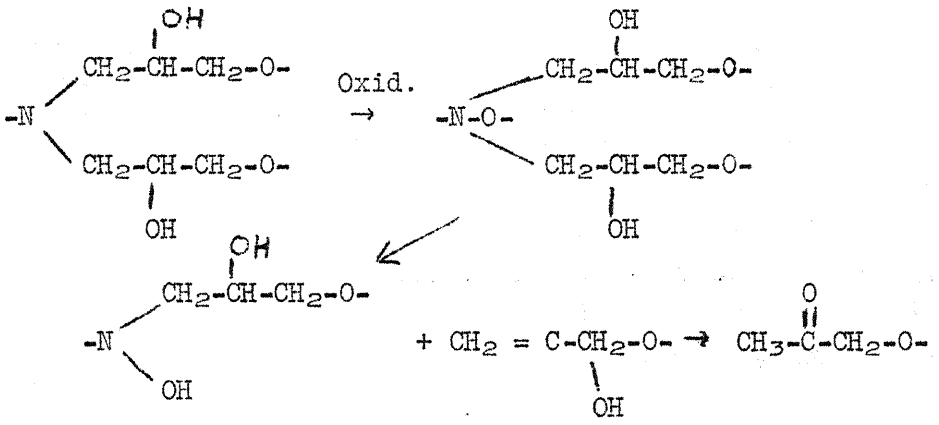

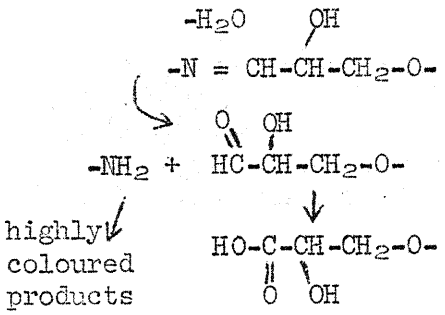

B.3 The infra-red spectra of epoxy resins

The work of O'Neill and Cole[28](1956), Dannenberg and Harp[11] (1956) and Dennenberg[10](1963) was reviewed in section B.1 by Bellamy[4]. Infra-red spectra of complex molecules provided an invaluable general reference and Lee and Neville's book 'Epoxy Resins' was consulted in this context.

Patterson[30](1956) published the spectra of twenty-six epoxy compounds. Correlation of the spectra indicated that absorption characteristic of the oxirane ring occured at about 8 μ and 11 μ and 12 μ. The position of the latter two bonds varied somewhat from compound to compound. Epoxy ethers studied also showed absorption at 12.2 μ which could have been due to the oxirane ring.

Feazel and Verchot[14](1957) reported the use of Potassium Bromide discs cemented together with an epoxy-resin/hardener mixture to study the cure of the resin.

Herbert, Mealcuir, Nicholls and Taylor[16](1957) studied the characteristic absorption due to the stretching of carbon-hydrogen bands in the epoxide ring, which appeared between 3050-2990 cm^{-1}.

Sugita and Ito[37](1965) studied the pyrolysates of cured unfilled epoxide resins. Identification of the hardener used was made possible by this technique. Assignments of peaks in the infra-red to absorptions due to specific groups were made.

Keenan[17](1966), whose work was reviewed in B:2.a., used infra-red spectra extensively. Absorptions in the infra-red spectra of degradation products were discussed in relation to the molecular processes supposed to occur during degradations. Absorptions in the infra-red spectrum of the diglycidyl ether of Bisphenol A were correlated as far as possible with individual chemical groups in the compound.

B:4 Dielectrics

B:4.a Recent comprehensive review articles on the general theory of the dielectric properties of matter, Wyllie[28](1960) and Cole[7](1961), specifically on the dielectric properties of solids (Meakins[22](1961)) and more specifically on the dielectric properties of polymeric systems (Curtis[9](1960)), Mikhailov and Borisova[23](1961) and Reddish[32](1962)) are summarised in sections C.1 and C.2.

B:4.b Dielectric properties of Epoxy Resins

Kobale and Lobl[18] studied the dielectric properties of a low molecular weight epoxide resin cured with tetrahydrophthalic anhydride under a variety of cure conditions. A dispersion region (at high frequencies and low temperatures) was associated with the movement of hydroxyl groups and another dispersion (at low frequencies and high temperatures) region was associated with the softening of the resin and was associated with the relaxation of the resin network. A study was made of the effects of cure-time, hardener concentrations, cure temperature and plasticisers on the dielectric properties, and in particular on the second dispersion region. A study was made on the change in dielectric properties during cure of the above resin/hardener system and also of a resin cured with p-p' diamino dihenyl methane. The specific resistance of resins cured with different amounts of hardeners was measured as a function of temperature. Eyring's absolute reaction rate theory was applied to the high temperature loss region. For this region, plots of the frequency of loss maxima against the reciprocal of the absolute temperatures gave straight lines and from these plots a study of the effect of hardener concentration on activation enthalpy and activation entropy was made. The results are discussed in the light of the molecular processes occurring during mixing of resin and hardener, and cure.

Dasqupta and Mital[13](1964) studied the dielectric properties in the frequency range 5 c/s to 50 kc/s and the temperature range 12-95°C of a commercial resin, a commercial hardener phthalic anhydride and cure mixtures of the two. The high loss exhibited by the pure components at frequencies below 1 kc/s was thought to be due to conduction by ionic impurities.

Havan, Guingras and Katz[15](1965) studied the changes in loss tangent and dielectric constant accompanying the curing of a commercial epoxide resin with diethylenetriamine at constant temperature. The loss tangent/time curves were typically represented by a decrease followed by an increase to a maximum and subsequent decrease. No attempt was made to explain the curves but their possible application to monitoring cure was discussed.

C. Summary of Dielectric Theory*

C.1. General Dielectric Theory

The theory may conveniently be split up into two parts:

a) that which concerns loss-free materials or lossy materials in a state of equilibrium viz. the theory of dielectric polarisation.

b) the theory of dielectric relaxation which attempts to describe the absorption of energy by a lossy material subjected to a non-constant field.

C.1.a. Dielectric Polarisation

The application of an electric field to a dielectric produces a polarisation of the dielectric i.e. dipoles are set up in the material such that over any large enough region there is a nett separation of charge. On a molecular level polarisation may be due to several processes.

i) Electronic polarisation i.e. the perturbation of electronic orbitals or, roughly speaking, the relative displacement of electrons and nuclei.

ii) Atomic polarisation i.e. the stretching, twisting and bending of chemical bonds.

iii) Orientation polarisations due to the tendency of permanent dipoles of the dielectric to aline themselves with the field.

In addition to the above three types, interfacial on Maxwell Wagner type polarisation may occur at the interface of two materials differing in electrical conductivity.

Macroscopically a vector $\bar{D}$, the displacement, may be defined as the charge moved/unit area. Experiments show that for low intensity fields applied to non-lossy isotropic dielectric $\bar{D}$ is related to the field $\bar{E}$ by the relation

$$\bar{D} = \epsilon\epsilon_o \bar{E}$$

where ϵ_o is a universal constant and ϵ a constant, at a fixed temperature and fixed frequency of the field, which is characteristic of the dielectric.

---

*Note the rationalised M.K.S. system of units will be used.

Any dielectric theory must relate measurable physical quantities to significant molecular quantities, calculable, at least in principle from molecular theories. Charges and currents should be put in terms of electrons and nuclei and their motions, macroscopic quantities then being obtained by averages over molecular quantities. By assuming Coulomb's Law for the force between charges and by some purely mathematical manipulation, the displacement $\bar{D}$ may be related to the field $\bar{E}$, the polarisation $\bar{P}$ (i.e. the no. of dipoles/unit volume) and higher multiple moment densities by the relation

$$\bar{D} = \epsilon_o \bar{E} + \bar{P} + \text{higher terms.}$$

The elimination of $\bar{D}$ from these two equations forms the basis for most of the equations which attempt to relate the macroscopically accessible ϵ with molecular quantities. The macroscopic field $\bar{E}$ in the equations is not in general equal to the field of external charges. The computation of the local field at a molecule, which is the vector sum of the macroscopic field and fields due to the other molecules present which are violently fluctuating quantities, provides difficulties.

At present, detailed theories exist for gases of simple molecules at low pressures. For more complicated molecules and gases at higher densities, liquids and solids, simplifying assumptions or models, often of dubious validity, have to be used.

C.1.a.i) Polarisation of Gases

The static polarisation of dilute gases may be treated by assuming that the molecules are independently polarised by an external field $\bar{E}_o$, thermal collisions only serving to maintain equilibrium between the internal and external motions of the molecules. Because of the independence of the polarisation, the total polarisation is given simply by the sum of the polarisations of individual molecules

$$\bar{P} = N \frac{\langle \bar{m} \rangle}{V}$$

where N is the no. of molecules in volume V and $\langle \bar{m} \rangle$, the average dipole moment of each molecule.

Ignoring any higher terms than the polarisation

$$\bar{D} = \epsilon_o \bar{E}_o + \bar{P}$$

$$\bar{D} = \epsilon \epsilon_o \bar{E}_o$$

where $(\epsilon - 1) \epsilon_o \bar{E}_o = \bar{P}$

$$= \frac{N}{V} \langle \bar{m} \rangle$$

$\bar{P}$ and $\bar{E}$ are aligned since the gas is isotropic whence

$$(\epsilon-1)\,\epsilon_o|\bar{E}_o| = \frac{N}{V}\langle\bar{m}.\bar{e}_o\rangle$$ where e_o is unit vector in the field direction.

Debye represented the moment $\bar{m}$ by the sum of an induced moment $\bar{\eta} = \alpha\,\bar{E}_o$ with α a scalar polarisability and a permanent moment $\bar{\mu}$ directed long some molecular axis.

$$\bar{m} = \alpha\,\bar{E}_o + \bar{\mu}$$

$$m.e_o = \alpha\,\bar{E}_o.\bar{e}_o + \bar{\mu}.\bar{e}_o$$

$$= \alpha\,|\bar{E}_o| + |\bar{\mu}|\cos\theta$$ where θ is the angle between the molecular axis and $\bar{E}_o$

$$\langle\bar{m}.\bar{e}_o\rangle = \langle\alpha|\bar{E}_o| + |\bar{\mu}|\cos\theta\rangle$$

$$= \alpha\,|\bar{E}_o| + |\bar{\mu}|\langle\cos\theta\rangle$$

$\langle\cos\theta\rangle$ was obtained by considering the energy of a dipole aligned at an angle θ related to the field direction and by using the first term of a Langevin expression for the distribution of orientations with respect to the field:

$$\langle\cos\theta\rangle = \frac{|\bar{\mu}|\,|\bar{E}_o|}{3kT}$$

substituting for $\langle\bar{m}.\bar{e}_o\rangle$ gives

$$(\epsilon-1)\epsilon_o|\bar{E}_o| \times \frac{V}{N} = \alpha|\bar{E}_o| + \frac{|\bar{\mu}|^2|\bar{E}_o|}{3kT}$$

whence $\epsilon-1 = \frac{N}{\epsilon_o V}\left(\alpha + \frac{\mu^2}{3kT}\right)$

where $\mu = |\bar{\mu}|$

Quantum Mechanical calculations show that representation of $\bar{m}$ by $\bar{m} = \alpha\bar{E}_o + \mu$ is approximately justified in most cases.

At moderate gas densities the assumption used in the above derivation that the macroscopic field is indistinguishable from the local field as the field of extent charges is no longer valid.

If a gas is introduced between the plates of a parallel-plate condenser such that the charges on the plates remain constant, the macroscopic field between the plates is given by

$$\vec{E} = \frac{\vec{E}_o}{\epsilon} \quad \text{where } \vec{E}_o \text{ is the original field.}$$

Lorentz calculated the local field at a molecule which had polarisability α and was situated on a regularly spaced lattice of cubic symmetry, as

$$\vec{E} = \vec{E}\,\frac{(\epsilon+2)}{3}$$

Representing the moment of the molecule as $\alpha\,\vec{E}_L$, and summing overall molecules substitution into

$$(\epsilon-1)\epsilon_o\vec{E} = \frac{N}{V}\,\alpha\;\vec{E}_L$$

gives $$\frac{(\epsilon-1)}{(\epsilon+2)} = \frac{N\alpha}{3\epsilon_o V}$$

Assuming that E_L is also the field which might tend to orientate permanent dipoles gives

$$\frac{(\epsilon-1)}{(\epsilon+2)} = \frac{N}{3\epsilon_o V}\left(\alpha + \frac{\mu^2}{3kT}\right)$$

The use of a field which is computed for a regularly spaced lattice, for a non-polar gas needs justification. The introduction of the term for permanent moments is even more suspect as the assumptions used by Lorentz in computing the local field are no longer valid. More detailed calculations of the local field show that the function

$$\frac{(\epsilon-1)}{(\epsilon+2)}\,\frac{V}{N} \quad \text{is not necessarily simply related to molecular quantities.}$$

In practice the expression

$$\frac{(\epsilon-1)}{(\epsilon+2)} = \frac{N\alpha}{3\epsilon_o V}$$

describes the polarisation of non-polar gases and some non-polar liquids quite well. For polar gases

$$\frac{(\epsilon-1)}{(\epsilon+2)} = \frac{N}{3\epsilon_o V}\left(\alpha + \frac{\mu^2}{3kT}\right)$$

is less good and can be very bad for polar liquids with high dielectric constants. The detailed theories are complicated, however.

C.1.a.ii) The polarisation of Liquids.

Since the expression

$$\frac{(\epsilon-1)}{(\epsilon+2)} = \frac{N}{3\epsilon_o V}\left(\alpha + \frac{\mu^2}{3kT}\right)$$

does not describe adequately the dielectric constant of polar liquids, a theory for these is needed. Most theories of liquids use variations of or modifications of Onsager's model. Onsager represented a polar molecule in a liquid as a point polarisable dipole at the centre of a sphere of exclusion of radius a, having molecular dimensions. The surroundings were taken to be a continuum of dielectric constant ϵ, and surrounding the void. A dipole of moment $\bar{m}$ in cavity induces a polarisation of the continuum surrounding the cavity which in turn gives rise to a reaction field in the cavity given by

$$\bar{\Omega} = \frac{2(\epsilon-1)}{(2\epsilon+1)}\,\frac{\bar{m}}{a^3}$$

Representing $\bar{m}$ by $\mu + \alpha\,\bar{R}$ gives

$$\bar{m} = \mu \Big/ \left(1 - \frac{2(\epsilon-1)}{(2\epsilon+1)}\,\frac{\alpha}{a^3}\right)$$

A uniform macroscopic field $\bar{E}$ outside the cavity gives rise to a uniform macroscopic field $\bar{G}$ inside the cavity

$$\bar{G} = \frac{3\epsilon\bar{E}}{2\epsilon+1}$$

The resultant field inside the cavity is $\bar{G} + \bar{R}$, but it is clear that, since $\bar{R}$ lies parallel to $\bar{m}$, only G plays any part in orienting the dipole. The sum of mean induced and mean square orientation moments gives

$$\epsilon-1 = \frac{N_o}{\epsilon_o}\,\frac{u}{V}\left(\frac{3\epsilon}{2\epsilon+1}\right)\left\{\frac{\alpha}{\left(1 - \frac{2(\epsilon-1)\alpha}{(2\epsilon+1)a^3}\right)} + \frac{\mu^2}{\left(1 - \frac{2(\epsilon-1)}{(2\epsilon+1)}\,\frac{\alpha}{a^3}\right)}\right\}$$

where u is the no. of moles and N_o the no. of molecules per mole.

Onsager assumed that the spherical molecules completely filled the volume they occupied:

$$u\,No\,\frac{4}{3}\pi a^3 = V$$

This is equivalent to saying that the mean resultant local field at each molecule is the Lorentz field i.e.

$$\langle \vec{R} + \vec{G} \rangle = \frac{(\epsilon+2)\vec{E}}{3}$$

Using this assumption and putting $\mu = 0$ yields the expression:

$$\frac{(\epsilon_\infty - 1)}{(\epsilon_\infty + 2)} = \frac{u\,No}{3\epsilon_o V}\alpha$$

where ϵ_∞ refers to the dielect ic constant at frequencies such that orientation polarisation is prohibited. This is the classical expression, using the Lorentz field, for the polarisation of polar gases or liquids. Putting $\mu \neq 0$ and again using the volume assumption leads to the expression

$$\frac{(\epsilon - \epsilon_\infty)(2\epsilon + \epsilon_\infty)}{\epsilon(\epsilon_\infty + 2)^2} = \frac{No}{3\epsilon_o}\,\frac{\mu^2}{3kT}\,\frac{u}{V}$$

which is a distinct improvement on the classical expression, using the Lorentz field, for the polarisation of a polar liquid.

Modifications of Onsager's treatment involve changing the shape of the molecular cavity or avoiding the volume assumption. Onsager's expression does not describe with even reasonable accuracy the dielectric constants of hydrogen bonded liquids. Theories have been put forward to describe the properties of these materials.

C.1.a.iii) The Polarisation of Solids.

Crystalline solids may be anisotropic. In this case the quantity ϵ in the relation

$$\vec{D} = \epsilon\epsilon_o\vec{E}$$

is a second rank tensor.

The dielectric properties of solids depend on the type of solid considered. In general, in ionic solids the forces involved in the relative displacements of electron clouds and nuclei are small, giving rise to absorption in the far infra-red, and hence only electronic distortions

contribute to the polarisability. At low frequencies, however, alkali halide crystals have dielectric constants of 5 to 30 or more, indicating that ionic displacements contribute to the polarisability.

Molecular crystals of non-polar compounds form the type of idealised system for which the Lorentz field was calculated and, apart from anomalies due to phase transitions, seldom show interesting properties. Molecular crystals of polar molecules show more interesting behaviour. It appears that in the crystal, orientation of the dipoles may be possible. In many polar molecular crystals, abrupt changes in the dielectric constant occur below the melting point and these are usually associated with changes in the rotational freedom of the dipoles which accompany changes or anomalies in other properties such as specific heats, volume, and crystal type.

Computation of dipole interactions is in general a complicated problem. Molecular orientation in solids is often discussed by considering one molecule whose rotational movements are supposed to be hindered by the presence of potential barriers whose form may be suggested by the packing of neighbouring molecules. Treatments of the pair-wise interaction of dipoles, however, show no features which may be represented by temperature dependence on fluctuating potential barriers related to the angular co-ordinates of a single molecule. There may be cases for which the one-molecule model is an adequate description, but it is not generally adequate and cannot be applied to any set of data. This is important since this model is often used when discussing relaxation processes.

C.1.b. Relaxation of Dielectrics

If a dielectric is submitted to a field which is a step function as shown in figure 1, the displacement often shows the behaviour shown by the curve in figure 1.

A practical instantaneous response of the dielectric is followed by a slower response which asymptotes to an equilibrium value. The rapid initial response is attributed to induced electrons or nuclear displacements and is hence as much a function of intra molecular structure as molecular interaction. The slower response for times longer than 10^{-12} seconds is usually considered the domain of dielectric relaxation. For these times the steady-state response to a sinusoidal field is more easily studied, than transients due to instantaneous changes in the applied field. Both types of response, however, are subject to the same molecular dynamics and, providing that the principle of super-position holds (viz. that the response to separate successive applications of fields is the sum of responses to each separate application of a field), can be related by Laplace or Fourier transform theory. The same theory shows that ϵ' and ϵ'' are not independent functions of frequency or temperature.

Clearly the relation

$$\vec{D} = \epsilon\epsilon_o\vec{E}$$

precludes any time dependent effects and this relation often holds at optical frequencies (where no resonance absorption occurs) at which orientation polarisation cannot occur because of the high frequencies.

Consider a field which varies with time as

$$E = E_o \cos \omega t$$

If dielectric absorption takes place $\bar{D}$ no longer follows $\bar{E}$ and there is a phase difference δ between them so that $\bar{D}$ can be written

$$D = Do \cos(\omega t - \delta)$$

$$= Do(\cos \omega t \cos \delta + \sin \omega t \sin \delta)$$

i.e. a component $\bar{D}o \cos \delta$ is in phase with E and a component Do sin δ $\frac{\pi}{2}$ radians out of phase with E.

$\bar{E}$ can be written concisely as

$E^* = Eoe^{i\omega t}$ where E^* denotes a complex quantity with the convention that the intensity of the field is given by the real part of the complex quantity. D^* is then given by

$$D^* = Do\, e^{i(\omega t - \sigma)}$$

Suppose $D^* = \epsilon^* \epsilon_o E^*$

i.e. $\underline{D}^* = \epsilon^*$

$\epsilon_o E^*$

Then $$\epsilon^* = \frac{Do\, e^{i(\omega t - \sigma)}}{\epsilon_o E_o\, e^{i\omega t}} = \frac{D_o}{\epsilon_o E_o} e^{-i\delta}$$

Expanding gives $\epsilon^* = \frac{D_o}{\epsilon_o E_o} (\cos \delta - i \sin \delta)$

so that ϵ^* can be written

$$\epsilon^* = \epsilon' - i\,\epsilon'' \text{ with}$$

$$\epsilon' = \frac{D_o}{\epsilon_o E_o} \cos \delta$$

and $$\epsilon'' = \frac{D_o}{\epsilon_o E_o} \sin \delta$$

and $$\frac{\epsilon''}{\epsilon'} = \tan \delta .$$

Implicit in the assumptions that D^* is related to E^* by

$$D^* = \epsilon_o \epsilon^* E^*$$

is the assumption of linear behaviour.

For a stepwise application of a field the simplest form of relaxation is an exponential rise in $\bar{D}$ after the initial rapid increase in $\bar{D}$. This is Debye's treatment of relaxation and one which is often found experimentally. The complex dielectric constant for a sinusoidal field is given in this case by

$$\epsilon^* = \epsilon_\infty + \frac{(\epsilon_o - \epsilon_\infty)}{(1+i\omega\tau)}$$

where τ is the macroscopic relaxation time, ϵ_o the dielectric constant at frequencies below the absorption and ϵ_∞ at frequencies above.

Separating real and imaginary parts gives

$$\epsilon' = \epsilon_\infty + \frac{\epsilon_o - \epsilon_\infty}{1+\omega^2\tau^2}$$

$$\epsilon'' = (\epsilon_o - \epsilon_\infty)\frac{\omega\tau}{1+\omega^2\tau^2}$$

This behaviour may be represented by figure 2.

A plot of ϵ'' against ϵ' (Cole-Cole plot in the complex plane) is a semi-circle.

Debye-type relaxation is also described by the 1st order differential equation for the polarisation $\bar{D}$.

$$\tau \frac{dP}{dt} + P(t) = (\epsilon_o - \epsilon_\infty)E(t)$$

Many models can give rise to this equation so that the conformation of experimental data to Debye-type relaxation is, of itself, no confirmation of the validity of any one particular model.

Often relaxation processes exhibit a different time dependence than that

described by Debye. Some examples of Cole-Cole plots are given in figure 3.

Formally such curves can always be constructed from a linear superposition of relaxation processes of the simplest type (i.e. Delyce-type), each with its own characteristic relaxation time τ_i

$$\epsilon^* - \epsilon\infty = \sum_i \frac{Fi}{1+i\omega\tau} \qquad \text{where} \sum F_i = \epsilon_o - \epsilon\infty$$

More generally for a continuous distribution of relaxation times

$$\epsilon^* - \epsilon\infty = \int_0^\infty \frac{F(\tau)d\tau}{1+i\omega\tau} \quad \text{where} \int_0^\infty F(\tau)d\tau = \epsilon_o - \epsilon\infty$$

$F(\tau)$ can be determined with difficulty from analytical representations of $\epsilon''(\omega)$ and $\epsilon'(\omega)$ of the right form.

What is important is the significance of sets of relaxation times or continuous spectra of relaxation times. A discrete set can be regarded as a collection of times each of which represents a Debye type equation and each of which contributes independently to the polarisation. Some experimental systems have a reasonable molecular basis for representation by a set of discrete relaxation times e.g. Fig. 3(a) suggests the overlapping of three single relaxation processes.

The flat arc and skewed arc loci (Figs. 3(b) and 3(c)) correspond to broader dispersion regions and flatter absorption peaks than those for Debye-type relaxation. The circular arc locus is given empirically by

$$\epsilon^* - \epsilon\infty = \frac{\epsilon_o - \epsilon\infty}{1+(i\omega\tau)^{1-\alpha}} \quad \text{with } 1 > \alpha \geq 0$$

$\alpha = 0$ gives the Debye equation. The corresponding spectrum $F(\tau/\ )$ is logarithmically symmetrical about $\tau \cong \tau_o$. For other systems which show broad absorption regions (Fig. 3c) there is more difficulty in finding molecular mechanisms which correctly predict spectra when a linear combination of simple differential equations is used. In these cases it appears that use of a linear combination of simple differential equations may not be justified and the resulting spectra of relaxation times are, therefore, of academic interest.

C.1.b.i Relaxation in Gases

In the case of gases at low pressures, theories assume that relaxation arises because the energy which the field imparts to the molecule is distributed to other degrees of freedom by collisions. As densities are increased this explanation becomes obscure since the molecules are almost continuously in a strong state of interaction. Models for dense gases consider the effect of the field on the probabilities of transition between rotational states of the molecule, assuming that in the absence of the field all states are equally probable.

C.1.b.ii Relaxation in Liquids

Models for dense gases cannot describe liquids for two reasons. Firstly, it was pointed out earlier that consideration of single molecules in dense systems is not justifiable. Secondly, the assumption that all orientations are equally probable in the absence of a field neglects dipole interactions between molecules. Two problems arise when attempting to describe relaxation in polar liquids: i) the satisfactory representation of an irreversible approach to equilibrium on a molecular level, ii) the relation of the macroscopic external field to the local microscopic field when both are time dependent.

Debye's model: Debye assumed 'orientation diffusion' to occur in time dependent fields. Energy is dissipated in overcoming molecular 'friction'. A function f can be defined which gives the probability that a number dN of molecules are oriented in solid angle $d\Omega$ such that

$$dN = f\, d\Omega$$

The molecular friction is represented by a constant ξ such that

$$h = \xi \frac{d\theta}{dt} \quad \text{where h is the torque and } \frac{d\theta}{dt} \text{ the angular velocity.}$$

Continuity equations lead to the Schmolukowski equation

$$\xi \frac{\partial f}{\partial t} = \text{div } (kT \text{ grad } f - Lf)$$

Delyce used the Lorentz field as the local molecular field and put the torque L equal to

$$L = -\mu E_2 \sin(\theta) \quad \text{where } (\theta) \text{ is the angle between } \mu \text{ and } E_2$$

For a sinusoidal field f can be calculated to be

$$4\pi f = \frac{1+\mu E_2{}^{\circ}\cos(\theta)}{kT(1+i\omega\tau)}$$

and the molecular relaxation time is $\tau = \xi/2kT$. f can then be used to evaluate the mean moment and time dependent polarisation. The result is the Debye equation for the relaxation

$$\epsilon^* - \epsilon\infty = \frac{(\epsilon_0 - \epsilon\infty)}{1+i\omega\tau} \quad \text{given above.}$$

Debye interpreted ξ by assuming that a dipole responds to a torque as a rigid sphere of radius a turning in a fluid of macroscopic viscosity η. Stokes formula

$\xi = 8\pi\eta a^3$ then gives

$\tau = 4\pi\eta a^3/kT$.

Replacing ξ by η does, in fact, go no further in explaining the process but experimental results for η and τ can give reasonable results for a.

C.1.b.iii) Relaxation in Solids

Debye's equation for the complex dielectric constant ϵ^* has been derived for solids as well as for liquids though using a different model. Broader relaxation regions involving a range of relaxation times may be described by Fuoss and Kirkwood's empirical relation

$$\epsilon'' = \epsilon''_{max} \operatorname{sech} [\alpha \ln(f/f_{max})] \quad \text{where } f \text{ is frequency and } \alpha$$

varies between 1 for a single relaxation time to 0 for an infinite range of relaxation times.

Diffusion models used to describe relaxation processes in liquids are not likely to be realistic models for relaxation in most types of solids. As mentioned earlier, models which are used for solids tend to consider a single dipole whose orientational increment is restricted by potential barriers. The dipoles normally have energies such that they may be considered to reside in potential triangles. Occasionally, due to thermal fluctuations, a dipole will possess enough energy to cross a potential barrier. In the absence of a field an equilibrium will exist such that over a large enough sample the distribution of dipoles in the available potential triangles is a constant. Application of a field will tend to change the distribution so that dipoles will tend to align themselves with the field.

Debye's Model: Debye assumed that each dipole possessed two positions of equilibrium equal in energy and separated by a potential barrier ΔE as in Figure 4.

The dipoles oscillate about the equilibrium positions and occasionally acquire enough energy to cross the potential barrier to the other equilibrium position. With no field applied, the equilibrium positions are equally populated. When a field is applied some dipoles will rotate such that more dipoles occupy the position favoured by the direction of the field, thus polarising the sample. The frequency of maximum absorption is given by

$$f_{max} = \frac{1}{2\pi\tau} = Ae^{-\frac{\Delta E}{RT}}$$

where A is a constant. In practice A varies and is sometimes written as an entropy term

$$f_{max} = \frac{f_o}{\pi} e^{\Delta S/R} e^{\Delta E/RT}$$

where f_o is the frequency of oscillation of the dipole in the potential triangles (of the order of 10^{-12}/sec).

f_{max} can therefore be written as

$$f_{max} = \frac{f_o}{\pi} e^{-\Delta F/RT}$$ where ΔF is the free energy of activation.

Some authors apply absolute reaction rate theory which gives $\frac{kT}{h}$ instead of $\frac{f_o}{\pi}$. The values of ΔS and ΔF derived from this method agree, at room temperatures, with those from the above equation.

Debye's equation is not, in fact, restricted to a model with only two equilibrium positions of equal energy but applies to a model with any number of potential triangles of equal energy separated by potential barriers of equal energy. In such a system, the magnitude of the absorption increases with decreasing temperature.

In most solids the energy of the potential triangles are unequal as are the energies of potential barriers separating them. The linearity of a plot of $L_u f_{max}$ versus $\frac{1}{T}$ gives an indication of how well Debye's model is approximated in the Temperature/Frequency range considered.

For a model in which there exist two triangles of unequal energy as in the diagram of figure 5, the molecular relaxation time is given approximately by the expression

$$f_{max} = \frac{1}{2\pi\tau} = Ae^{-\frac{\Delta E_1}{RT}}$$ where ΔE_1 is approximately the smaller energy barrier.

Clearly, this is a better approximation as $\Delta E_1 \rightarrow \Delta E_2$ and Debye's model is more closely approximated.

The above two-site model gives one relaxation time. Two relaxation times are given by a slightly more complicated model. Extensions of the model to give three or more relaxation times have been made.

The magnitude of the absorption is not given by the expression relating f_{max} and T. Frohlich concluded that the two site model with equal energies can be described by an equation for the magnitude of the absorption in liquids. This type of equation is difficult to formulate but Ousager's formula for the dispersion

$$\epsilon'_o - \epsilon'_\infty = \frac{4\pi N_o \mu^2}{9kT} - \frac{\epsilon'_o(\epsilon_\infty+2)^2}{2\epsilon'+\epsilon_\infty}$$

has been found to apply to a number of systems. For the two site model with triangles of unequal energies, the dispersion is given by

$$\epsilon'_o - \epsilon'_\infty = \frac{C}{T}\left(1 + \cosh\frac{\Delta E_o}{RT}\right)^{-1}$$

where C is a constant.

For $\Delta E_o \gg RT$ this reduces to

$$\epsilon'_o - \epsilon'_\infty = \frac{B}{T} e^{-\frac{\Delta E_o}{RT}} \quad \text{with B a constant.}$$

Some polar solids e.g. long chain aliphatic ketones do not absorb at temperatures up to the melting point. This indicates that ΔE_o for the dipoles involved must be large.

Summary: The Dielectric Theory gives an adequate description of the equilibrium polarisa tion of gases at low pressures. For denser gases, liquids and solids, the problem involved in specifying properly the molecular processes responsible for equilibrium polarisation are such that models which may be of dubious validity have to be employed. In the case of dielectric relaxation which is essentially a non-equilibrium irreversible process, the difficulties of describing the responsible underlying molecular processes are even greater than in the equilibrium case. The result of this is that, in the study of dielectric relaxation, emphasis is shifted from attempts to apply detailed theoretical calculations to empiricism. Results may be compared with data obtained by other means and with data for the dielectric absorption of samples whose structure is known to be closely related to that of the sample under consideration. In this way a qualitative understanding of the process may emerge.

The position is closely paralleled by the state of knowledge of absorption in the infra-red. In this case detailed calculations can be

successfully made for simple molecules. The infra-red spectra of complex molecules, however, are seldom subjected to any mathematical analysis which would be prohibitively complicated. The usefulness of the technique lies in the vast accumulation and correlation of qualitative results. In this respect studies of dielectric relaxation suffer in that there does not exist the wide range of experience such as is available in the field of infra-red absorption.

C.2 Dielectric Relaxation of Polymers[9] [23] [32]

C.2.a Introduction

The connection between the measured electrical properties and the molecular structure of a polymer cannot be simply expressed. The molecular structure is often not known exactly; small amounts of impurities may contribute to and even dominate the measurements; the sample may not be stable. Molecular mechanisms proposed to account for dielectric behaviour are the result of experience and a range of related data from studies by techniques using Nuclear Magnetic Resonance, X-rays, optical properties, infra-red spectra, mechanical and thermal properties.

The detailed dielectric theory developed for simpler molecules generally breaks down when applied to polymers since the underlying assumptions are no longer valid. There are, however, semi-empirical relations which may be of use in analysing data. These include activation energy relations between the maximum frequency and temperatures and relations which may estimate the spread of relaxation times characterising the process.

C.2.b The dielectric properties of polymers depend on molecular relaxation processes which affect other properties, in particular mechanical properties. In general, polymers appear to be characterised by several distinguishable relaxation processes which can be attributed to the thermal motion of different molecular units. These may be side chains or pendant groups or portions of the main chain itself. When the movement of such a unit involves a change in dipole moment, dielectric loss is exhibited. The movement of a unit may be characterised by a relaxation time or, if the movement is complicated, by a spectrum of relaxation times. Unfortunately, no complete theory exists which relates polymer structure to relaxation times and their temperature dependence. Hence the connection between dielectric properties and polymer structure tends to be made on the basis of experience and related experimental studies.

Experimental evidence indicates that in general, linear polymers and lightly crosslinked polymers exhibit two types of dielectric relaxation. One involves movement of dipoles independently of the main chain and the other involves movement of a portion of the main chain with a dipole

incorporated (i.e. the movement of dipolar segments of the main chain). In Mikhaelov's terminology, the former gives rise to 'dipole-radical' losses and the latter to 'dipole-elastic' losses. Dipole radical losses generally appear, in the frequency and temperature ranges normally studied, in the glassy state of the polymer, but this need not be the case. Mikhaelov reports dipole-radical losses in Polymethyl Methacrylate at a frequency of 5 Mc/s at 190°C, well above the glass-transition temperature at this frequency.

The characteristics of dipole-radical losses are closely connected to the immediate surroundings of the dipole and hence are independent of the movement of the main chain unless this specifically alters the surroundings of the dipole. This may occur in crystalline parts of the polymers where neighbouring chains are closely packed in a specific way or where there is interaction such as hydrogen bonding between different chains or portions of a chain.

Dipole-elastic losses are related to movements of the chain and are hence ultimately connected with the glass-transition temperature. It is clear, therefore, that the presence of plasticisers will substantially affect the characteristics of dipole-elastic losses while, in general, not affecting those of dipole-radical losses. Stretching likewise affects only dipole-elastic losses. Co-polymerisation may affect both types of loss.

Some evidence appears to indicate that the segments responsible for dipole-elastic losses cannot be very long (e.g. consisting of three or four methylene groups) and light crosslinking has no effect on dipole losses. Extensive crosslinking, however, limits the possibilities for segmental motion and hence profoundly affects dipole-elastic losses.

Roughly speaking, dipole-elastic losses and dipole-radical losses may be distinguished by plots of log f_{max} versus $\frac{1}{T}$ where f_{max} i.e. the frequency of maximum absorption at temperature, T. The former generally show apparent activation energies very much greater (40-120 k cals/mole) than the latter (5-30 k cals/mole). The mechanism providing for dipole-elastic losses is usually a complicated one and the apparent activation energy calculable, even if the log f_{max} versus $\frac{1}{T}$ plot is linear, is of dubious significance. These processes are usually characterised by a range of relaxation times.

Ferny et al.'s method of reduced variables to determine the spectrum of relaxation times characterising a certain process involves the implicit assumption that the distribution function for relaxation times is independent of temperature, which in turn implies that all the elementary processes contributing to the whole process have the same temperature dependence. This is not generally the case in practice and so the method is of limited applicability. A method of estimating the spread of relaxation times is from a Cole-Cole plot. If the locus of ϵ^* in the complex plane is a

circular arc, α, the distribution parameter, in the expression

$$\epsilon^* - \epsilon_\infty = \frac{\epsilon_o - \epsilon_\infty}{1+(i\omega\tau)^{1-\alpha}}$$

can be calculated.

Polymers may be divided into the two classes - linear/slightly cross-linked, and extensively cross-linked. There is little experimental data concerning the investigation of basic molecular structure in highly cross-linked systems. General theoretical discussions about the dielectric properties of such systems do not appear to exist. The first class may be divided into polar and non-polar polymers and these can be arbitrarily divided into crystalline and non-crystalline polymers. These types will be briefly described.

Non-polar polymers: As would be expected, non-polar polymers (e.g. polyethylene and polytetrafluoroethylene) are characterised by values for the dielectric constant which indicate that only electronic and atomic polarisations are effective, and by low values of tan δ. These are, however, not insignificant. For polyethylene, several well defined loss regions have been reported. Experimental studies (in particular infra-red investigations) have shown that the loss is due to extraneous carbonyl groups introduced during polymerisation or processing. Likewise in the case of P.T.F.E., the very low dielectric losses are probably due to oxidation, impurities or end groups. Dispersion regions corresponding to phase transformations in P.T.F.E. have been reported.

Polar Polymers:

It is reasonable that the dielectric behaviour of crystalline regions in polymers would be different from that of amorphous regions in view of the different mechanisms which must be operative to provide for dielectric loss in each case. In particular, the glass transition is a characteristic of amorphous material while a well-defined melting point is characteristic of crystalline material, both transformations being accompanied by changes in dielectric properties. Dipole-radical losses may well be modified in crystalline material because of interaction between groups responsible for this type of loss.

Typical of amorphous polar polymers are the acrylics which have been extensively studied. A general formula is

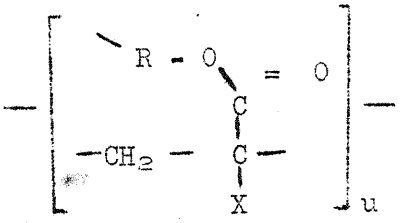

where both X and R may be varied. Polymethyl methacrylate has $R = X = CH_3$. It is clear that in changing R, the properties of the pendant group can be changed and by changing X, the properties of the polymer chain itself can be varied. Systematic studies have been made of polymers with differing X and R and some general characteristics have been brought to light. Generally, the polymers exhibit two well defined loss regions termed α and β respectively. Perhaps the greatest benefit which has accrued from a systematic study has been a clear-cut distinction between the two processes. The α-peak has been characterised as due to dipole-elastic losses and the β-peak as due to dipole-radical losses. The dipole-elastic loss appears to be unanimously related to the glass-transition temperature and the motion of segments of the main chain. The mechanism responsible for the β-peak is not so obvious, but the evidence indicates that it is due to motion of the ester side-group.

Dipolar motions which are possible in amorphous material may be inhibited or modified in crystalline material because of steric hinderance due to the close packing of polymer chains in the crystal or because of specific interactions between the dipoles which characterise the crystalline state. Dipolar movement may, however, be able to occur in the crystalline state of polymers just as it is possible in crystals of monomeric polar organic compounds.

D. Experimental Procedure

D.1 The Starting Materials

It was stated in the introduction that it was felt important to degrade a resin whose chemical structure was known as well as possible. For this reason a pure sample of the diglycidyl ether of Bisphenol A was cured with pure p-p' diamino diphenyl methane.

The diglycidyl ether (dge-BPA) was recrystallised from a commercial sample of the crystalline material (Ciba EP274) according to a method recommended by the manufacturers. The recrystallisation was from an ethanolic solution of the commercial material and, after filtering, the recrystallised product was dried under vacuum for several days. Relatively large crystals (approximately 1 m.m. across) could be grown from a melt of the dge BPA. The crystals melted over the range 39-42°C, complete melting occurring only at 42°C.

Elemental analyses* gave the following results, which are compared with figures for the pure compound whose formula is:

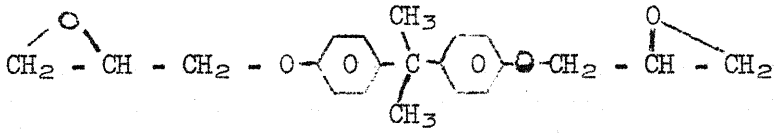

	% N	% C	% H	% Cl	% O (by difference)
Experimental:	0	73.17	7.14	.74, .68	18.95, 19.01
	0	73.40	7.07	.25, .21	19.28, 19.32
Theoretical:	0	74.08	7.105	0	18.8

The most likely reason for the chlorine content is the presence of molecules with structure

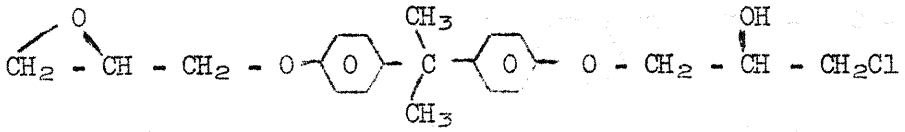

in which ring closure to form one of the terminal epoxide groups during the synthesis of the dge BPA from epichlorhydrin and Bisphenol A has not been successful. Calculations based on the figure of 0.47% chlorine showed that, if all the chlorine present were due to this substance then

---

* Messrs. Weiler and Strauss.

for very 1,000 molecules of the dge BPA there were some molecules with the above formula present in the resin.

This calculation did not explain the rather large discrepancy between the experimental and theoretical figures for carbon content. It was supposed that the relatively low carbon content found might have been due to the presence of residual ethanol in the solid dge BPA which could be relatively strongly incorporated into the crystal by hydrogen bonding. Rough calculations to estimate the percentage of ethanol required to resolve the discrepancy between the calculated and experimental results showed that a mole ratio of 17% could account for them.

Accordingly a sample of the dge BPA was melted and then vacuum was applied for three hours to the melt. Elemental analyses on this sample of dge BPA gave results considered, within the experimental error, to agree with those for the pure resin:

	%C	%H	%O	%N	%Cl
Experimental:	73.76	7.22	18.41, 18.56	0	.61, .46
	73.92	7.00	18.78, 18.70	0	.30, .38
Theoretical:	74.08	7.105	18.8	0	0

In the preparation of discs, the solid dge BPA was always melted and evacuated before being weighed finally. In fact a typical weight loss due to evacuation for 20 minutes was 0.1% which is not consistent with figure of 2.4% corresponding to a mole % of ethanol present of 17%. It appears therefore that little ethanol remained in the recrystallised material and that unless some of the non-volatile species is present, the discrepancies between the calculated and experimental values for carbon content are a result of experimental uncertainty in the latter.

The manufacturers stated* that molecules of the form

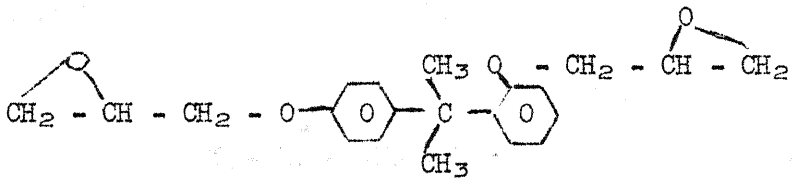

are present in the original material in 1-2% quantities. Recrystallisation may have reduced this quantity.

In summary, the resin used in the preparation of discs was a fairly pure sample of the diglycidyl ether of Bisphenol A. Chlorinated molecules with the structure

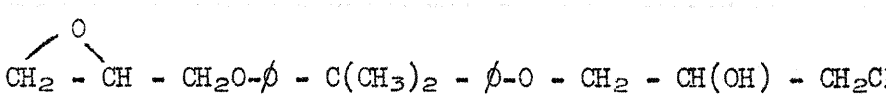

---

*private communication

are present in some ½% mole ratio, and isomeric molecules (2:4 disubstituted diphenyl dimethyl methane instead of 4:4 disubstituted) in some 1% mole ratio.

The hardener, p-p' diamino diphenyl methane, was recrystallised from a solution in hot water of a commercial product. Elemental analyses on the recrystallised product gave

	%C	%H	%N	%O (by difference)	%Cl
Experimental	78.13	7.15	14.16	.27	.29, .29
	78.50	7.00	14.52	0	
Theoretical:	78.70	7.11	14.13	0	0

D.2: Preparation of discs

The preparation of the discs used in the degradation and dielectric studies was as follows:

A sample of the recrystallised dge-BPA was weighed out. It was melted and evacuated for 20 minutes. The weight was taken again and the weight loss due to evacuation calculated. This was never greater than 0.1%. A weight of DDM calculated as 28.8% of the final weight of the dge-BPA was added. The mixture was heated until a mobile, homogeneous liquid resulted. This was then evacuated for 20 minutes to rid the mixture of air bubbles. After evacuation, the mixture was again weighed - a typical weight loss figure was 0.1%. Elemental analyses showed that evacuation of the mixtures had no significant effect on the C:H:O:N ratios i.e. neither component was significantly more volatile than the other. The mixture was then heated till mobile and cast in polythene moulds which were air tight. The resin was cured for approximately 20 hours at a temperature of 95°C. The resulting discs were honey-coloured, circular of diameter approximately 5½ cms. and approximately 0.13 cms thick. After filing off extraneous matter, the discs were weighed before cure/degradation under low pressure and an infra-red spectrums taken.

Two discs were prepared for any one experiment, one being used for dielectric studies, the other for infra-red studies.

D.3: Infra-red studies on the Discs and on Degradation Products

Infra-red spectra of cured and degraded discs were obtained by filing the discs and incorporating the filings into KBr discs in the normal way. Infra-red spectra of solid crystalline substances were obtained by grinding the substance with KBr and making a KBr disc; spectra of liquid substances were obtained from smears between KBr and rock-salt plates. Infra-red spectra of gases were obtained in a cell of 10 cm, path length.

Perlsin Elmer model '21' spectrometer was used to obtain all infra-red spectra. The KBr used was analar grade and was heated strongly before being stored at 120°C. The spectro of discs of pure kBv which had been evacuated for 10 minutes before pressing at a pressure of 8 tons/in^2 showed negligible hydroxyl absorption and so all kBv discs were evacuated for 10 minutes or more before pressing.

D.4: Infra-Red studies of Initial Cure

In these studies small quantities of the crystalline dge-BPA and DDM in a w/w ratio of 100:28.8 were weighed out and the powders thoroughly mixed. Continued mixing of the mixture with a spatula produced a paste. Two discs of pure Potassium Bromide (kBv) were made in the normal way and a small quantity of paste pressed between the discs. The resulting sandwich was mounted in a KBr disc holder and the infra-red spectrum of the paste obtained. This technique was reported by Feazel and Verchot(14)(1957). The cure was followed by heating the sandwich, at first gently and then strongly, to about 100°C by means of a commercial hairdrier. The cures studied were hence by no means isothermal, but served to relate the spectra of discs cured at 95°C (D.2) with those of the starting materials, and also to identify particular absorptions with particular chemical groups involved in the cure reactions.

D.5: Post-cure and degradation were performed at low pressure (of the order of 0.7 m.m. of mercury) to prevent oxidation. In fact, post-cure and degradation were not distinguished for reasons explained fully in section F. The discs of resin which had been cured at 95°C were weighed and then clipped with 'Bulldog' clips onto a flat clean aluminium plate to avoid distortion during heating, care being taken that the clips did not come into contact with any portion of the disc which would be subsequently situated between the electrodes of the cell used for dielectric measurements. This assembly was placed in the degradation vessel shown in Fig. 6.

The vessel was sealed by bolting the cap on. The copper gasket was compressed by a lip on the reaction vessel into a groove in the cap thus providing a seal. The reaction vessel was connected by rubber pressure tubing to the glass-apparatus shown in Fig. 7.

The first trap was for condensible products produced during degradation. The second trap served to prevent back diffusion of oil vapours from the pump into the first trap.

The procedure for the post-cure/degradation of a sample was as follows:

(1) The discs of resin were weighed, clipped to the aluminium plate and introduced into the reaction vessel which was then closed and connected via the traps to the pump.

(2) The whole apparatus was pumped down with taps T1, T2, and T3 open.

Meanwhile the traps were immersed in liquid air. The pressure was read periodically and, when a minimum (usually after a few minutes pumping), it was noted and tap T2 shut.

(3) The reaction vessel was introduced into an oven at the desired temperature and the time noted. The temperature of the reaction vessel was continuously monitored by a chromel-alumel thermocouple connected to a recording potentiometer with the cold junction at 0°C. The thermocouple gave the temperature of the outside of the reaction vessel.

(4) Pumping was continued and the temperature monitored for the duration of the post-cure/degradation.

(5) At the desired time, the reaction vessels was removed from the oven and taps T1 and T3 shut. Liquid air was placed around the side-arms A and tap T2 opened. The first tap was warmed to room-temperature and thus any degradation products volatile at room temperature condensed into A. A was then sealed and removed from the apparatus.

(6) Condensible products remaining in the first tray were removed by dissolving them in methanol. Both the capsule containing any volatile products and the methanolic solution of condensible products were reserved for analysis.

(7) The discs were removed from the cooled reaction vessel and were both weighed to determine weight loss and physically examined. An infra-red spectrum of one disc was taken and the other disc was reserved for dielectric studies. In the last experiment at a degradation temperature of 309°C, quantities of tar were produced in the reaction vessel. This was removed and reserved for analysis. The discs in this experiment were unfit for dielectric studies.

The apparatus suffered two very serious disadvantages. The first was that since the reaction vessel had a very high heat capacity, the post-cure/degradations were isothermal only after a considerable time had elapsed. The second and more serious was that, although the pressure was shown to be low enough to prevent oxidation of the discs, considerable quantities of air were pumped through the system. This meant that, in particular, Carbon Dioxide and Water were condensed in the first tray. Any Water or Carbon Dioxide which may have been produced in the degradation could not, therefore, be detected.

D.6: Dielectric Measurements

The dielectric properties of the resin discs were measured at nine fixed frequencies in the frequency range 210 c/s to 90 kc/s and in the temperature range for approximately 180°C to 240°C. The discs formed the dielectric of a parallel plate capacitor, or cell, whose capacitance and loss were measured on a dielectric bridge.

The construction of the cell is given in Fig. 8.

The resin disc was placed between two electrodes of aluminium, machined flat. One electrode was circular of diameter some 5.5 cms; the other electrode was circular with diameter accurately 3.1 cms, surmounted by an anular guard ring approximately 1 cm wide. The electrodes were cemented to bakelite plates which were backed with steel plates so that the whole assembly could be bolted together without distortion of the electrodes. The steel backing plates and bolts were all earthed. Terminals from the electrodes and guard ring were connected to the bridge by means of leads insulated with PTFE and each sheathed in a copper spiral to eliminate mutual capacitance effects. After measurements at high temperatures the bakelite plates showed evidence of degradation. Tests proved, however, that their insulation was in no way impaired.

The dielectric bridge used in the measurements was designed and built by Baker (AEI Ltd.). The circuit diagram is shown in Fig. 9.

X was the lossy capacitance to be measured. S was a standardised variable capacitor. R is a variable resistance and C a variable capacitance and a voltmeter with a range 1 mV to 10V was necessary for the detector.

At balance X = S and the loss tangent

$\tan\delta = wrk = wRC = 2\pi fRC$ where f is frequency in c/s.

S was standardised by comparing S with known capacitances. In this way a proportionality factor between readings on S and capacitors was found. The absolute capacitance of S, including the self and mutual capacitors of the leads to the cell was measured by substituting various standard non-lossy capacitances (accurate to 1%) for the cell, thus balancing the bridge. In this way the capacitance of the cell was related to readings on S. The standardisation was important as the self-capacitance of the leads was of the order of the capacitance of the cell (several pF)

The dielectric constant of the resin disc were calculated using the standard equations for the capacitance of a parallel-plate condenser

$$C = \frac{\epsilon\epsilon_o A}{d}$$

C = capacitance in farads

A = area of electrode in m^3

d = width of dielectric in m.

ϵ_o = absolute

ϵ = dielectric constant

This was considered to give accurate enough values of ϵ since a guard-ring was used and very accurate values of ϵ were not required. Values of the loss tangent were given directly from readings of R and C on the bridge.

For readings in the temperature range - 185°C to room temperature the cell was wrapped in two separate layers of polythene sheeting which

prevented condensation of water from the atmosphere onto or into the cell. The wrapped cell was placed in a massive iron cylinder of very high heat capacity which was cooled to liquid air temperatures and placed in a thermos flask. Readings at temperatures between liquid air temperatures and room temperatures were taken while the cell and cylinder heated up slowly to room temperature. The maximum rate of temperature rise was less than 1°C/minute which enabled the bridge to be easily balanced. Values of ϵ calculated from these readings were not strictly isothermal but the rate of temperature change was such that the difference between the experimental values and isothermal values of ϵ was negligible. For readings at temperatures greater than room temperature the cell was placed in an oven which maintained the temperature between $\mp$ 1°C of the desired value. Helium was circulated around the cell for readings at room temperatures greater than 140°C to prevent any oxidation of the resin discs. Examination of the discs after dielectric measurements had been taken showed that some slight superficial darkening had occurred. The extent of this was such that it did not affect the results.

The temperature of the cell was measured by measuring the E.M.F. of a chromel-alumel thermocouple with one junction sunk into one of the bakelite plates of the cell and the other maintained at 0°C. Temperature variations across the sample was likely to be minimal as the electrodes and steel backing plates would seem to even out any temperature variations. Heating of the dielectric due to the measurement was negligible.

E. Experimental Results

E.1: Infra-Red spectra of Starting Materials and Initial Cure

Figure 10 shows the infra-red spectrum of the crystalline diglycidyl ether of Bisphenol A used in the experiments. The allocation of peaks was as follows (a question mark signifies an allocation which is not beyond doubt):

Frequency cm^{-1}	Allocation	Ref. or reason for allocation
~ 3070	Aromatic C-H	Bellamy[4]
~ 3030	C-H in Oxcious Ring	Herbert et. al.; disppears on curing.
~ 3000	CH_3	Bellany[4]
~ 2980	CH_2	Bellamy
~ 2910	CH_2 and CH_3	Bellamy
~ 1900 }	1:4 disubstituted	Bellamy
~ 1770 }	Aromatic ring	Bellamy
1615	C=C in Aromatic ring	Bellamy
1590	C=C in Aromatic ring	Bellamy
1520	C=C in Aromatic ring	Bellamy
1490	CH_2	Bellamy
1460	CH_3	Bellamy
1440	C=C in Aromatic ring	Bellamy
1420	?	-
1390	CH_3 ?	Bellamy[4]
1370 }	$C(CH_3)_2$ doublet	Bellamy
1350 }		
1300	Ether	Keenan[17]
1250	Ether + Epoxy	Bellamy[4], Keenan[17]
1190	Ether and $C(CH_3)_2$	Bellamy[4], Keenan[17]
1155	ϕ-O-R ?	Keenan[17]
1135		
1110	1:4 disubstitution of Aromatic Ring	Bellamy[4]
1090	ϕ-O-R	Bellamy[4], Keenan[17]
1040	ϕ-O-R	Bellamy[4], Keenan[17]
1015	1:4 disubstituted Aromatic Ring or ϕ-O-R ?	Bellamy[4], Keenan[17]

Frequency cm^{-1}	Allocation	Ref. or reason for allocation
970	Oxirane ring	f notes; disappears on curing
915	Oxirane ring	Patteron(30), Bellamy(4), Lee and Neville, O'Neill and Cole(28), Dannenberg and Harp(11); disappears on curing.
865	Oxirane ring	" " " "
830	1:4 disubstituted Aromatic Ring	Bellamy(4)
805	ϕ-O-R ?	Keenan(17)
770	Oxirane Ring	Patterson(30); disappears on curing.

Notes:

(1) The peak at 970 cm^{-1} is very poorly developed in the solid. It is a medium intensity peak in the melted dge-BPA (Fig. 11), which completely disappears on curing. It appears certain, therefore, that it is some absorption characteristic of the oxirane ring. No mention could be found in the literature of this allocation. The fact that this mode of absorption is suppressed in the crystallised state may give some indication of the crystal structure.

(2) Peaks allocated as due to absorption of the group ϕ-O-R were found in the spectra of many compounds having this structure (Keenan, 1966); the three peaks at 1300 cm^{-1}, 1250 cm^{-1} and 1190 cm^{-1} appear to form a pattern characteristic of aryl alkyl ethers (Keenan(17)(1966)).

(3) One of the benefits which accrued from the use of a pure compound was that peaks in the infra-red spectrum could be correlated, with some certainty, with chemical groups known to be in the compound.

The infra-red spectrum of crystalline p-p diamino-diphenyl methane is shown in Fig. 12. Absorptions were allocated as follows:

Frequency cm^{-1}	Allocation	Ref. or reason for allocation
3500, 3420, 3380	N-H stretch	Bellamy(4)
3070	C-H in Aromatic Ring	Bellamy(4)
2940, 2880	CH_2	Bellamy
1900, 1800	1:4 disubstituted Aromatic Ring	Bellamy

Frequency cm^{-1}	Allocation	Ref. or reason for allocation
1640	Primary amine	Bellamy[4]
~ 1620 (not resolved)	C=C in Aromatic Ring	Bellamy
1590	C=C in Aromatic Ring	Bellamy
1525	C=C in Aromatic Ring	Bellamy
1440	CH_2	Bellamy
1435	C=C in Aromatic Ring	Bellamy
1325	Amine ?	Keenan[17]
1295 and 1280	Primary Amine	Bellamy; disappears on curing.
1210	1:4 disubstitution of Aromatic Ring	Bellamy; disappears on curing
1185	Amine ?	Keenan[17]
1130, 1085, 1015	1:4 disubstitution of Aromatic Ring	Bellamy[4]
962, 952	?	-
910, 845	$-\phi-CH_2-\phi-$?	Keenan[17]
820	1:4 disubstitution of Aromatic Ring	Bellamy[4]
765	$-\phi-CH_2-\phi-$?	Keenan[17]

For the spectra shown in Fig. 13, amounts of dgeBPA and DDM were weighed out separately, ground and made up into two separate KBr discs such that the relative concentrations in the KBr discs were roughly in the ratio 100:28.8, dgeBPA:DDM. A spectrum of the dgeBPA and a spectrum of the DDM were run separately. A spectrum of both discs together was run in an attempt to simulate the spectrum of a completely unreacted mixture and to relate the composite spectrum to those of the individual components.

Notes on the composite spectrum:

(1) The primary amine absorption at 1640 cm^{-1} is not well resolved from the Aromatic C=C absorption at 1615 cm^{-1} but appears as a shoulder.

(2) Aromatic C=C absorptions are all very well resolved.

(3) The CH_3 absorptions at 1460cm^{-1} and 1390 cm^{-1} are well resolved as is

the $C(CH_3)_2$ doublet at 1370 cm^{-1} and 1350 cm^{-1}.

(4) The main primary amine peak (1295 and 1280 cm^{-1}) falls between two strong absorptions (1300 and 1250 cm^{-1}) due to ether, and ether and epoxy; it does not appear as a peak at all.

(5) The peak at 910 cm^{-1} due to ϕ-CH_2-ϕ in the amine overlaps the epoxy peak at 915 cm^{-1}.

(6) Generally speaking the result of the relatively low concentration of DDM is that its spectrum is largely overwhelmed by that of the dgeBPA except where strong absorptions due to DDM occur.

Fig. 14 shows spectra of a 100:28.8 mixture of dgeBPA and DDM in various stages of cure, obtained by the method described in section D.4.

Notes:

(1) The spectra cover a range of the reaction which the degree of conversion of epoxide groups varies from near zero to an estimated 70 to 80%. The degree of cross linking was probably not near that which would characterise a properly cured resin.

(2) In the 3000 to 3500 cm^{-1} region the conversion of amine groups and the formation of hydroxyl groups are clear, though the two absorptions overlap.

(3) The primary amine absorption at 1640 cm^{-1} disappears progressively.

(4) Some increased background absorption occurs in the range 1470 to 1300 cm^{-1} probably due to secondary hydroxyl, but despite this the CH_2 absorption at 1390 cm^{-1} and the $C(CH_3)_2$ doublet at 1370 and 1350 cm^{-1} remain clear.

(5) Some decrease in absorption in the region 1300 to 1260 cm^{-1} which accompanies amine conversion can be detected.

(6) Increased absorption in the region 1120 to 1070 cm^{-1} accompanies the formation of secondary hydroxyl groups.

(7) The epoxy peaks at 970 cm^{-1}, 915 cm^{-1}, 865 cm^{-1} and 770 cm^{-1} all decrease progressively in intensity. The peak at 1250 cm^{-1} surprisingly remains unchanged. This may mean that epoxide absorption at this frequency is slight. The decrease in epoxy concentration can also be seen in the C-H stretch region where the absorption due to C-H stretch in the oxirane ring disappears on curing.

(8) Generally speaking, curing results in a 'blurring' of the spectrum. Despite this, characteristic features of the spectrum of the cured product can be picked out:

a) Broad hydroxyl absorption in the 3500 cm^{-1} region and the 1100 cm^{-1} region.

b) Resolved absorptions due to aromatic C-H, CH_3 and CH_2 groups in the C-H stretch region.

c) 1:4 disubstitution patterns between 2000 cm^{-1} and 1650 cm^{-1}.

d) Aromatic C=C absorptions at 1615 cm^{-1}, 1590 cm^{-1} and 1520 cm^{-1}.

e) CH_3 absorption at 1390 cm^{-1} and $C(CH_3)_2$ absorptions at 1370 cm^{-1} and 1350 cm^{-1}.

f) The three characteristic ether absorptions at 1300 cm^{-1}, 1250 cm^{-1} and 1190 cm^{-1}, the last overlapping $C(CH_3)_2$ absorption.

g) Anyl-Alkyl ether absorption at 1040 cm^{-1}.

h) 1:4 disubstitution absorption at 820 cm^{-1}.

i) No absorption appears which can be attributed to the nitrogen present.

The fact that the spectrum of the cured product is reasonably resolved is probably because both the resin and the hardener contain the unit

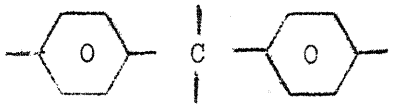

E:2. Post Cure/Degradation Details

In all the experiments, the resin discs were cured for 20 hours at 95°C in airtight polythene moulds.

Fig. 15 shows a typical spectrum of a disc after this cure.

E.2.a Experiment I. After the 95°C cure the discs were post cured in air at 130°C for $16\frac{1}{2}$ hours.

i) The infra-red spectrum of the discs after this cure is shown in Fig. 16. The spectrum is not different from that obtained for discs cured at 95°C except for very slightly reduced epoxide absorption at 915 cm^{-1}.

ii) The discs retained their transparent honey colour.

E.2.b. Experiment II.

In this experiment discs cured at 95°C in polythene were post cured for $16^{1}/_{4}$ hours at 136°C in air and a further 16 hours at 180°C in air.

i) The discs were extensively reddened in colour though still transparent.

Filing showed that the discolouration was a maximum on the surface and that no discolouration had occurrred in the centre of the discs.

ii) Infra-red spectra of the surface and the centre of the discs are given in Fig. 17 and 18 respectively. Absorption at 1700 cm^{-1} and 1660 cm^{-1} in the former spectrum indicated that considerable oxidation had taken place. The discs were discarded as being unsuitable for dielectric studies.

E.2.c Experiment III.

i) Discs cured at 95°C were post-cured at an initial pressure of 0.7 m.m. of mercury in the apparatus described in section D.5. The temperature-time history is given in Fig. 19.

ii) The discs emerged from the post-cure the same honey colour as before.

iii) The discs suffered no weight loss.

iv) An infra-red spectrum of the discs after post-cure is given in Fig. 20.

E.2.d Experiment IV.

i) Discs cured at 95°C were post-cured/degraded at an initial pressure of 0.7 m.m. of mercury in the apparatus described in section D.5. The temperature-time history is given in Fig. 21.

ii) The discs emerged from the heat treatment the same honey colour as before.

iii) Weight losses of 0.0628% and 0.0627% were recorded for the two discs.

iv) Products in the first trap occupied three distinct regions shown in Fig. 24.

On warming the trap, the light white deposit sublimed or evaporated and was distilled into the capsule (section D.5), together with quantities of the heavy white crystalline deposit which proved to be water. The oily yellow substance was dissolved in methanol and the solution reserved for analysis.

v) An infra-red spectrum of the discs after heat treatment is given in Fig. 25.

E.2.f Experiment VI.

i) Discs cured at 95°C were post-cured/degraded at an initial pressure

of 0.7 m.m. of mercury in the apparatus described in section D.5. The temperature-time history is given in Fig. 26.

ii) The discs emerged from the heat treatment darkened in colour and the darkening was uniform throughout the discs.

iii) Weight losses of 7.87% and 4.94% were recorded for the two discs.

iv) Products in the trap occupied distinct regions shown in Fig. 27.

On warming, both the light white deposit (8) and the clear crystals (7) sublimed or evaporated and were distilled into the capsule (section D.5). The heavy white crystalline deposit (6) melted and some evaporated. Meanwhile the other regions had melted, and mixed together and with the melted portion of (6). These formed two immiscible mobile phases - one yellow and the other cloudy white. These were reserved for analysis.

v) An infra-red spectrum of the discs after heat treatment is given in Fig. 28.

E.2.g Experiment VII.

i) In this experiment four discs were used so that large quantities of degradation products would be produced. They were post-cured/degraded at an initial pressure of 0.6 m.m. of mercury in the apparatus described in section D.5. The temperature-time history is shown in Fig. 29.

ii) The discs emerged from the heat treatment very much darkened to a dark brown colour and were opaque. They were considerably distorted and very brittle. For this reason no dielectric studies were possible for Experiment VII.

iii) Weight losses of 20.8%, 17.5%, 9.75% abd 26.0% were recorded for the discs.

iv) During the degradation quantities of a colourless liquid condensed in the glass lines before the first trap. After the degradation this was flame distilled into the first trap. Products in the trap occupied distinct regions shown in Fig. 30.

Probably because of the increased quantities of products formed and because of the distillation into the trap of the colourless liquid which had collected in the lines, the regions were not as well separated as those in Experiment VI. On warming the trap the powdery white deposit (6) sublimed or evaporated off and was sealed in the capsule. (Section D.5). The crystalline white deposit (5) melted and some evaporated. The other deposits melted slowly and all products not volatile enough to be distilled into the capsule were removed as a methanolic solution which was reserved for analysis.

v) An infra-red spectrum of the discs after heat treatment is shown in Fig. 31.

vi) Large quantities of a reddish-brown very viscous tar were formed.

Discs from experiments I, III, IV, V and VI were reserved for dielectric measurements.

E.3 Results of Dielectric Measurements

E.3.a Accuracy of Dielectric Measurements

A preliminary experiment to test the reproducibility of results was carried out on a disc of cured epoxide resin. The results showed that where values of the loss tangent were of the order of 10^{-2}, values could be quoted to 0.5×10^{-3} i.e. a spread of 10^{-3}. The source of greatest uncertainty appeared to be the readings of frequency on the oscillator. Values of ϵ are accurate to two decimal places.

E.3.b Except for Experiment I results for loss tangent and dielectric constant will be tabulated, values for various temperatures at a fixed frequency being grouped together; the results will be plotted in concise form as contour diagrams. The discs of resin used in Experiment I, which were cured at 130°C proved unstable when measurements at temperatures near the and particularly about cure temperature were attempted. This point is taken up in the Discussion (section F). The full results are, therefore, not given for these discs; only values at a frequency of 1.05 kc/s will be tabulated for the sake of the Discussion.

E.3.b.1. Dielectric Results in Tabular Form. (see end of Note printed separately under this title).

Notes on dielectric results:

(1) In all four experiments (Experiment III, IV, V and VI) the effect of leaving a disc of the resin at a temperature greater than 100° was a lowering of the value of the dielectric constant ϵ without any significant change in tan δ values. The same effect occurred when when discs were heated to temperatures above 100°, cooled and then reheated. In making dielectric measurements the discs had to be left at elevated temperatures for appreciable times (some hours) and since the measurements extended over a period of days the discs were usually cooled and left at room temperature overnight.

The effect can be seen in Experiment III in the region of 160°C, in Experiment IV at all temperatures above 100°C, in Experiment V at all temperatures above 100°C and particularly around 160°C, and in Experiment VI in the region of 160°C. In Experiment IV and V, the effect was such that the normal rise with temperature of ϵ, which should have accompanied the rapid rise with temperature of tan δ was not noted except at the lowest frequencies.

There appeared no way of obviating this effect which was characteristic of the resin. The result is that values of ϵ at the higher temperatures are not simply related to those at lower temperatures and in fact may not have any quantitative significance.

(2) As will be shown fully in the Discussion (Section F) values of tan δ and ϵ at temperatures in the region of 220°C and above are time dependent. The reported values of tan δ and ϵ at these temperatures have only qualitative significance.

E.4: Degradation Products

E.4.a Experiment IV

The minute quantity of non-volatile degradation products collected in the first trap proved too small for analysis.

E.4.b. Experiment V

The methanolic solution of the non-volatile degradation products was evaporated to dryness and an infra-red spectrum taken (Fig. 40). This was badly resolved; a puzzling feature is the complete lack of absorption at frequencies below 900 cm^{-1}. Both effects may have been due to a fault in the spectrometer.

E.4.c. Experiment VI

The methanol from the methanolic solution of the non-volatile degradation products was evaporated off. The residue consisted of two distinct liquid phases, one yellow and viscous and the other mobile and cloudy white. The yellow phase (i) smelt strongly of phenol and gave a violet colouration with ferric chloride solution. On exposure to air the yellow phase darkened in colour to red. An infra-red spectrum was taken (Fig. 41) and this proved identical with the spectrum of phenol (Fig. 42), except for very minor differences. The yellow phase (i) therefore consisted of phenol with some small quantities of other substances.

The mobile white phase (ii) proved to be mainly water. A portion was extracted with carbon disulphide which was then evaporated. An infra-red spectrum of the residue (iii) was taken (Fig. 43). The spectrum showed strong absorption in the 3,400 cm^{-1} region which could have indicated O-H or N-H absorption or both; plus strong CH stretch absorption, evidence of aromatic C=C, and evidence of mono-substituted aromatic rings in the 850 to 650 cm^{-1} region. The spectrum showed some strong similarities to that of phenol. Phenol was almost certainly present.

Both the yellow phase (i) and the white phase (ii) were combined in a solution in methanol which was then dried over anhydrous sodium sulphate. This solution was evaporated to dryness. Two distinct residues appeared, one oily and dark brown (iv) and the other yellow and apparently crystalline, having a sharp, fishy smell (v). Infra-red spectra of (iv) (Fig. 44) and (v) (Fig. 45) were taken. The infra-red spectrum of (iv) was similar to that of (iii), and, similarly, (iv) was probably a mixture of phenol and other compounds.

The whole residue was dissolved in methanol and the solution passed through an alumina column in an effort to separate the coloured components of the mixture. Some separation was achieved into two bands, both yellow coloured. The solution corresponding to the two bands were collected and

evaporated to dryness. Infra-red spectra were taken of the residues. The infra-red spectrum of the first residue (vi) shown in Fig. 46 is similar to that in Fig. 45. The residue (vi) did not give a nitroso derivative. The infra-red spectrum of the second residue (vii) is shown in Fig. 47. The second residue (vi) appeared to give a nitroso-derivative though the test was not conclusive. It may, therefore, have been a primary or secondary amine.

During the chromatographic separation any colourless components were not detected, notably phenol.

In summary the existence of phenol in the degradation products was shown. Smaller quantities of other components, some of which may have been amines were present. The crude analyses made in this case served to indicate the line of approach used for the analysis of the non-volatile reaction products of Experiment VII.

E.4.d Experiment VII

In this experiment larger quantities of products were available for analysis. The methanolic solution of the non-volatile degradation products was distilled; the methanol distilled was retained for further examination. A yellow liquid residue resulted.

This residue was subjected to a chemical separation into acidic, basic and neutral components.

A: Acidic components

The yellow residue was treated with sodium hydroxide solution and then extracted with ether. The ethereal solution (i) which was yellow, was reserved for future separation.

The sodium hydroxide solution was acidified and a milky white suspension was produced. This was extracted with ether and the remaining clear water solution (ii) retained. The ethereal solution was dried over sodium sulphate (anhydrous) and the ether removed under reduced pressure to leave a pink mobile oil which had a phenolic smell. The oil gave a violet-blue colouration with ferric chloride solution. An infra-red spectrum of the oil was taken (Fig. 48) which was identical with that of phenol (Fig. 42). A p-toluene sulphonyl derivative was prepared from the oil. The melting point of the crude product was 91.5°C. An infra-red spectrum of this derivative (Fig. 49) was identical with that of the p-toluene sulphonyl derivative of phenol (Fig. 50).

The acidic component of the non-volatile degradation products probably consisted therefore of phenol.

B: Basic Components

The ethereal solution (i) from the separation of the acidic compound was treated with hydrochlorine acid to remove basic components. The hydrochloric acid turned a light yellow 'fluorescent' colour leaving a yellow ethereal solution (iii) which was retained. The acidic solution was rendered alkaline with sodium hydroxide to produce a white emulsion which was extracted with ether, the remaining aqueous layer being discarded. The ether was distilled off leaving a mobile brown liquid and a dark brown oil. Infra-red spectra of the mobile brown oil (Fig. 51) and the dark brown oil (Fig. 52) were taken.

These spectra indicated that a mono-substituted aromatic ring was present. A p-toluene sulphonyl derivative of the mobile brown oil was successfully prepared, the melting point of the crude product being 80°C. An infra-red spectrum of this derivative was taken (Fig. 53). This proved identical with the spectrum of the p-toluene sulphonyl derivative of N-methyl aniline (Fig. 54). This indicated that N-methyl aniline was certainly present and that no significant quantity of primary amine was present. There existed the possibility of the presence of some tertiary amine since these do not, in general, give p-toluene sulphonyl derivatives.

The spectra of the original residues of basic components (Figs. 51 and 52) were compared with the spectra of N-methyl amiline (Fig. 55) and N-N-dimethyl aniline (Fig. 56). Both spectra corresponded exactly to a mixture of N-methyl aniline and N-N dimethyl aniline. To confirm this the amines were dissolved in hydrochloric acid and sodium nitrate added The solution turned red. On rendering alkaline, the solution turned yellow and the colour could be extracted with ether. On evaporation of the ether a yellow oil together with crystals resulted. The presence of a tertiary amine was thus proved by the formation of a crystalline p-nitroso derivative. The yellow oil gave Liebermann's reaction proving that it was the nitroso derivative of a secondary amine.

The basic component of the non-volatile degradation products consisted of N-methyl aniline and N-N dimethyl aniline. Very much smaller quantities of other amines could have been present.

The colourless liquid which condensed in the glass lines during degradation proved to be these two amines.

C: Neutral Components

The ethereal solution (iii) from the separation of basic components was distilled. The ether distilled off leaving a trace of a brown oily residue with a slightly fish-glue smell. The residue was redissolved in ether, dried over anhydrous sodium sulphate and then freed of the solvent by distillation. An infra-red spectrum of the residue was taken (Fig. 57).

The spectrum indicated that aromatic rings were present which could have been mono-substituted, p-disubstituted or 1:2:4 trisubstituted (medium intensity bond at 880 cm^{-1}). The most interesting feature of the spectrum was very strong absorption at 1680 cm^{-1} which may have been due to a carbonyl group.

The residue was therefore extracted from the potassium bromide disc with ether. The ether was evaporated off and the residue dissolved in methanol. A solution of 2:4 dinitrophenyl hydrazine was added and a red precipitate was formed when the solution was diluted with water. This suspension was boiled to coaqulate the precipitate, the distillate (iv) being collected. The precipitate was washed with a 50:50 methanol hydrochloric acid solution to free it from excess 2:4 DNPH and, since the quantity was too small for a melting point determination an infra-red spectrum was taken, (Fig. 58).

The distillate (iv) was extracted with ether. The ether solution was dried over anhydrous sodium sulphate and evaporated to dryness. A trace of a yellow residue resulted whose infra-red spectrum is given in Fig. 59. This spectrum showed the existence of aromatic rings whose substitution was not clear. The peaks at 1680 cm^{-1} and 1540 cm^{-1} may have indicated a secondary amide. The peak at 1345 cm^{-1} would, if this were so, indicate that the nitrogen substituent was an aromatic ring. The quantity present, however, precluded any attempts at hydrolysis and subsequent analysis. The peak at 1680 cm^{-1} may, on the other hand, have indicated unsaturation.

D: The Original Methanol Distillate

The methanol distillate from the distillation of the original solution of the degradation products was redistilled leaving a mobile brown liquid when the methanol had distilled off. This was proved to consist mainly of phenol together with small quantities of secondary amine.

E:

The solution (ii) from the separation by acidification of the acidic component from solution in sodium hydroxide, was treated with a solution of 2:4 dinitro phenyl hydrazine. A red precipitate was formed which was coagulated, filtered, thoroughly washed and dried. Because of the small quantity available the determination of its melting point was not conclusive but the 2:4 dinitro phenyl hydrazone did not appear to melt below 280°C. An infra-red spectrum of the 2:4 dinitro phenyl hydrazone is shown in Fig. 60.

F: Tar

In Experiment VII large quantities of a very viscous red-brown coloured tan were found in the reaction vessel. The tar had a strong 'phenolic' smell. An infra-red spectrum of the tar is shown in Fig. 61. The spectrum shows some strong similarities to that of the original resin -

hydroxyl absorption at 3450 cm^{-1}, aromatic and aliphatic C-H stretch absorption, evidence of aromatic rings whose substitution patterns in the 900-650 cm^{-1} region are complicated, and evidence of aryl alkyl ether linkages.

The tar was separated into acidic, basic and neutral components in exactly the same way that was used for the non-volatile degradation products. Further analysis was not attempted in view of the probable diversity of tarry products.

An infra-red spectrum of the acidic component of the tar is given in Fig. 62. The spectrum shows strong hydroxyl absorption at 3400 cm^{-1}; aromatic and aliphatic C-H stretch: a peak at 1695 cm^{-1} which may show unsaturation; aromatic C=C absorption; phenolic absorption at 1370 cm^{-1}; evidence of ether linkages; substitution patterns in the 900-650 cm^{-1} region which may indicate mono substitution, p-disubstitution or 1:2:4 tri-substitution.

An infra-red spectrum of the basic component of the tar is given in Fig. 63. The spectrum shows amine absorption at 3400 cm^{-1}; strong aromatic and aliphatic C-H stretch absorption; p-disubstitution pattern at 1880 cm^{-1}; aromatic C=C absorption; some evidence of ether linkages; strong p-disubstitution absorption at 820 cm^{-1}; and some mono-substitution absorption at 750 and 690 cm^{-1}.

An infra-red spectrum of the neutral component of the tar is given in Fig. 64. The spectrum shows strong hydroxyl and/or amine absorption at 3400 cm^{-1} weak aromatic C-H absorption but strong aliphatic C-H absorption; a peak at 1700 cm^{-1} which may be due to unsaturation; C=C (aromatic) absorption; evidence of ether linkages; complicated absorption in the 900-650 cm^{-1} region; mono substitution is very weak if present.

E.4.e Volatile Products

An infra-red spectrum of the volatile products from the capsules (section D.5) from all the experiments after drying of the volatiles showed no absorption. A 10 cm. path length cell was used and it was estimated that some tens of millograms would have been detectable by this means. No volatile products other than perhaps water were therefore found in quantities of this order or greater.

E.4.f A summary of the products of degradation at 309°C is given below with estimates of the quantities:

Product	Quantity
Tar	very large quantities
Phenol	large quantities
N-methyl/aniline	smaller quantities
N:N-dimethyl/aniline	still smaller quantities
products with carbonyl groups together with traces of other products unidentified.	traces

It must be re-emphasised that water could not be detected and may well have been a degradation product. (Section F - Discussion).

During degradation at lower temperatures, no tar was found, large quantities of phenol were found together with smaller quantities of other products, in particular amines.

F: Discussion and Analysis of Results

The dielectric results of Experiments III, IV, V and VI are presented as contour plots of the real part, ϵ of the complex dielectric constant and the loss tangent, tan δ, as functions of frequency and temperature, in Figs. 32 to 39. The results for Experiment III are for a fully cured resin which has not been degraded. The term 'fully cured' will be considered in detail in Section F.2. The results for Experiments IV, V, VI are for increasingly degraded specimens.

The results for all four experiments show that in the frequency/temperature range considered the samples are characterised by two distinct dispersion regions, roughly speaking a low temperature region and a high temperature region.

The low temperature region, or β- region as it will be termed in this discussion, is broad and is characterised by relatively low values of tan δ. A plot of log f_{max} versus $\frac{1}{T}$ (where f_{max} is the frequency of maximum absorption and T is the absolute temperature) for the results of the undegraded sample is roughly a straight line and gives an apparent activation energy of some $16\frac{1}{2}$ k cals/mole. In Mikhaelov's terminology this value characterises the β-region as due to a dipole-radical type of loss as opposed to a dipole elastic type of loss. On this basis the loss is therefore probably due to the movement of a dipole essentially independently of the main chain and this is consistent with the temperature/frequency range in which the loss occurs.

Cole-Cole plots of the locus of the complex dielectric constant $\epsilon = \epsilon' - j\epsilon''$ in the complex plane for the sample of Experiment III at temperatures of - 50°C, 0°C, and 50°C are shown in Figs. 65, 66 and 67 respectively. It is at once clear that the absorption is not an ideal Debye-type absorption. While the locus of the complex dielectric constant at temperatures of 0°C and 50°C might conceivably be a circular arc in the experimental range covered, that at - 50°C is very clearly not since it appears to be concave upwards. It is therefore likely that, if the full frequency range were available, the locus of the complex dielectric constant would not be a circular arc, or even a skewed arc. Since the theories so far developed have only been for these cases, further theoretical analysis is impossible. It is likely, however, that the process giving rise to this dispersion region is a complicated one. In view of this, the apparent activation energy for the process quoted earlier is of dubious significance.

There is a hint in the results that the loss peak is a result of two overlapping loss peaks. This is clear in Fig. 68 which shows tan δ as a function of temperature at a frequency of 1.05 kc/s for Experiments III, IV, V and VI. This is most obvious in Experiment V which concerned a degraded sample, however, but is also discernible in the result of Experiment III. This may imply that at least two processes are operative in giving rise to the loss.

From a consideration of the chemical structure of the cured resin (Section F.2) it is clear that the only dipolar group which could be responsible for the β loss region is the hydroxyl group. As far as the resin network is concerned, these groups are the only pendant dipolar groups which could be responsible for a dipole-radical type of loss; the movement of any other dipole in the network structure would necessarily involve a change in the configuration of the network involving a dipole-elastic type of loss. There are other dipolar groups present in the fully cured system which could give rise to dipole-radical type losses. These include residual epoxide and amine groups and impurities in the original resin such as

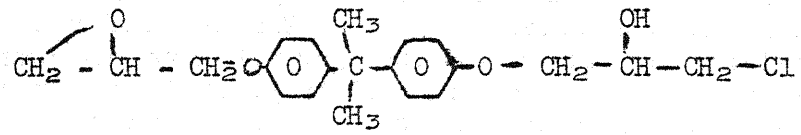

which, being only mono functional, would constitute a dipolar pendant group capable of movement independently of the main network. The concentration of any of these groups is, however, so small that their contribution to the dielectric properties is not likely to be measurable.

Fig. 69 shows the results of measurements of tan δ as a function of temperature at a frequency of 1.05 kc/s for the resin disc of Experiment I. This disc had only received a preliminary cure at a temperature of 130°C. For reasons given in Section F.2, it was clear that the disc was by no means fully cured. In Figs. 68 and 69 it is clear that as the discs were more fully cured so the maximum value of tan δ in the β loss region increased, the greatest value being recorded for the disc of Experiment IV which had in fact been cured up to a temperature such that some slight degradation had occurred. For increasingly degraded specimens in Experiments V and VI the maximum value of tan δ in the β loss region decreased. It is known from the work of Lee[20] on the degradation of a commercial low molecular weight commercial resin cured with p-p′ diamino diphenyl methane that water is one of the main products that this is produced by a dehydration reaction involving the hydroxyl group. Although it would be unreasonable to postulate that the concentration of hydroxyl groups in the resin is the only factor controlling the extent of the absorption, the results of this investigation showed clearly a direct relation between the concentration of hydroxyl groups, which increases with increasing cure and decreases with increasing degradation, and the maximum value of tan δ in the β loss region. This was taken as further evidence

that the hydroxyl groups were responsible for the loss.

Work by Dannenburg[10] on the spectra in the near infra-red of epoxide resins during cure with amine hardener showed that the hydroxyl groups in the cured resin can be hydrogen bonded. A consideration of the possible configurations of the unit

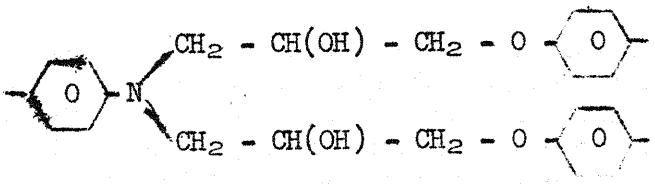

showed that mutual hydrogen bonding between the two hydroxyl groups is possible; hydrogen bonding of the hydrogen of one hydroxyl group with both the ether oxygen and the nitrogen are also possible. In addition to these possibilities, hydrogen bonding between the hydroxyl hydrogen and oxygen and even nitrogen atoms of neighbouring chains is possible. The characteristics of orientation of the hydroxyl group in an electric field are governed by the change in energy accompanying the orientation which in turn depends upon the forces involved. The many different possibilities for hydrogen bonding of the one hydroxyl group are probably responsible for the broadness and the non-ideality of the β loss region. The underlying property is the random nature of the resin structure which is one of its chief characteristics.

The high temperature region or α loss region has two main characteristics. The first is that in the temperature range covered no local maximum or peak in values of tan δ was found. It was shown that degradation, as measured by weight loss, occurred at temperatures above 240°C approximately so measurements were not continued much above this temperature. The second was that very high values of tan δ, approaching 1, were recorded in this temperature range. It should be noted that the assumptions implicit in the reduction of the dielectric properties to a statement of ϵ and tan δ as functions of frequency and temperature (in particular that of linear behaviour) are unlikely to be valid when such values of tan δ are found and, for this reason, the values of tan δ recorded are of qualitative significance.

The α dispersion region was associated with the resin network. Since no peaks in the values of tan δ were found it was not possible to characterise the region as due to dipole-elastic losses or an apparent activation energy approach. The reasons for characterising the α loss region as being a property of the network are reserved for Section F.3.

Kobale and Löbl[18] give the dielectric properties of a commercial epoxide resin cured with an anhydride hardener, tetrahydro phthallic anhydride. As in this investigation two distinct loss regions were found. The low temperature region was a broad region characterised by low maximum values of tan δ. An apparent activation enthalpy for the process was quoted as 11 k cals/mole, activiation entropies being too small

to measure. From a consideration of the chemical structure of the cured resin network Kobale and Löbl concluded that movement of the OH group was responsible for this loss region. In support of this they quote activation enthalpys for the movement of the OH dipole in Terylene and Ice. This is to be criticised. The forces involved in the highly cross linked random structure of the cured epoxide resin with all the attendant different possibilities of hydrogen bonding and differing steric barriers are likely to be very different from the forces involved in the linear partially crystalline Terylene and the perfectly ordered molecular crystal, Ice. The rough agreement of the values for the activation enthalpy for the movement of the OH dipole in these three solids is probably fortuitous and, in any event, is not sufficient evidence to identify the processes.

In contradiction to the results of this investigation, Kobale and Löbl found well defined peaks in the values of tan δ for the high temperature loss region, the maximum values of tan δ being in the region of 0.1. They showed clearly the relation of this region with the properties of the network and characterised the losses as dipole-elastic losses.

F.2 Cure

The chemical reactions involved in the curing of dge BPA with DDM are fairly simple and involve the reaction of epoxide groups with both the primary and secondary amine groups:

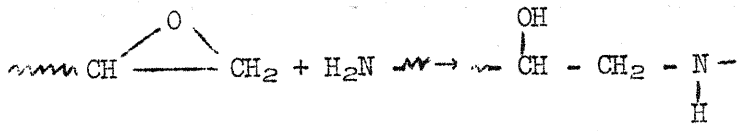

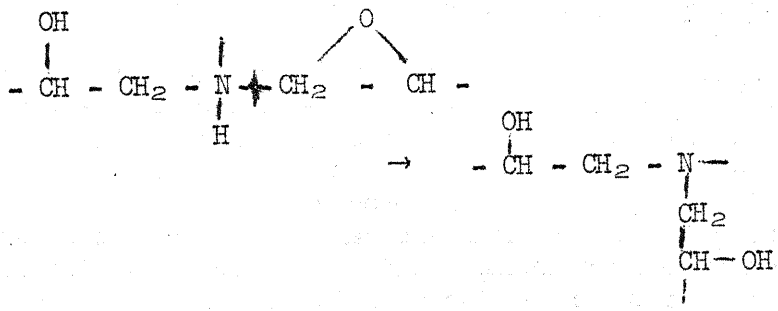

Work on model compounds by Shechter, Wynstra and Kurkjy[34] showed that etherification of the aliphatic hydroxyl by epoxide groups

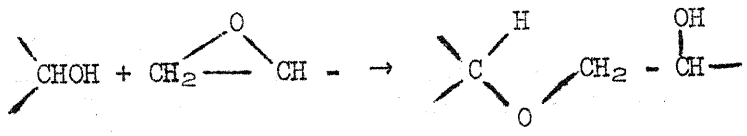

does not occur to any appreciable extent. This is supported by the fact

that optimum properties are obtained for this resin/hardener system when equi-equivalent amounts of hardener and epoxide resin, calculated on the basis of one epoxide group for every basic hydrogen present, are used.

As cure proceeds molecules with the structure

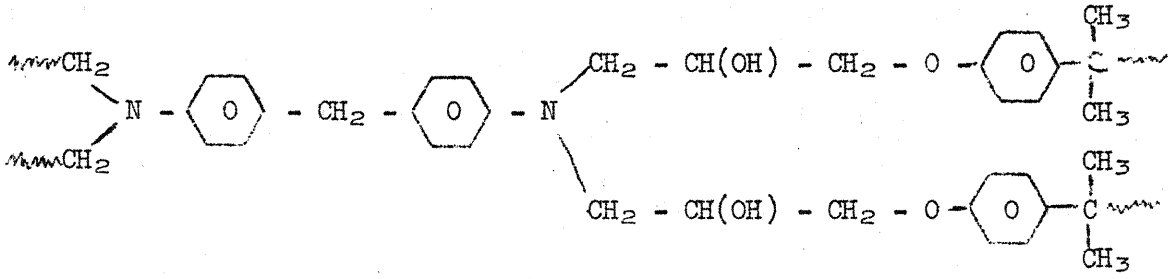

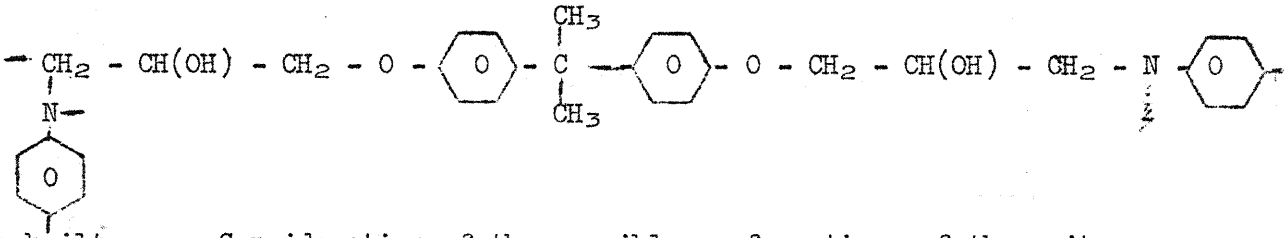

are built up. Consideration of the possible conformations of the unit

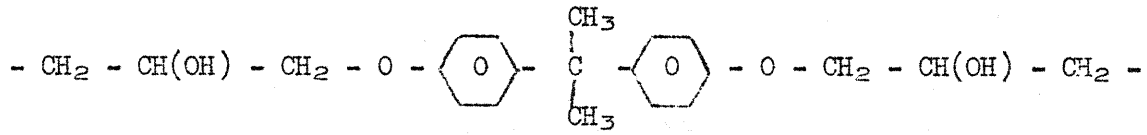

show that the number of pairs of these units joined by the same two nitrogen atoms is small and that a truly random structure is found.

At a certain stage, the gel point, a sharp increase in viscosity of the system marks the appearance of a large three-dimensional network molecule which forms a phase which is essentially distinct from the liquid phase which existed before and now co-exists and which consists of small molecules and small fragments of addition products. Molecular motion and hence chemical reaction are by no means halted; the cure process continues by reaction in the remaining liquid phase and by an increase in the size of the network and by an increase in the degree of cross linking of the network. Reaction is accompanied by a decrease in the amount of liquid phase present and an increase in the rigidity of the network.

The network may be characterised by its glass transition temperature which, for the purposes of this discussion, may be defined as the temperature below which segmented motion of the network is not possible. The word 'motion' implies the specification of frequency if an attempt is made to

measure this property. It is clear that as cure proceeds the role of cure reaction shifts from that of building onto the network to increasing the cross linking of the molecule so that in the later stages of cure, when the liquid phase has for all practical purposes disappeared, the latter is the only process. If cure is carried out isothermally there may come a time when the degree of cross linking and the amount of liquid phase present are such that the glass transition temperature of the network corresponds to the cure temperature.

At this stage cross-linking must practically cease, for this implies molecular motion and this is frozen in all but any remaining liquid phase. The results of Experiment I (Fig. 67) exemplify these predictions. The disc used in these measurements was cured finally at 130°C. The graph of tan δ/temperature shows a rise in values of tan δ as 130°C is approached but the expected peak at 130°C is not realised. The value of tan δ at 135°C is lower than would be expected and successive measurements at this temperature show a progressive decrease in tan δ. The temperature of measurement was raised to 160°C and then lowered. The results appear to indicate a peak in the region above 160°C.

These results are simply explained on the basis of the above predictions. The disc originally cured at 130°C cured up until the glass-transition temperature corresponded to the cure temperature. As the temperature of measurement approached 130°C a rise in tan δ was noted which signified the approach of a peak in tan δ characterising the glass transition. As the temperature was raised further, however, molecular motion became possible and the sample became unstable as further cure reactions occurred until the glass-transition temperature corresponded to the new cure temperature i.e. the temperature of measurement. Raising the temperature to 160°C provided the opportunity for further cure until the glass-transition temperature corresponded to this temperature. Subsequent measurements at temperatures below 160°C confirmed the apparent appearance of a peak characterising the glass transition temperature somewhere above 160°C.

Information in a technical bulletin by CIBA(ARL) Ltd.[6] on the properties of a low molecular weight epoxy resin cured with DDM confirms the correspondence of the deflection temperatures (which is related to the glass-transition temperature) and the cure temperature.

Information gained in Experiment I dictated the heat treatment of discs used in further experiments. The discs were given an initial cure at 95°C. Since the discs were to be post cured/degraded at temperatures above 240°C there appeared no point in post curing for any length of time at temperatures below these. A feature of the apparatus was that in the degradation vessel the final post-cure/degradation temperature was reached relatively slowly, allowing ample time for cure as the temperature increased. Increased cure implied an increase in the glass-transition temperature by increased cross linking, and hence increased cure temperatures were necessary to provide for molecular movement and hence reaction. All this was achieved

progressively in the degradation vessel. Oxidation, which becomes appreciable in air at 180°C, was precluded.

The sample which exists after cure at an elevated temperature consists mainly of a random three-dimensional network molecule extending throughout the sample. Ideally the sample would consist of nothing else. In fact it is obvious that when cure has reached a certain stage it may be impossible for two pendant unreacted groups (one epoxide, the other amine) to meet and react. To put it more succintly, the probability of co-ordinated segmented motions of the network which would allow previously separated pendant groups to approach closely and react is prohibitively small. In the 'fully-cured' resin, therefore, there must exist unreacted epoxide, primary and secondary amine groups and possibly very small numbers of unreacted dge-BPA and DDM molecules. The concentration of all these is very low. In addition to these impurities, molecules originally of the structure

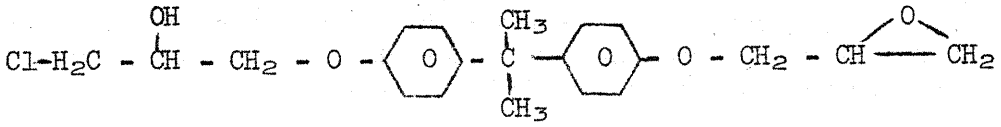

which were present in the dge-BPA will form pendant groups through reaction of the one epoxide group. Other trace impurities may be present.

F.3 Discussion of the α loss region.

The α loss regions recorded for the sample of Experiments III, IV, V and VI were regions in which sharp rises in both tan δ and ϵ were noted for rises in temperature. The maximum in the values of tan δ which is usually associated with a dispersion region was not noted. Measurements could not be extended to higher temperatures in an attempt to locate a peak since the temperatures were such that degradation occurred.

The temperature/frequency range of the α-loss region is such that it would be unlikely to be due to dipole-radical type losses even if there were a dipole available other than the hydroxyl group to provide for such a loss. It appears reasonable, therefore, that the loss is associated with movement of the network i.e., that it is due to relaxation of the network. This cannot provide the whole explanation of the results however, since a simple relaxation of the network should provide definite peaks in tan δ/temperature curves.

Weight loss measurements showed that degradation is appreciable at temperatures around 240°C. The identity of the main degradation products found in this investigation namely phenol, N-methyl aniline and N:N-dimethyl aniline, which all contain phenyl groups, is such that degradation must involve the resin network; further, it must involve a break down of the network by the scission of chemical bonds to produce these chemical species. Their production from unreacted amine or epoxide groups is not reasonable;

firstly, because of the extremely low concentration of these in a fully cured resin and, secondly, because the chemical nature of the phenol and N:N dimethyl aniline is not compatible with this origin. The production of separate small molecules from the network presupposes at least two scissions of chemical bonds in the network. These are unlikely to be simultaneous and so it appears established that appreciable scission of chemical bonds in the network occurs in the 240°C temperature range, some of which leads by further scission to the appearance of small molecules.

The possible fates of two free radical ends produced by the homoly scission of a chemical bond in the network are many. The most obvious and most likely is recombination to form the same chemical bond. For this reason it seems likely that appreciable scission occurs, only a small fraction of which leads to the production of small molecular weight products.

The 'free ends' produced by scission which exist in the resin at elevated temperatures must contribute to the dielectric properties if they are free to oscillate in the field. Providing the network is above its glass transition temperature such motion is possible. The abnormality of the α loss region is attributed to the existence of these free ends at the temperatures involved. That superposition of dielectric loss due to the motion of the free ends on top of the dielectric loss due to relaxation of the network provides for the measured very high values of tan δ is clear since, as the temperature of measurement is raised, so scission is a more likely event and the rate of production of free ends is increased. The instability of the samples at elevated temperatures is almost certainly due to the same effect.

At any particular temperature the rate of production of free ends by scission of network bonds is roughly constant. If their only fate was to recombine then eventually an equilibrium would be set up such that the concentration of free ends is constant. This may be the case at the lower end of this temperature region (210°C - 220°C). Any irreversible process such as stabilisation of the free radical by isomerisation by splitting off a smaller molecule, or by disproportionation, which follows scission means that the concentration of free ends may not be constant. This implies that the dielectric properties in this temperature region are a function of time. This is a further reason why the data on tan δ and ϵ for this temperature range are of qualitative significance only.

The results for the α loss region recorded in this investigation for an amine cured epoxide resin appear to contrast strongly with those recorded by Kobale and Löbl[18] for an anhydride cured epoxide resin. The α loss region in the latter investigation was shown clearly to be a relaxation phenomenon. The extra chemical stability of anhydride cured epoxide resins compared with amine cured resins is well known. In the case of an anhydride cured resin it appears that at the glass transition temperature no significant scission occurs. Alternatively, it is possible that we did not observe a full α

peak due to the fact that correct temperature and frequency conditions were not attained. In view of the wide range of temperatures and frequencies used this explanation of the observed phenomena seems less probable than that based on degradation of the network, which is further described below.

As increased cross linking of the resin increases the glass transition temperatures, so it would be expected that degradation of the resin network, which involves scission of chemical bands in the network, would decrease the glass transition temperature. The results of Experiments III, IV, V and VI confirm this (Fig. 68). The results for Experiments III and IV show rises in tan δ in the α loss region which almost lie on the same line. The disc in Experiment IV was post cured/degraded at higher temperatures than that in Experiment III. While the weight loss measurements of Experiment IV indicated that some degradation had occurred the maximum value of tan δ in the β loss region appeared to indicate that the disc was better cured than that in Experiment III. This is perfectly credible since degradation and cure reactions may occur simultaneously at a high enough temperature. The α loss regions for the discs in Experiment V and VI which were increasingly degraded specimens were shifted to lower temperatures as predicted.

As emphasised earlier the results for this temperature region must only be a qualitative guide to the properties of the discs. The time scale of the measurement of the dielectric properties was such that some degradation must have occurred during the measurement at the higher temperatures.

The prediction that the α loss region be shifted to lower temperatures on degradation, which implies scission of chemical bonds of the network, is not dependent on the assumption that the loss is due solely to relaxation phenomena since the nature of the free ends produced by scission is such that they are unlikely to be capable of relaxation independently of the network.

The important conclusion drawn from the data on the α loss region was that the degradation of the cured resin used in this investigation was by degradation of the resin network itself and did not concern simply the reactions of unreacted reactants as has been suggested by some workers (Neiman, Kovarskaya, Golubenkova, Strizhkova, Levantovskaya, and Akutin)[27].

The results also have a bearing on the practical uses of this resin/hardener system. It is clear that cure at a temperature of 240°C under conditions which prohibit oxidation will produce a sample which will retain good dielectric properties and, therefore, presumably good mechanical properties at temperatures up to 200°C, providing oxidation is inhibited.

F.4 The Chemistry of Degradation

The fact that degradation involves a breakdown of the resin network by scission of chemical bonds in the network has been discussed. It remains to discuss which chemical bonds in the network are most liable to rupture and how the main products found in this investigation - phenol, N-methyl aniline and N:N dimethyl aniline - may be produced. It would be presumptious, however, on the basis of the chemical evidence of this investigation and previous investigations to attempt to put forward a detailed reaction mechanism.

The resin network consists ideally of a molecule with the structure:

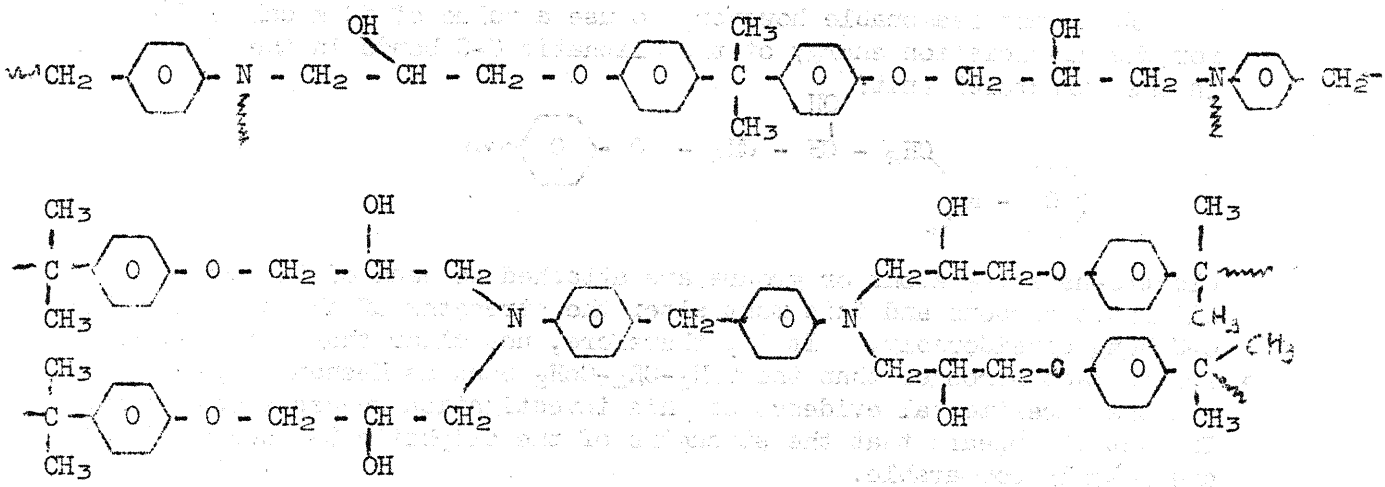

Keenan[17] has examined this structure theoretically and has come to the following conclusions:

1. The strongest chemical bands in the structure are the

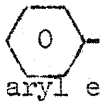 aryl ether and the 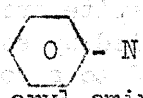 aryl amine bonds with the former the stronger of the two.

2. In order of decreasing bond strengths the remaining bonds were as follows:

$$C\text{-}H > C\text{-}O > H_2C\text{-}\phi > C\text{-}C > (CH_3)_2C\text{-}\phi > C\text{-}N$$

The appearance of phenol as the main degradation product with N-methyl aniline and N-N dimethyl aniline as the next most important degradation products would certainly seem to confirm the first conclusion. The second conclusion needs some qualification. Keenan used standard values of 80 k cals/mole for the C-C bond and 66 k cals/mole for the aliphatic C-N bond. The $H_2C\text{-}\phi$ bond was considered stronger than the aliphatic C-C bond because of hyperconjugation between the $-CH_2-$ group

and the benzene rings attached. Semenov[23] quotes a value of 76.5 k cals/mole for the dissociation:

$$C_6H_5CH_2C_6H_5 \rightarrow C_6H_5CH_2^{\bullet} + C_6H_5^{\bullet}$$

It is reasonable that the dissociation

$C_6H_5\,C(CH_3)_2\,C_6H_5 \rightarrow C_6H_5C^{\bullet}(CH_3)_2 + C_6H_5^{\bullet}$ would require less energy because of some strain caused by steric crowding with the bulkier methyl groups attached to the central carbon and since hyperconjugation is no longer possible.

It is not reasonable however, to use a value of 80 k cals/mole for the dissociation energy of the aliphatic C-C bonds in the structure. In the structural unit:

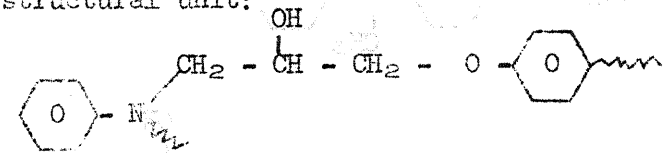

electro-negative atoms or groups are attached to each of the three aliphatic carbons and this must alter the strengths of the two aliphatic C-C bond considerably. It is, therefore, not clear that these bonds are in fact stronger than the C_6H_5-CH_2-CoH_5 bond as Keenan suggests and the experimental evidence of this investigation suggests otherwise. In fact it appears that the strengths of the aliphatic C-C and C-N bonds are roughly comparable.

If simple scission of chemical bonds were the only possible process of degradation it would be fairly simple, if the bond strengths were accurately known, to work out mechanisms of degradation. Degradation is, however, almost certainly complicated by a dehydration reaction involving hydroxyl groups and, despite precautions taken to rid the resin of entrapped air, may be accompanied by some oxidation. The discussion of the degradation will be limited to a consideration of the most likely shear points in the structure and of the role of the dehydration reaction in the degradation. Keenan[17] has given a detailed discussion of the role of oxidation in the degradation of this resin/hardener system.

The most likely scission points are the N-C, C-C and the $(CH_3)_2C$-ϕ bonds provided that the structure in the vicinity of these bonds has not been modified by other reactions. Scission of these bonds is probably responsible for the abnormal dielectric properties discussed earlier. Concurrent with pure thermal scission reaction is a dehydration reaction involving the hydroxyl groups. Lee's[20] results show that degradation of a low molecular weight commercial epoxide resin cured with p-p' diamino diphenyl methane at 350°C results in water as one of the main products. The dehydration reaction distorts the previous picture of bond strengths.

Dehydration involving the hydroxyl groups could occur in various ways. A study of the possible conformations of the element:

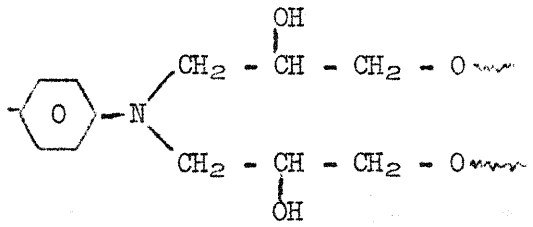

shows that the reaction:

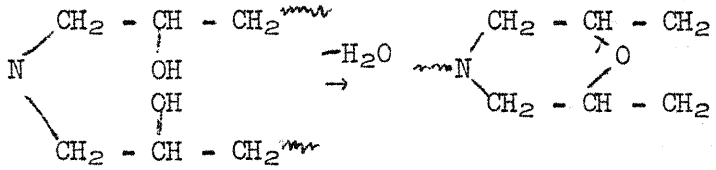

is possible. The morpholine type ring is not strained and the reaction is unlikely to be followed by further reaction. Dehydration may alternatively involve hydrogen atoms on carbons adjacent to that with the hydroxyl group:

Either

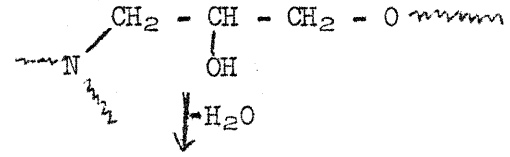

or

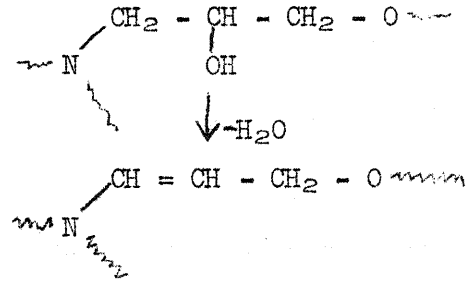

Dehydration to produce a cis-substituted double bond adjacent to the nitrogen atom

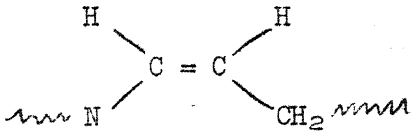

results in a very strained system because of steric obstruction and is an

unlikely process. Dehydration to produce a cis-substituted double bond adjacent to the oxygen atom

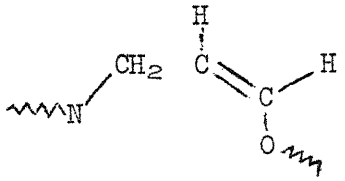

results in a less strained structure. Dehydration to produce unstrained trans-substituted double bonds are more likely.

Keenan[17] suggested that the double bonds produced by dehydration in this way may be delocalised:

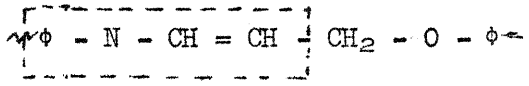

and

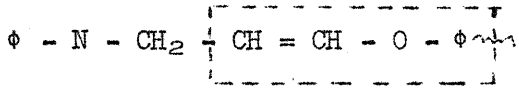

Such delocalisation results in a strengthening of the single bonds involved and a relative weakening of bonds not involved.

The production of phenol may be explained on this basis: scission of the weak $C(CH_3)_2C-\phi$ bond may occur:

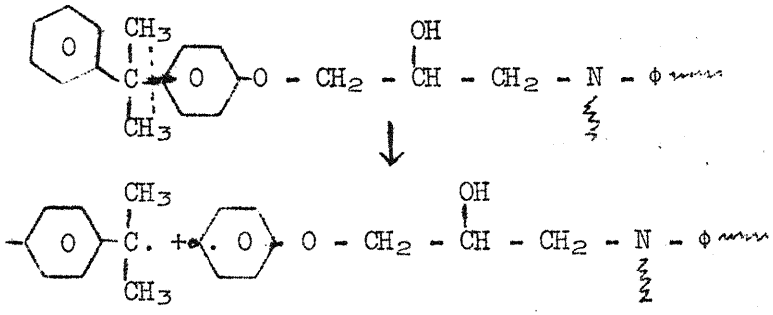

The free radical 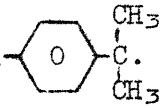 is resonance stabilised. The other radical may abstract hydrogen to produce:

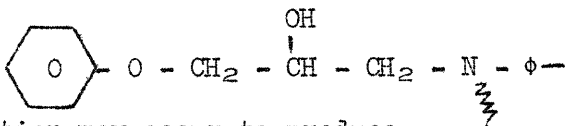

Dehydration may occur to produce

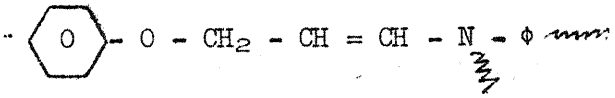

followed by scission of the now relatively weak CH_2-O bond to produce:

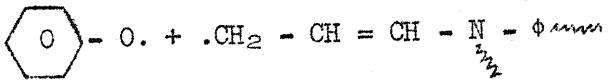

The radical  may abstract hydrogen to produce phenol. The remaining radical is likely to be stabilised by resonance.

N-methyl aniline must be produced by three different scissions:

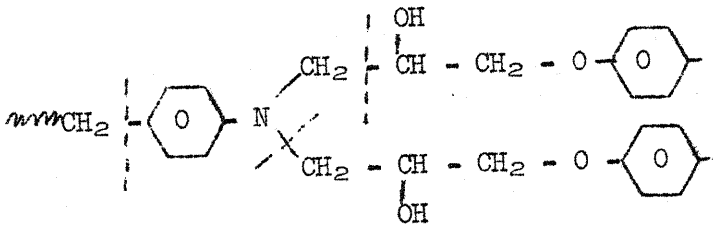

Both the C-C and the C-N bonds involved appear to be weak bonds and it is not clear in which order scission occurs and whether or not dehydration is involved. Nor is it clear whether the radical produced by one scission is stabilised by hydrogen abstraction before a further scission takes place.

N:N dimethyl aniline must also be produced by three different scissions:

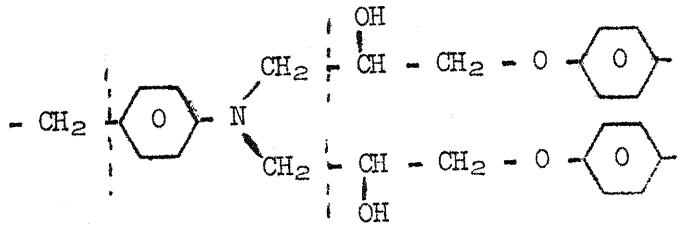

The fact that the primary amine, aniline, was not detected may indicate that the aliphatic C-C bonds are in fact weaker than the aliphatic C-N bonds. If this is the case then the fact that more of the monomethyl substituted amine was produced may indicate that dehydration precedes scission of the C-N bond:

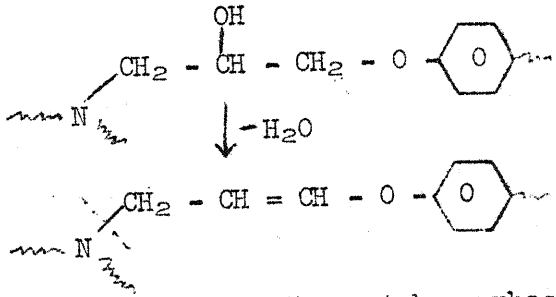

This is conjectural. It must be emphasised that before a detailed reaction

mechanism may be put forward with any confidence, a thorough quantitative kinetic study of the degradation must be made. This requires a positive and complete identification of every reaction product and its quantitative analysis as a function of time under varying experimental conditions.

The large quantities of tar formed during degradation at 309°C appeared to consist of large molecular fragments where structure was little changed from that of the cured resin. This is consistent with the idea that scission of chemical bonds in the network takes place during degradation.

The essential difference between the tar and the low molecular weight products lies in their mode of formation. The tarry products are presumably formed by unrelated random scissions of chemical bonds in the network to produce large molecular fragments of varying size and complexity. Low molecular weight products are produced by scission of chemical bands in the network followed by further specific reactions of the free ends so formed which must occur in an effect to stabilise the free ends. This is fairly clear for phenol production but it is not so obvious for the production of the N-methyl/substituted aniline. The amount of these amines produced, however, precludes their formation by the random scission of the chemical bands involved. Work with tagged atoms would prove invaluable in elucidating these mechanisms if the synthesis of hardeners with the basic hydrogen tagged proved practicable.

F.5 Summary

This work has emphasised the need to consider the physical state of the cured resin during degradation as well as the chemical processes involved. Much work in this field[20][21][24][25][27] has been devoted to the degradation of uncured epoxide resins and the results of this work have been applied with apparently little concern to the discussion of the degradation of cured epoxide resins. It should be clear that the uncured resin degrades, at least initially, in the liquid or even vapour state and that reaction must therefore occur by collision of molecules. This is a very different case to the degradation of a three-dimensional network molecule whose degradation involves scission of chemical bonds. In the same way, work on model compounds, while perhaps providing some data on the strengths of chemical bonds, cannot be applied directly to give any understanding of the degradation processes which occur in a cured resin since degradation of model compounds again occurs in the liquid or vapour phase.

The work has also shown that reactions of residual reactant molecules in the cured resin do not contribute materially to the degradation of the cured system studied. For this reason, too, it is unreasonable to attempt to use results for the degradation of uncured epoxide resins to understand the degradation processes which occur in a cured epoxide resin.

Classical chemical methods were used to analyse some of the products

of degradation, backed up by infra-red analysis. Sophisticated analytical techniques such as gas chromatography and mass spectrometry by themselves, seldom give unambiguous results. As mentioned in the Introduction, the use of gas chromatography to study the degradation of epoxide resins[17][19][20][36] has often resulted in the employment of unreasonably high degradation temperatures. In the interests of simplicity it appears important to study the degradation at as low temperatures as possible. Furthermore, it appears important to study all the products of the degradation. Neimann et al.[24][25][26][27] have concentrated almost exclusively on the gaseous products of degradation which form only some few percent of the reaction products and base their degradation scheme on these results only. This appears unreasonable. The work of Lee[19][20] and the results of this investigation emphasise the importance of phenol as a reaction product. Lee did not, however, detect any amines which is surprising in the light of the present results.

This work may be extended in several directions. Firstly, it would be interesting to study the time dependence of the dielectric properties at high temperatures of the resin/hardener system used in this investigation. Secondly, a study of the dielectric properties of cured resins made from epoxide resins and hardeners with different but related chemical structures, may permit confirmation that dielectric loss at high temperatures may be due to movement of free ends produced by scission as well as relaxation of the network and would allow a systematic study of the relationship between the chemical structure and the rigidity of the network. Thirdly, a thorough quantitative kinetic study of the low temperature degradation of a cured epoxide resin system, involving the quantitative determination of the concentrations of all products formed as a function of time under various experimental conditions, is necessary before a reaction scheme for the degradation may be proposed in any detail and with any confidence. The last two items present formidable experimental programmes.

F.6 Conclusion

1. The dielectric properties of fully cured and increasingly degraded samples prepared from equi-equivalent proportions of the diglycidyl ether of bisphenol A and p-p' diaminodiphenyl methane have been studied in the frequency range 210 c/s to 90 kc/s and the temperature range - 200°C to 250°C.

2. The main condensible product of the degradation was phenol, N-methyl aniline and N:N dimethyl aniline were found in small quantities. Very much smaller quantities of other products were formed containing amine, carbonyl and other groupings. At 309°C large quantities of tar were formed. Water could not be detected through a weakness in the apparatus but was probably a major product. No other gaseous products were detected.

3. The dielectric and anlytical results suggest that degradation proceeds by scission of chemical bonds in the network.

4. Suggestions have been made for the extension of this work.

Section G: References

1. Anderson, H.C. — Polymer, 2, p. 451, (1961).
2. Anderson, H.C. — Kolloid-Z, 184, p.26, (1961).
3. Anderson, H.C. — J. Appl. Polym. Sci., 6, p. 484, (1962)
4. Bellamy, L.J. — 'Infra-red spectra of complex molecules' Methuen (1964).
5. Bishop, D.P., and Smith, D.A. — Unpublished review on epoxide degradation.
6. — Ciba Technical Bulletin. 'Araldite MY750 and MY750 with hardener HT972' January, 1964.
7. Cole, R.H. — 'Theories of dielectric polarisation and relaxation'. Progress in Dielectrics, Vol. III, (1961). Heywood, London.
8. Conley, R.T. — S.P.E. Baltimore - Regional Tech. Corp. (1964). Preprints, p. 118, (1964).
9. Curtis, A.J. — 'Dielectric properties of polymeric systems'. Progress in Dielectrics, Vol. II (1960) Heywood, London.
10. Dannenburg, H. — S.P.E. Trans., Jan. (1963), p. 78.
11. Dannenburg, H., and Harp, W.R. — An. Chem. 28, p. 86, (1956)
12. Dante, M.F., and Conley, R.T. — Amer. Chem. Soc., Div. of Org. Coatings and Plastics Chem. Chicago Meeting, 24, No. 2, p. 135. Aug-Sept. 1964.
13. Dasgupta, S., and Mital, P.K. — J. Appl. Polym. Sci., 8, p. 2299, (1964).
14. Feazel, C.E., and Verchot, E.A. — J. Polym. Sci., 25, p. 351, (1957).
15. Havan, E.N., Gringras, H., and Katz, D. — J. Appl. Polym. Sci., 9, p. 3305, (1965).
16. Henbest, H.B., Meakins, G.D. Nicholls, B., and Taylor, K.J. — J. Chem. Soc. (1957). p. 1459.

17. Keenan, M.A. — 'Some aspects of the degradation of an epoxide compound by the flash filament technique'. Thesis, College of Aeronautics, Cranfield, Bedford, England. May, 1966.

18. Kobale, M.von and Löbl, H. — Z. fur Eletrochemie, 65, p. 662, (1962).

19. Lee, H., and Neville, K. — 'Epoxy resins'. McGraw Hill, (1957).

20. Lee, L.H. — J. Polym. Sci., 3, p. 859 (1965).

21. Lee, L.H. — J. Appl. Polym. Sci., 9, p. 1981, (1965).

22. Meakins, R.J. — 'Mechanisms of dielectric absorption in solids'. Progress in Dielectrics, Vol. II (1961). Heywood, London.

23. Mikhaelov, G.P., and Borisova, T.I.B. — 'The dielectric investigation of molecular relaxation in polymers' Russian Chem. Rev., 30, No. 7, 386, (1961).

24. Moiseev, V.D., Neiman, M.B., Kovarskaya, B.M., Zenova, I.E., and Guryanova, V.V. — Soviet Plastics, 6, p. 12, (1962).

25. Neiman, M.B., Golubenkova, L.I., Kovarskaya, B.M., Strizhkova, A.S., Levantovskaya, I.I., Akutin, M.S., and Moiseev, V.D. — Vysokomol. Soed., 1, p. 1531, (1959).

26. Neiman, M.B., Kovarskaya, B.M., Yazvikova, M., Sidnev, A., and Akutin, M.S. — Vysokomol. Soed., 3, p. 602, (1961).

27. Neiman, M.B., Kovarskaya, B.M., Golubenkova, L.I., Strizhkova, A.S., Levantovskaya, I.I., and Akutin, M.S. — J. Polym. Sci., 56, p. 383, (1962).

28. O'Neill, L.A., and Cole, C.P. — J. Appl. Chem., 6, p. 356, (1956).

29. Park, W.R.R., and Blount, J. — American Chem. Soc., Div. of Org. Coatings, Plastics, and Pv. Inks. 16, No. 2, p. 56, (1956).

30. Patterson, W.A. — An. Chem., 26, p. 823, (1954).

31. Pearman, D.E., Tolberg, W., and Floyd, D.E. — Ind. Eng. Chem., 49, No. 7, p. 1091, (1957).

32. Reddish, W. — The Off. Jnl of the Int. Union of Pure and Appl. Chem., 5, p. 723, (1962).

33. Semenov, N.N. — 'Some problems of chemical kinetics and reactivity'. Vol. I, Pergammon Press, 1958.

34. Shechter, L., Wynstra, J. and Kurkjy, R.P. — Ind. Eng. Chem., 48, p. 94, (1956).

35. Smith, I.T. — Polymer, 2, p. 95, (1961).

36. Stuart, J.M., and Smith, D.A. — J. Appl. Polym. Sci., 9, p. 3195, (1965).

37. Sugita, T., and Ito, M. — J. Chem. Soc., Japan 38, p. 1620, (1965).

38. Wyllie, G. — 'Theory of polarisation and absorption in dielectrics'. Progress in Dielectrics, II, (1960). Heywood, London.

Dielectric Results

E.3.b.1.

Frequency: 1.05 kc/s.

Temperature (°C)	tan δ (X 10^{-2})	ε
-178	0.10	1.27
-157	0.15	1.29
-137	0.25	1.30
-123	0.30	1.31
-105	0.35	1.33
- 92½	0.45	1.33
- 86	0.45	1.36
- 76½	0.55	1.36
- 72	0.55	1.38
- 56½	0.65	1.40
- 47½	0.80	1.42
- 37½	0.95	1.44
- 32	1.05	1.45
- 27½	1.10	1.46
- 25½	1.05	1.47
- 23½	1.10	1.47
- 20	1.15	1.48
- 17	1.15	1.49
- 15½	1.15	1.49
- 9½	1.10	1.51
1½	0.90	1.50
7½	0.80	1.53
25	0.55	1.57
37½	0.35	1.59
58½	0.20	1.58
67	0.10	1.67
88	0.15	1.63
105	0.20	1.66
116	0.50	1.71
132	0.40	1.83
134	0.25	2.26
135	0.10	2.28
135	0.50	1.89
141	0.10	2.32
149	0.15	2.46
160	0.35	2.54

E.3.b.2

Frequency: 90 kc/s.

Temperature (°C)	tan δ (X 10^{-2})	ε
-171	0.15	1.94
-155	0.25	1.97
-141	0.30	1.99
-131	0.35	2.02
-121	0.40	2.04
-111	0.50	2.06
-100	0.55	2.09
- 91	0.75	2.12
- 81	0.90	2.16
- 70	1.00	2.19
- 59	1.05	2.23
- 52	1.15	2.24
- 49½	1.15	2.26
- 46	1.20	2.26
- 43	1.25	2.29
- 39½	1.35	2.30
- 35½	1.40	2.33
- 31	1.45	2.34
- 28½	1.50	2.36
- 25	1.60	2.37
- 21	1.65	2.39
- 18½	1.70	2.41
- 14½	1.75	2.42
- 10	1.85	2.45
- 4½	1.95	2.47
6	2.10	2.53
12½	2.25	2.56
20	2.30	2.60
25	2.40	2.64
32	2.40	2.68
42½	2.30	2.74
65	1.85	2.85
83	1.35	2.94
97	0.95	3.00
118	0.40	3.10
132	0.30	3.21
143	0.25	3.19
152	0.20	3.22
161	0.20	3.28
162	0.25	3.25
173	0.25	3.33
178	0.35	3.48
184	0.50	3.53
194	0.85	3.63
204	1.25	3.84
217	1.80	4.21
230	2.30	4.48
245	3.15	4.47

Frequency: 22 kc/s

Temperature (°C)	tan δ (X 10^{-2})	ε
-169	0.25	1.95
-152	0.30	1.98
-140	0.35	2.00
-129	0.45	2.03
-118	0.50	2.05
-109	0.60	2.08
- 98	0.65	2.11
- 89	0.75	2.15
- 79	0.85	2.18
- 69	0.95	2.22
- 57	1.05	2.25
- 50½	1.10	2.26
- 48	1.15	2.29
- 45½	1.15	2.29
- 42	1.20	2.32
- 38½	1.30	2.33
- 34½	1.35	2.36
- 30½	1.55	2.37
- 27½	1.60	2.40
- 24½	1.65	2.41
- 20½	1.75	2.43
- 18	1.75	2.45
- 14	1.85	2.46
- 9½	1.85	2.49
- 3½	2.05	2.52
6	2.10	2.58
12½	2.20	2.61
20	2.15	2.66
25	2.15	2.70
32	2.05	2.74
42½	1.85	2.80
65	1.10	2.88
83	0.70	2.96
97	0.45	3.02
118	0.25	3.12
132	0.20	3.22
143	0.20	3.20
151	0.15	3.22
161	0.20	3.29
162	0.25	3.26
173	0.25	3.34
178	0.50	3.49
184	0.65	3.55
194	1.00	3.67
205	1.75	3.90
217	2.60	4.32
230	4.31	4.57
245	7.67	4.60

Frequency: 46 kc/s

Temperature (°C)	tan δ (X 10^{-2})	ε
-169	0.20	1.95
-154	0.25	1.97
-141	0.35	2.00
-130	0.45	2.02
-119	0.50	2.05
-110	0.60	2.07
- 99	0.65	2.10
- 90	0.75	2.13
- 80	0.85	2.17
- 69	1.00	2.20
- 58	1.05	2.24
- 51	1.10	2.25
- 49	1.15	2.28
- 45½	1.20	2.28
- 42½	1.25	2.31
- 39	1.30	2.31
- 35	1.35	2.34
- 31	1.45	2.36
- 28	1.45	2.38
- 24½	1.55	2.39
- 20½	1.60	2.41
- 18½	1.65	2.43
- 14½	1.75	2.44
- 10	1.80	2.47
- 4	1.90	2.49
6	2.10	2.53
12½	2.15	2.58
20	2.20	2.63
25	2.20	2.67
32	2.15	2.71
42½	2.05	2.77
65	1.45	2.86
83	1.00	2.95
97	0.65	3.01
118	0.40	3.10
132	0.20	3.21
143	0.20	3.20
152	0.20	3.22
161	0.20	3.28
162	0.20	3.26
173	0.25	3.34
178	0.45	3.49
184	0.60	3.54
194	0.90	3.65
205	1.40	3.87
217	2.00	4.27
230	2.95	4.52
245	4.75	4.51

Frequency: 10.5 kc/s			Frequency: 4.8 kc/s		
Temperature (°C)	tan δ (X 10^{-2})	ε	Temperature (°C)	tan δ (X 10^{-2})	ε
-168	0.25	1.95	-167	0.25	1.96
-151	0.30	1.98	-150	0.35	1.99
-139	0.40	2.01	-138	0.40	2.01
-128	0.40	2.03	-127	0.45	2.04
-118	0.50	2.05	-117	0.50	2.06
-108	0.60	2.09	-107	0.60	2.10
- 97	0.65	2.12	- 97	0.70	2.13
- 89	0.80	2.16	- 88	0.80	2.16
- 79	0.85	2.19	- 78	0.85	2.20
- 68	1.00	2.23	- 67	1.00	2.24
- 57	1.05	2.27	- 56	1.15	2.28
- 50½	1.15	2.28	- 50	1.25	2.29
- 48	1.20	2.31	- 47½	1.25	2.32
- 45	1.25	2.31	- 45	1.30	2.32
- 41½	1.25	2.34	- 41½	1.35	2.36
- 38½	1.35	2.35	- 38	1.40	2.36
- 34	1.40	2.38	- 34	1.50	2.39
- 30	1.50	2.39	- 29½	1.60	2.41
- 27	1.55	2.42	- 27	1.60	2.44
- 24	1.65	2.43	- 24	1.75	2.45
- 20	1.70	2.45	- 20	1.80	2.48
- 18	1.70	2.47	- 18	1.75	2.49
- 14	1.85	2.48	- 14	1.90	2.51
- 9½	1.85	2.52	- 9½	1.90	2.54
- 3	2.00	2.54	- 2½	2.00	2.57
5½	2.00	2.60	5½	1.95	2.63
12½	2.05	2.64	12½	1.90	2.66
20	1.95	2.69	20	1.80	2.71
25	1.90	2.73	25	1.65	2.75
32	1.70	2.77	32	1.45	2.79
42½	1.45	2.82	42½	1.20	2.84
65	0.90	2.90	65	0.65	2.90
83	0.50	2.96	83	0.35	2.97
97	0.30	3.02	97	0.25	3.02
118	0.20	3.12	118	0.15	3.12
132	0.15	3.22	132	0.15	3.22
143	0.20	3.20	143	0.15	3.20
151	0.15	3.22	151	0.15	3.22
161	0.20	3.29	161	0.20	3.29
161	0.20	3.28	162	0.30	3.27
162	0.25	3.27	173	0.35	3.35
173	0.30	3.34	178	0.60	3.51
178	0.55	3.50	184	0.90	3.58
184	0.75	3.57	194	1.60	3.72
194	1.20	3.69	206	2.85	3.98
206	2.20	3.93	217	5.30	4.45
217	3.55	4.38	230	11.70	4.93
230	7.30	4.66	245	21.85	5.10
245	13.10	4.78			

Frequency: 1.05 kc/s

Temperature (°C)	tan δ (X 10^{-2})	ε
-164	0.25	1.97
-148	0.30	2.00
-136	0.40	2.03
-125	0.45	2.05
-116	0.55	2.08
-105	0.60	2.12
- 95	0.65	2.15
- 86	0.80	2.19
- 77	0.85	2.23
- 66	1.05	2.27
- 53	1.20	2.32
- 49	1.25	2.33
- 46½	1.35	2.36
- 44	1.40	2.36
- 40½	1.40	2.39
- 37½	1.55	2.40
- 33	1.55	2.44
- 29	1.70	2.46
- 26½	1.75	2.48
- 23½	1.80	2.50
- 19	1.80	2.52
- 17½	1.80	2.54
- 13	1.85	2.56
- 9	1.75	2.59
- 2	1.75	2.63
5	1.55	2.67
12½	1.45	2.71
20	1.20	2.76
25	1.15	2.79
32½	0.95	2.82
43	0.75	2.86
65	0.35	2.91
83	0.20	2.98
97	0.15	3.03
118	0.10	3.13
132	0.15	3.23
143	0.15	3.21
151	0.15	3.22
161	0.25	3.30
161	0.25	3.29
162	0.40	3.27
173	0.50	3.36
178	1.05	3.54
184	1.70	3.62
194	3.15	3.79
207	5.70	4.15
217	12.40	4.79
230	32.70	5.67
245	69.25	7.96

Frequency: 2.4 kc/s

Temperature (°C)	tan δ (X 10^{-2})	ε
-166	0.25	1.96
-149	0.30	1.99
-137	0.35	2.02
-126	0.45	2.05
-117	0.50	2.07
-107	0.60	2.11
- 96	0.70	2.14
- 87	0.80	2.17
- 78	0.85	2.21
- 66	1.00	2.25
- 53	1.10	2.30
- 49½	1.15	2.31
- 47	1.25	2.34
- 44½	1.25	2.34
- 41	1.30	2.37
- 38	1.40	2.38
- 33½	1.50	2.41
- 29½	1.70	2.43
- 26½	1.60	2.46
- 23½	1.80	2.47
- 19½	1.90	2.50
- 17½	1.90	2.51
- 13½	1.95	2.53
- 9½	1.88	2.57
- 2	1.95	2.60
+ 5½	1.85	2.64
12½	1.80	2.69
20	1.50	2.73
25	1.35	2.78
32	1.15	2.81
43	0.95	2.85
65	0.45	2.91
83	0.25	2.97
97	0.20	3.03
118	0.10	3.13
132	0.10	3.23
143	0.15	3.20
151	0.15	3.22
161	0.20	3.29
161	0.25	3.29
162	0.30	3.27
173	0.40	3.35
178	0.75	3.52
184	1.15	3.59
194	2.15	3.74
207	4.00	4.04
217	7.85	4.57
230	19.85	5.10
245	54.30	5.77

Frequency: 445 c/s			Frequency 210 c/s		
Temperature (°C)	tan δ (X 10^{-2})	ε	Temperature (°C)	tan δ (X 10^{-2})	ε
-162	0.30	1.97	-159	0.25	1.98
-147	0.40	2.01	-146	0.35	2.02
-135	0.40	2.03	-133	0.40	2.04
-125	0.55	2.06	-124	0.55	2.07
-115	0.60	2.09	-115	0.60	2.10
-104	0.60	2.12	-103	0.60	2.13
- 95	0.75	2.16	- 94	0.90	2.17
- 85	0.80	2.20	- 85	0.90	2.22
- 77	0.95	2.24	- 76	0.95	2.25
- 65	1.06	2.28	- 65	1.25	2.30
- 53	1.30	2.34	- 52	1.45	2.36
- 48½	1.40	2.35	- 48	1.55	2.36
- 46½	1.30	2.38	- 46	1.55	2.39
- 43½	1.45	2.38	- 43½	1.65	2.39
- 40½	1.55	2.41	- 40	1.65	2.43
- 37	1.60	2.42	- 36½	1.70	2.45
- 33	1.70	2.46	- 32½	1.60	2.48
- 29	1.75	2.48	- 28½	1.75	2.50
- 26	1.70	2.51	- 25	1.70	2.53
- 23	1.85	2.52	- 23	1.80	2.54
- 19	1.80	2.55	- 18½	1.75	2.58
- 17	1.75	2.57	- 16½	1.75	2.57
- 13	1.75	2.59	- 13	1.70	2.61
- 9	1.65	2.62	- 8½	1.60	2.64
- 1½	1.60	2.66	- 1	1.40	2.68
5	1.35	2.69	5	1.20	2.71
12½	1.20	2.73	12½	1.00	2.74
20	0.95	2.77	20	0.95	2.79
25	0.85	2.80	25	0.75	2.81
32½	0.70	2.83	32½	0.55	2.84
43	0.55	2.87	43	0.45	2.87
65	0.25	2.92	65	0.15	2.92
83	0.20	2.98	83	0.20	2.98
97	0.15	3.03	97	0.15	3.03
118	0.15	3.13	118	0.20	3.13
132	0.10	3.23	132	0.20	3.23
143	0.20	3.21	143	0.25	3.21
151	0.15	3.22	151	0.15	3.22
161	0.35	3.30	161	0.50	3.30
162	0.50	3.29	161	0.50	3.31
178	1.55	3.56	162	0.80	3.29
184	2.40	3.66	173	0.95	3.38
194	4.50	3.87	178	2.10	3.59
207	8.25	4.31	184	3.30	3.71
217	20.00	5.16	194	5.85	3.95
230	> 36.35*	no balance	208	12.30	4.50
245	> 36.35	no balance	217	> 17.15	no balance
			230	> 17.15	no balance
			245	> 17.15	no balance

*At these temperaturees the value of tan δ exceeded the maximum value which could be measured at this frequency (viz. 36.35 x 10^{-2}) and the bridge could not therefore be balanced. The maximum value of tan δ that the bridge could measure at 210 c/s was 17.15 x 10^{-2} and at 1.05 kc was 85.80 x 10^{-2}.

Contour diagrams showing ε and tan δ as functions of frequency and temperature are given in Figures 32 and 33 respectively.

E.3.b.3 Experiment IV

Frequency: 90 kc/s

Temperature (°C)	tan δ (X 10^{-2})	ε
-176	0.15	2.36
-149	0.25	2.43
-140	0.30	2.46
-131	0.40	2.50
-123	0.45	2.52
-112	0.55	2.56
-102	0.75	2.60
- 90	0.90	2.66
- 78	1.05	2.72
- 67	1.20	2.78
- 56	1.30	2.83
- 45½	1.45	2.90
- 36	1.65	2.97
- 20½	2.00	3.10
- 12½	2.10	3.14
- 1½	2.40	3.23
11	2.65	3.35
21½	2.75	3.45
31½	2.80	3.55
40½	2.80	3.63
55	2.70	3.82
77	2.10	4.02
98	1.25	4.16
111	0.90	4.21
134	0.35	4.18
156	0.25	4.30
175	0.30	4.41
188	0.60	4.45
198	1.20	4.51
216	1.70	4.57
231	2.05	4.66

Frequency 46 kc/s

Temperature (°C)	tan δ (X 10^{-2})	ε
-176	0.20	2.36
-149	0.35	2.44
-140	0.45	2.47
-131	0.50	2.50
-123	0.55	2.53
-111	0.65	2.57
-102	0.75	2.61
- 90	0.90	2.68
- 78	1.05	2.74
- 66	1.20	2.80
- 55½	1.30	2.85
- 45	1.45	2.92
- 35½	1.60	3.00
- 20½	1.95	3.13
- 12½	2.10	3.16
- 1½	2.40	3.27
11½	2.55	3.39
21½	2.65	3.49
32	2.65	3.60
40½	2.55	3.68
55	2.25	3.86
77	1.60	4.05
98	0.95	4.17
111	0.60	4.21
134	0.30	4.19
156	0.20	4.31
175	0.30	4.42
188	0.80	4.47
198	1.25	4.54
216	1.80	4.60
231	2.55	4.69

Frequency: 22 kc/s

Temperature (°C)	tan δ (X 10^{-2})	ε
-176	0.25	2.36
-148	0.35	2.45
-139	0.40	2.48
-130	0.50	2.51
-123	0.55	2.53
-111	0.65	2.58
-102	0.70	2.63
- 89	0.85	2.69
- 79	1.00	2.75
- 65	1.15	2.82
- 55	1.30	2.87
- 44½	1.55	2.95
- 35½	1.75	3.03
- 20	2.00	3.16
- 12½	2.15	3.20
- 1½	2.35	3.30
11½	2.50	3.44
21½	2.50	3.54
32	2.45	3.64
40½	2.30	3.72
55	1.35	3.94
77	1.15	4.07
98	0.60	4.19
112	0.40	4.22
134	0.20	4.19
156	0.20	4.31
175	0.35	4.42
188	0.80	4.48
198	1.45	4.57
216	2.20	4.64
231	3.90	4.73

Frequency: 10.5 kc/s

Temperature (°C)	tan δ (X 10^{-2})	ε
-176	0.25	2.37
-148	0.35	2.46
-139	0.40	2.49
-130	0.50	2.52
-122	0.55	2.55
-111	0.65	2.59
-101	0.80	2.64
- 89	0.90	2.70
- 79	1.00	2.77
- 65	1.20	2.84
- 54½	1.30	2.89
- 44½	1.45	2.98
- 35	1.65	3.05
- 20	2.00	3.19
- 12	2.25	3.23
- 1	2.35	3.35
12	2.45	3.49
22	2.35	3.59
32	2.20	3.68
40½	1.90	3.76
55	1.35	3.94
77	0.90	4.10
98	0.40	4.20
112	0.30	4.23
135	0.20	4.20
156	0.15	4.31
175	0.35	4.43
188	1.00	4.50
198	1.70	4.59
216	2.90	4.69
232	6.45	4.80

Frequency: 4.8 kc/s			Frequency: 2.4 kc/s		
Temperature (°C)	tan δ (X 10^{-2})	ε	Temperature (°C)	tan δ (X 10^{-2})	ε
-176	0.20	2.37	-176	0.20	2.37
-147	0.40	2.46	-147	0.40	2.47
-138	0.45	2.50	-138	0.45	2.50
-129	0.55	2.53	-129	0.50	2.54
-122	0.60	2.56	-121	0.60	2.57
-110	0.65	2.60	-109	0.70	2.61
-101	0.75	2.65	-101	0.80	2.67
- 89	0.90	2.72	- 88	0.90	2.73
- 79	1.10	2.79	- 79	1.05	2.80
- 65	1.30	2.86	- 64	1.20	2.88
- 54½	1.35	2.91	- 53½	1.35	2.94
- 43½	1.55	3.00	- 43½	1.75	3.03
- 34½	1.70	3.08	- 34½	1.90	3.11
- 19½	2.00	3.22	- 19	2.15	3.25
- 12	2.15	3.27	- 11½	2.30	3.30
- 1	2.25	3.39	- ½	2.25	3.43
12	2.15	3.53	12½	2.10	3.57
22	2.05	3.63	22½	1.90	3.66
32½	1.80	3.72	32½	1.50	3.74
40½	1.60	3.79	40½	1.30	3.81
55	1.15	3.96	55	0.90	3.98
77	0.65	4.11	77	0.50	4.12
99	0.35	4.21	99	0.25	4.21
112	0.25	4.24	112	0.20	4.24
135	0.15	4.20	135	0.10	4.21
156	0.15	4.31	156	0.15	4.31
175	0.40	4.43	175	0.45	4.44
188	1.20	4.52	188	1.50	4.55
198	2.15	4.63	198	3.00	4.68
216	4.30	4.74	216	6.50	4.82
232	11.90	4.93	232	20.40	5.23

E.3.b.4 Experiment V

Frequency: 210 c/s

Temperature (°C)	tan δ (X 10^{-2})	ε
-176	0.20	2.38
-146	0.45	2.50
-136	0.50	2.53
-128	0.65	2.57
-170	0.65	2.61
-108	0.70	2.65
-100	0.95	2.71
- 88	1.05	2.79
- 77	1.25	2.87
- 63	1.40	2.96
- 52½	1.55	3.02
- 42	1.75	3.12
- 33½	2.00	3.21
- 18½	2.00	3.37
- 11	1.90	3.43
- ½	1.65	3.55
13	1.25	3.67
23	1.05	3.74
32½	0.75	3.81
40½	0.65	3.87
55	0.45	4.02
77	0.25	4.14
99	0.15	4.22
112	0.15	4.25
135	0.15	4.21
156	0.25	4.32
175	1.25	4.48
188	4.95	4.70
198	9.30	5.02
216	> 17.15	no balance
234	17.15	no balance

Frequency: 90 kc/s

Temperature (°C)	tan δ (X 10^{-2})	ε
-184	0.15	2.26
-176	0.15	2.28
-164	0.25	2.31
-149	0.30	2.35
-139	0.35	2.38
-129	0.40	2.41
-117	0.50	2.45
-105	0.60	2.50
- 92	0.85	2.55
- 79	1.00	2.61
- 67	1.15	2.67
- 54½	1.30	2.73
- 44	1.50	2.80
- 32½	1.70	2.88
- 24	1.90	2.95
- 11½	2.10	3.05
- 2½	2.30	3.13
7	2.70	3.27
19½	2.75	3.35
30	2.50	3.55
43½	2.50	3.76
64	2.55	4.05
74	2.20	4.09
95	1.40	4.26
123	0.50	4.29
132	0.40	4.24
149	0.30	4.27
165	0.25	4.31
181	0.50	4.42
194	1.15	4.49
207	1.70	4.52
222	1.95	4.53
236	2.40	4.52

Contour diagrams showing ε and tan δ as functions of frequency and temperature are given in Figures 34 and 35 respectively.

Frequency: 1.05 kc/s

Temperature (°C)	tan δ (X 10^{-2})	ε
-176	0.25	2.37
-147	0.40	2.48
-137	0.50	2.52
-129	0.55	2.55
-121	0.60	2.58
-109	0.75	2.63
-101	0.85	2.68
- 88	1.00	2.75
- 78	0.75	2.83
- 64	1.30	2.91
- 53½	1.45	2.97
- 42½	1.70	3.05
- 34	1.85	3.14
- 19	2.05	3.29
- 11½	2.25	3.34
- ½	2.05	3.48
12½	1.75	3.61
22½	1.55	3.69
32½	1.25	3.77
40½	1.05	3.84
55	0.70	4.00
77	0.40	4.12
99	0.20	4.21
112	0.15	4.24
135	0.10	4.21
156	0.15	4.31
175	0.60	4.45
188	2.20	4.58
198	4.35	4.75
216	10.25	4.98
234	37.60	6.02

Frequency: 445 c/s

Temperature (°C)	tan δ (X 10^{-2}	ε
-176	0.25	2.38
-146	0.45	2.49
-137	0.50	2.53
-128	0.55	2.56
-120	0.65	2.60
-108	0.75	2.64
-100	0.85	2.70
- 88	1.05	2.77
- 78	1.20	2.85
- 63	1.45	2.93
- 53	1.55	2.99
- 42½	1.75	3.09
- 33½	1.85	3.18
- 19	2.00	3.34
- 11	2.00	3.39
- ½	1.75	3.51
13	1.55	3.64
23	1.25	3.72
32½	0.95	3.79
40½	0.80	3.86
55	0.55	4.01
77	0.35	4.13
99	0.20	4.21
112	0.15	4.24
135	0.10	4.21
156	0.15	4.32
175	0.95	4.46
188	3.45	4.64
198	6.60	4.86
216	16.50	5.29
234	> 36.35	no balance

Frequency: 46 kc/s

Temperature (°C)	tan δ (X 10^{-2})	ε
-184	0.15	2.26
-175	0.20	2.29
-162	0.25	2.31
-148	0.35	2.36
-138	0.45	2.38
-128	0.50	2.42
-116	0.60	2.46
-103	0.70	2.51
- 91	0.85	2.56
- 79	1.00	2.63
- 66	1.10	2.69
- 53½	1.30	2.75
- 43½	1.45	2.82
- 32	1.65	2.91
- 23½	1.80	2.98
- 11½	2.10	3.08
- 2½	2.25	3.17
7	2.70	3.30
19½	2.60	3.39
30	2.90	3.60
43½	2.75	3.81
64	2.10	4.09
74	1.70	4.12
95	1.00	4.27
123	0.45	4.30
132	0.30	4.25
149	0.25	4.27
165	0.25	4.32
181	0.60	4.44
194	1.30	4.51
208	1.90	4.56
222	2.25	4.56
234	3.40	4.55

Frequency: 22 kc/s

Temperature (°C)	tan δ (X 10^{-2})	ε
-184	0.15	2.26
-174	0.25	2.29
-161	0.30	2.32
-147	0.35	2.36
-137	0.40	2.39
-127	0.45	2.43
-116	0.55	2.47
-103	0.65	2.52
- 91	0.75	2.58
- 78	0.90	2.64
- 65	1.05	2.70
- 53½	1.20	2.77
- 43	1.35	2.84
- 32	1.70	2.94
- 23½	1.90	3.01
- 11	2.10	3.12
- 2	2.25	3.20
7	2.50	3.34
19½	2.40	3.44
30	2.55	3.65
43½	2.30	3.86
64	1.65	4.12
74	1.30	4.15
95	0.65	4.29
123	0.30	4.31
132	0.30	4.26
149	0.25	4.27
165	0.25	4.32
181	0.65	4.45
194	1.60	4.54
208	2.40	4.59
223	3.50	4.59
233	5.50	4.58

Frequency: 10.5 kc/s

Temperature (°C)	tan δ (X 10^{-2})	ε
-184	0.20	2.26
-173	0.25	2.30
-160	0.25	2.33
-147	0.35	2.37
-137	0.40	2.40
-125	0.45	2.43
-115	0.55	2.48
-102	0.65	2.53
- 90	0.80	2.59
- 78	0.95	2.66
- 65	1.10	2.72
- 53	1.25	2.79
- 42½	1.40	2.87
- 31½	1.70	2.96
- 23½	1.85	3.04
- 10½	2.05	3.15
- 1½	2.20	3.24
7	2.55	3.40
19½	2.35	3.48
30	2.25	3.70
43½	1.90	3.90
64	1.20	4.15
74	1.00	4.17
95	0.45	4.30
123	0.25	4.31
132	0.25	4.26
149	0.20	4.27
165	0.25	4.33
181	0.80	4.46
194	2.05	4.56
208	3.50	4.63
223	5.45	4.63
233	10.60	4.65

Frequency: 4.8 kc/s

Temperature (°C)	tan δ (X 10^{-2})	ε
-184	0.20	2.27
-171	0.25	2.30
-159	0.25	2.33
-146	0.35	2.37
-134	0.45	2.41
-125	0.50	2.44
-114	0.55	2.49
-102	0.65	2.54
- 90	0.80	2.60
- 78	1.00	2.67
- 65	1.15	2.74
- 52½	1.35	2.81
- 42½	1.45	2.89
- 31½	1.70	2.99
- 23	1.90	3.07
- 10	2.10	3.19
- 1	2.15	3.28
7	2.30	3.45
19½	2.00	3.52
30	1.89	3.74
43½	1.55	3.93
64	0.95	4.17
74	0.70	4.18
95	0.35	4.31
123	0.20	4.31
132	0.20	4.27
149	0.20	4.28
165	0.30	4.33
181	1.05	4.48
194	2.70	4.60
208	5.60	4.67
223	10.50	4.70
233	20.80	4.85

Frequency: 2.4 kc/s

Temperature (°C)	tan δ (X 10^{-2})	ε
-184	0.15	2.27
-168	0.25	2.31
-158	0.30	2.34
-144	0.35	2.38
-133	0.45	2.42
-124	0.55	2.45
-113	0.65	2.50
-101	0.75	2.56
- 90	0.85	2.61
- 77	1.00	2.69
- 64	1.20	2.75
- 52½	1.35	2.83
- 42	1.65	2.91
- 31	1.90	3.02
- 23	2.05	3.10
- 10	2.20	3.22
- ½	2.20	3.32
7	2.40	3.48
19½	1.95	3.56
30	1.80	3.77
43½	1.30	3.96
64	0.75	4.19
73	0.55	4.19
95	0.30	4.31
123	0.20	4.32
132	0.15	4.27
149	0.20	4.29
165	0.35	4.34
181	1.35	4.50
194	4.00	4.64
208	9.80	4.75
223	20.40	4.87
234	48.0	5.68

Frequency: 1.05 kc/s

Temperature (°C)	tan δ (X 10^{-2})	ε
-184	0.20	2.27
-168	0.25	2.31
-157	0.30	2.35
-143	0.40	2.39
-132	0.45	2.43
-124	0.55	2.46
-113	0.65	2.51
-101	0.80	2.57
- 89	0.95	2.63
- 77	1.05	2.70
- 64	1.25	2.78
- 52	1.45	2.85
- 42	1.65	2.94
- 30½	1.90	3.05
- 22½	2.00	3.14
- 9½	2.05	3.26
0	1.95	3.36
7	2.00	3.53
19½	1.55	3.59
30	1.35	3.80
43½	1.05	3.99
64	0.55	4.20
73	0.40	4.20
95	0.25	4.32
123	0.20	4.32
132	0.15	4.27
149	0.25	4.29
165	0.50	4.35
181	2.25	4.52
194	6.85	4.70
208	20.40	4.94
223	42.60	5.66
234	> 85.8	no balance

Frequency: 445 c/s

Temperature (°C)	tan δ (X 10^{-2})	ε
-184	0.10	2.28
-167	0.25	2.32
-156	0.30	2.36
-142	0.45	2.40
-132	0.50	2.43
-123	0.60	2.47
-112	0.70	2.53
-100	0.75	2.58
- 88	0.90	2.65
- 76	1.15	2.72
- 63	1.30	2.80
- 51½	1.50	2.88
- 41½	1.70	2.98
- 30½	1.90	3.09
- 22½	2.10	3.18
- 9½	1.90	3.30
1	1.75	3.41
7	1.70	3.56
19½	1.30	3.62
30	1.05	3.82
43½	0.80	4.01
65	0.50	4.23
73	0.35	4.21
95	0.20	4.32
123	0.20	4.32
132	0.20	4.27
149	0.35	4.29
165	0.90	4.36
181	4.25	4.56
194	6.85	4.70
208	> 36.35	no balance
223	> 36.35	no balance
234	> 36.35	no balance

Frequency: 210 c/s

Temperature (°C)	tan δ (X 10^{-2})	ε
-184	0.15	2.28
-166	0.15	2.33
-152	0.20	2.37
-141	0.40	2.41
-131	0.60	2.44
-122	0.90	2.48
-111	0.90	2.53
- 99	0.95	2.59
- 87	1.05	2.67
- 76	1.20	2.74
- 62	1.30	2.84
- 51	1.60	2.91
- 41	1.90	3.00
- 30	1.85	3.12
- 22	2.00	3.20
- 9	1.75	3.34
1½	1.45	3.44
7	1.50	3.60
19½	1.05	3.64
30	0.80	3.83
43½	0.60	4.02
65	0.45	4.23
73	0.35	4.22
95	0.20	4.32
124	0.20	4.33
132	0.25	4.27
149	0.50	4.30
165	1.80	4.36
181	7.60	4.60
195	> 17.15	no balance
208	> 17.15	no balance
223	> 17.15	no balance
234	> 17.15	no balance

Contour diagrams showing ε and tan δ as functions of frequency and temperature are given in Figures 36 and 37 respectively.

E.3.b.5 Experiment VI

Frequency: 90 kc/s

Temperature (°C)	tan δ (X 10^{-2})	ε
-168	0.10	1.81
-158	0.15	1.83
-147	0.20	1.84
-134	0.25	1.86
-124	0.30	1.88
-112	0.35	1.90
-102	0.40	1.92
- 92	0.45	1.95
- 81	0.55	1.97
- 70	0.70	2.00
- 56	0.80	2.03
- 45½	0.90	2.06
- 37	1.00	2.09
- 28½	1.10	2.12
- 17	1.25	2.16
- 6½	1.45	2.21
+ 5	1.55	2.25
20½	1.70	2.34
37	1.55	2.46
46	1.45	2.52
63	1.10	2.68
78	0.90	2.80
94	0.55	3.09
111	0.50	3.19
127	0.85	3.41
134	1.05	3.52
145	1.80	3.70
161	3.00	3.68
182	4.00	3.83
194	5.10	3.90
206	6.90	3.95
226	12.00	4.09
236	17.90	4.24

Frequency: 46 kc/s

Temperature (°C)	tan δ (X 10^{-2})	ε
-168	0.15	1.81
-157	0.20	1.83
-146	0.20	1.85
-134	0.25	1.86
-123	0.30	1.88
-111	0.40	1.91
-101	0.50	1.93
- 91	0.55	1.95
- 80	0.65	1.98
- 69	0.70	2.01
- 56	0.80	2.04
- 45	0.95	2.07
- 36½	1.05	2.10
- 28½	1.15	2.13
- 16½	1.30	2.18
- 6	1.40	2.22
5	1.50	2.27
20½	1.55	2.36
37	1.35	2.47
46	1.15	2.54
63	0.90	2.69
78	0.65	2.81
94	0.50	3.09
111	0.50	3.20
127	0.80	3.42
134	1.10	3.54
145	1.90	3.72
161	3.35	3.73
182	4.65	3.89
194	6.90	3.97
206	9.75	4.04
226	19.90	4.28
236	30.50	4.64

Frequency 22 kc/s

Temperature (°C)	tan δ (X 10^{-2})	ε
-168	0.15	1.82
-156	0.20	1.83
-144	0.25	1.85
-133	0.25	1.87
-122	0.35	1.89
-110	0.35	1.91
-100	0.45	1.93
- 91	0.50	1.96
- 79	0.55	1.98
- 68	0.65	2.02
- 55½	0.75	2.05
- 44½	0.80	2.08
- 36½	0.95	2.11
- 28	1.10	2.15
- 16	1.25	2.19
- 5½	1.35	2.24
+ 5½	1.50	2.29
20½	1.35	2.37
37	1.00	2.49
46	0.85	2.55
63	0.60	2.70
78	0.50	2.81
94	0.35	3.10
111	0.40	3.21
127	0.75	3.44
134	1.05	3.56
145	2.10	3.76
161	3.60	3.79
182	5.55	3.96
194	10.30	4.08
206	16.80	4.20
226	36.50	4.88
236	58.90	5.96

Frequency: 10.5 kc/s

Temperature (°C)	tan δ (X 10^{-2})	ε
-168	0.15	1.82
-156	0.20	1.84
-143	0.25	1.85
-132	0.25	1.87
-121	0.30	1.89
-109	0.40	1.92
- 99	0.45	1.94
- 90	0.50	1.97
- 79	0.55	2.00
- 67	0.65	2.03
- 55	0.80	2.06
- 44½	0.90	2.09
- 36	1.00	2.12
- 27½	1.20	2.16
- 15½	1.30	2.21
- 5	1.40	2.25
+ 6	1.35	2.31
20½	1.10	2.39
37	0.85	2.50
46	0.70	2.56
63	0.45	2.71
78	0.35	2.82
94	0.30	3.11
111	0.35	3.22
127	0.80	3.45
134	1.20	3.58
145	2.45	3.80
161	4.15	3.85
181	7.90	4.05
194	18.40	4.28
206	30.00	4.63
226	64.40	6.85
236	94.40	10.03

Frequency: 4.8 kc/s

Temperature (°C)	tan δ (X 10^{-2})	ε
-167	0.15	1.82
-154	0.20	1.84
-141	0.25	1.86
-131	0.25	1.88
-119	0.35	1.90
-109	0.40	1.92
- 98	0.45	1.95
- 90	0.45	1.97
- 78	0.55	2.00
- 67	0.65	2.04
- 54½	0.80	2.06
- 44	0.95	2.10
- 36	1.15	2.13
- 27½	1.30	2.17
- 15	1.35	2.23
- 5	1.35	2.28
+ 6	1.20	2.32
20½	0.90	2.40
37	0.60	2.51
46	0.55	2.57
63	0.40	2.71
78	0.30	2.83
94	0.25	3.11
111	0.35	3.22
127	0.90	3.47
134	1.45	3.61
145	2.80	3.85
162	5.30	3.94
181	12.00	4.17
194	32.50	4.81
206	50.90	5.83
226	94.10	11.46
236	130.0	19.17

Frequency: 2.4 kc/s

Temperature (°C)	tan δ (X 10^{-2})	ε
-166	0.15	1.83
-152	0.20	1.84
-141	0.25	1.86
-130	0.30	1.88
-118	0.35	1.90
-108	0.40	1.93
- 97	0.45	1.95
- 89	0.50	1.98
- 78	0.65	2.01
- 66	0.75	2.04
- 53½	0.85	2.08
- 44	1.05	2.11
- 35½	1.20	2.15
- 27	1.35	2.19
- 15	1.40	2.25
- 4	1.30	2.29
+ 6	1.05	2.34
20½	0.75	2.41
37	0.50	2.52
46	0.40	2.57
63	0.30	2.71
78	0.25	2.83
94	0.25	3.11
111	0.35	3.23
127	1.05	3.49
134	1.75	3.64
146	3.45	3.90
162	7.10	4.03
181	20.15	4.37
194	55.80	6.11
206	77.60	8.51
226	116.00	19.34
236	103.20	20.93

Frequency: 1.05 kc/s			Frequency: 445 c/s		
Temperature (°C)	tan δ (X 10^{-2})	ε	Temperature (°C)	tan δ (X 10^{-2})	ε
-166	0.15	1.83	-165	0.20	1.83
-151	0.20	1.85	-149	0.25	1.85
-140	0.25	1.87	-138	0.30	1.87
-130	0.30	1.89	-129	0.40	1.89
-117	0.40	1.91	-117	0.40	1.91
-107	0.40	1.94	-106	0.50	1.94
- 97	0.45	1.96	- 96	0.50	1.97
- 89	0.55	1.99	- 88	0.50	2.00
- 77	0.65	2.02	- 77	0.65	2.03
- 66	0.85	2.05	- 65	0.95	2.06
- 53½	1.00	2.09	- 53	1.10	2.10
- 42½	1.25	2.13	- 42½	1.40	2.15
- 35	1.35	2.16	- 35	1.45	2.18
- 27	1.40	2.21	- 26½	1.45	2.20
- 14½	1.35	2.27	- 14	1.20	2.29
- 3½	1.20	3.30	- 3	1.00	2.33
+ 7	0.85	2.35	+ 7½	0.60	2.36
20½	0.60	2.42	26½	0.40	2.43
37	0.40	2.52	37	0.40	2.53
46	0.35	2.58	46	0.35	2.58
63	0.25	2.72	63	0.20	2.72
78	0.25	2.84	78	0.20	2.84
94	0.20	3.12	94	0.20	3.12
111	0.40	3.24	111	0.50	3.24
127	1.30	3.52	127	1.70	3.54
134	2.05	3.67	134	2.65	3.72
146	4.40	3.98	146	5.80	4.09
162	11.00	4.16	162	19.15	4.41
180	35.95	5.02	180	> 36.35	no balance
194	76.20	9.33	194	> 36.35	no balance
206	> 85.80	no balance	206	> 36.35	no balance
226	> 85.80	no balance	226	> 36.35	no balance
236	> 85.80	no balance	236	> 36.35	no balance

Frequency: 210 c/s

Temperature (°C)	tan δ (X 10^{-2})	ε
-164	0.15	1.84
-148	0.25	1.86
-137	0.45	1.87
-127	0.45	1.90
-116	0.60	1.91
-105	0.65	1.94
- 95	0.70	1.98
- 86	0.85	2.00
- 76	1.00	2.04
- 64	1.10	2.08
- 52½	1.30	2.11
- 42	1.75	2.16
- 34½	1.40	2.20
- 26	1.15	2.24
- 13½	0.85	2.30
- 1½	0.85	2.33
+ 8	0.40	2.38
20½	0.30	2.43
37	0.30	2.54
46	0.25	2.59
63	0.15	2.73
78	0.25	2.85
94	0.20	3.13
111	0.45	3.25
127	2.00	3.58
134	3.30	3.77
146	7.90	4.20
162	> 17.15	no balance
180	> 17.15	no balance
194	> 17.15	no balance
206	> 17.15	no balance
226	> 17.15	no balance
236	> 17.15	no balance

Contour diagrams showing ε and tan δ as functions of frequency and temperature are given in Figures 38 and 39 respectively.

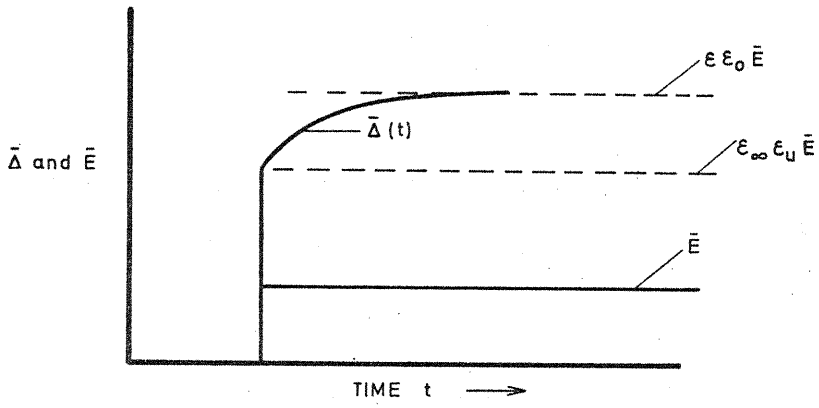

Figure 1

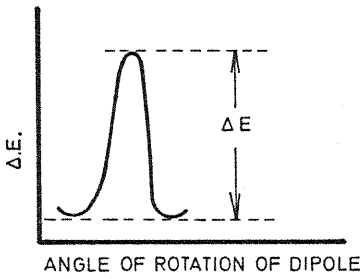

Figure 4

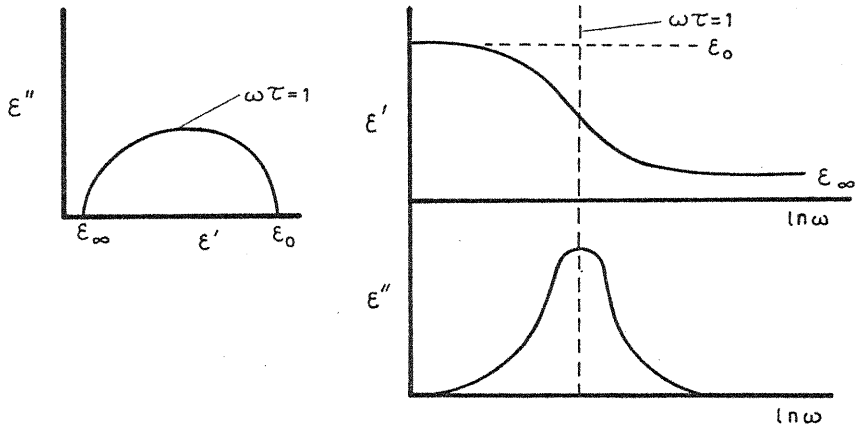

Figure 2

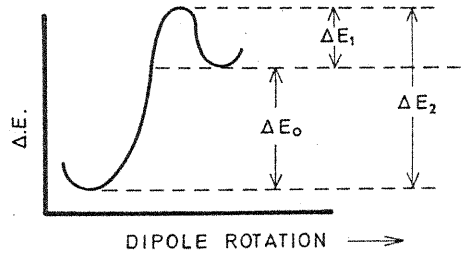

Figure 5

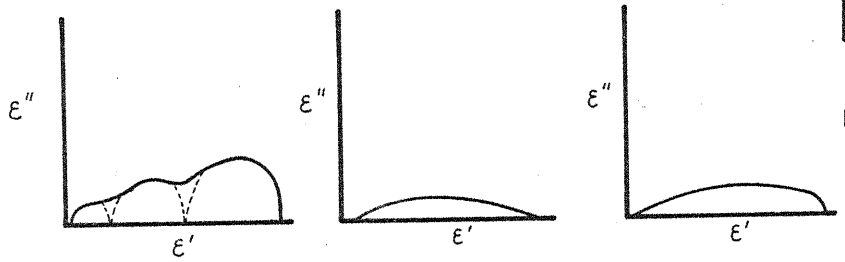

a) MULTIPLE b) CIRCULAR ARC c) SKEWED ARC

Figure 3

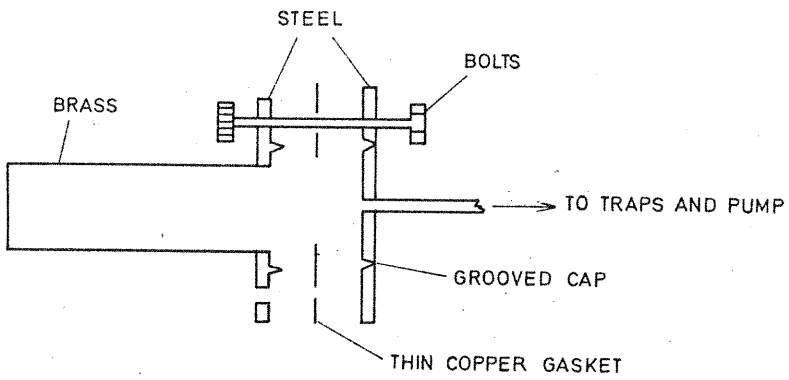

Figure 6 DEGRADATION CHAMBER OR REACTION VESSEL

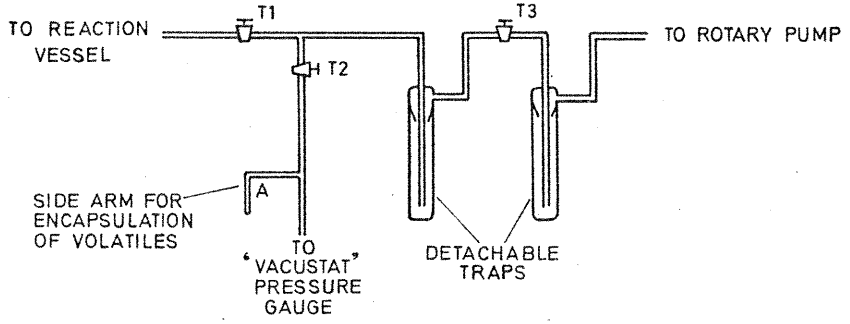

Figure 7 VACUUM LINE CONNECTED TO DEGRADATION CHAMBER

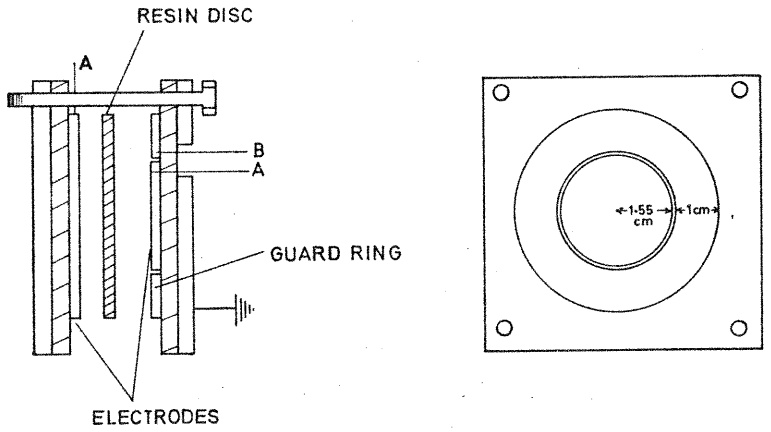

Figure 8 DIELECTRIC CELL

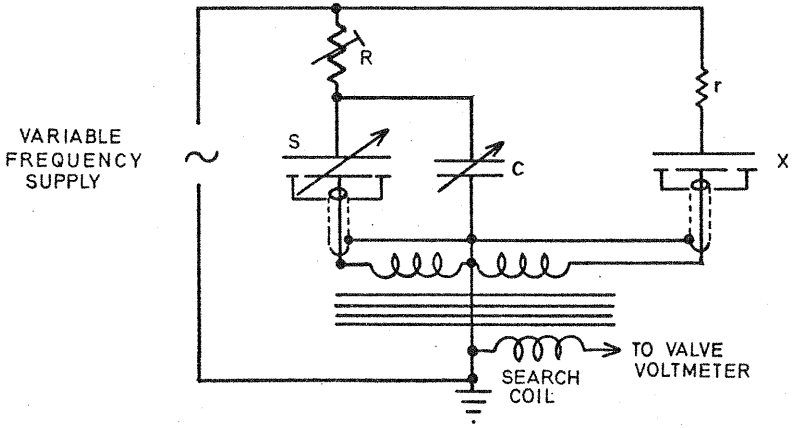

Figure 9 CIRCUIT DIAGRAM BAKER DIELECTRIC BRIDGE

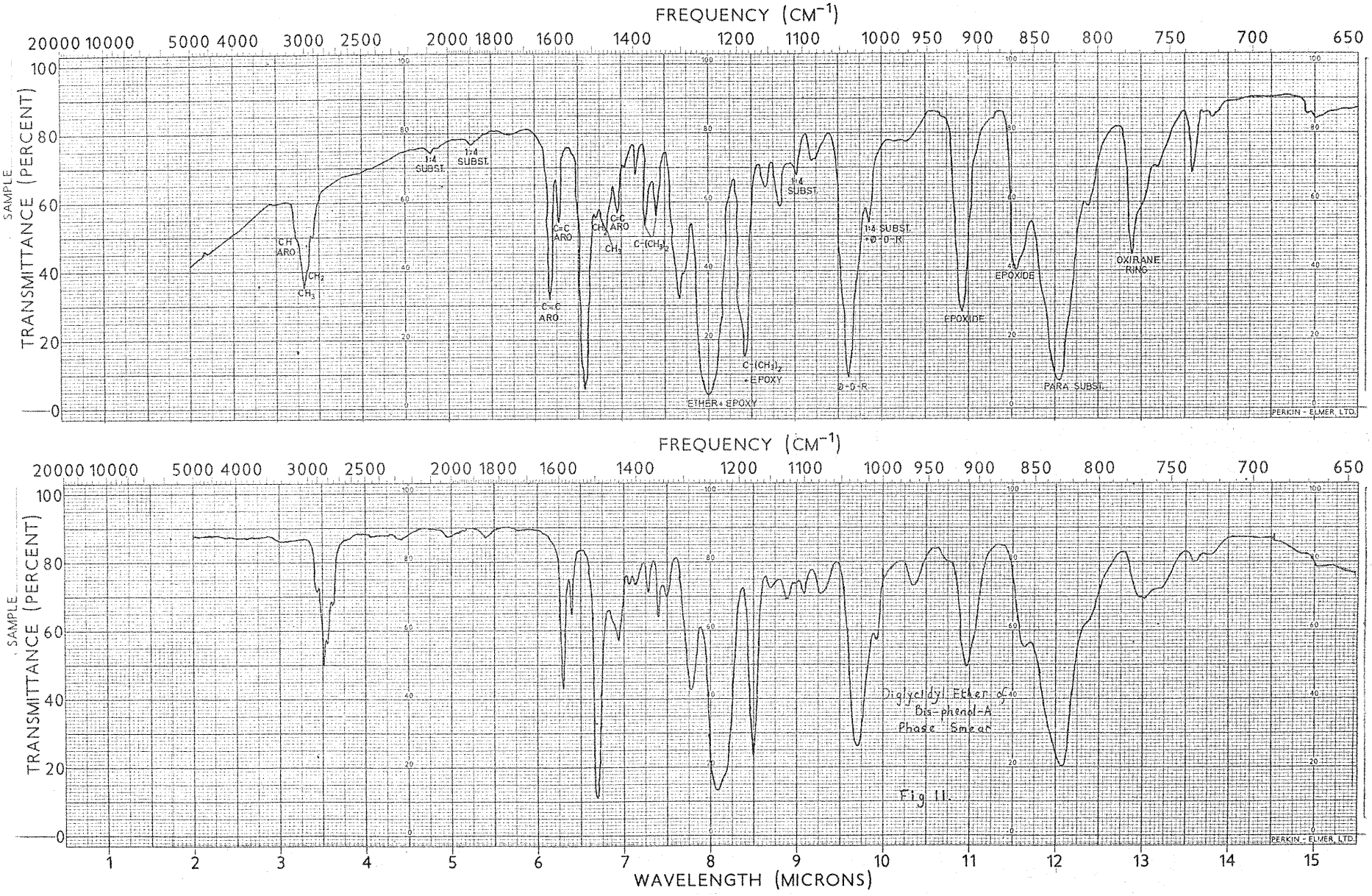

FIGURE 10 DIGLYCIDYL ETHER OF BIS-PHENOL-A CRYSTALS
PHASE KBr DISC

FIGURE 11 DIGLYCLDYL ETHER OF BIS-PHENOL-A PHASE SMEAR

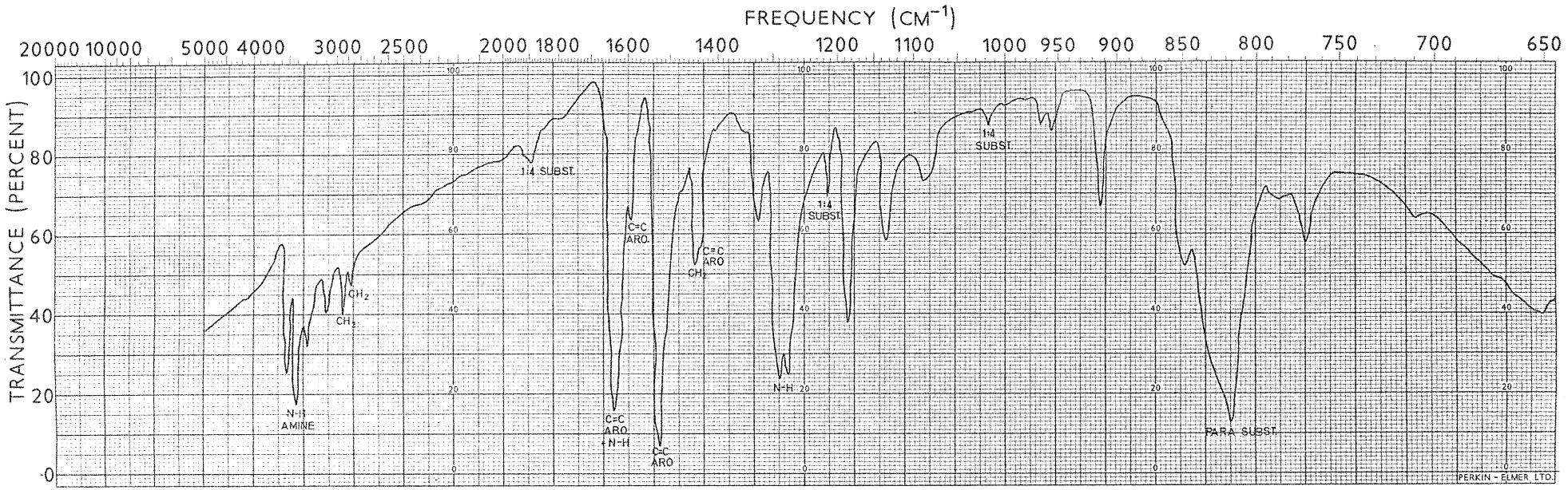

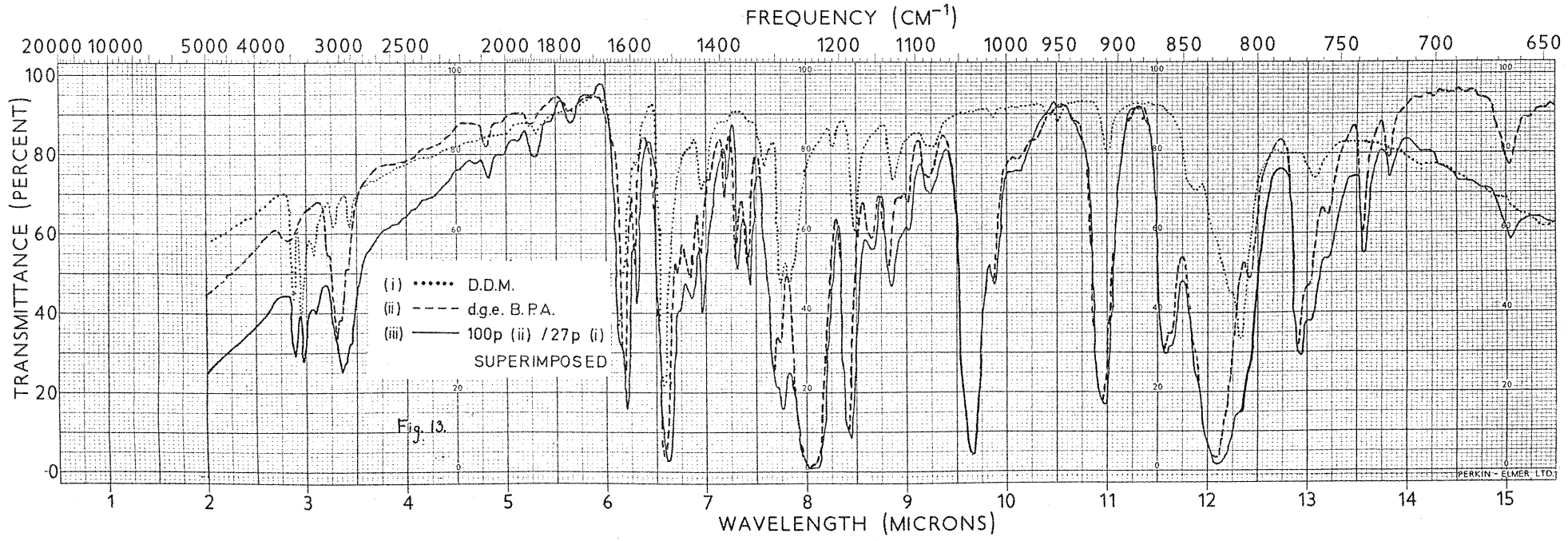

FIGURE 12 p p' - DIAMINO-DIPHENYL METHANE PHASE K Br DISC

FIGURE 13 PHASE KBr DISC

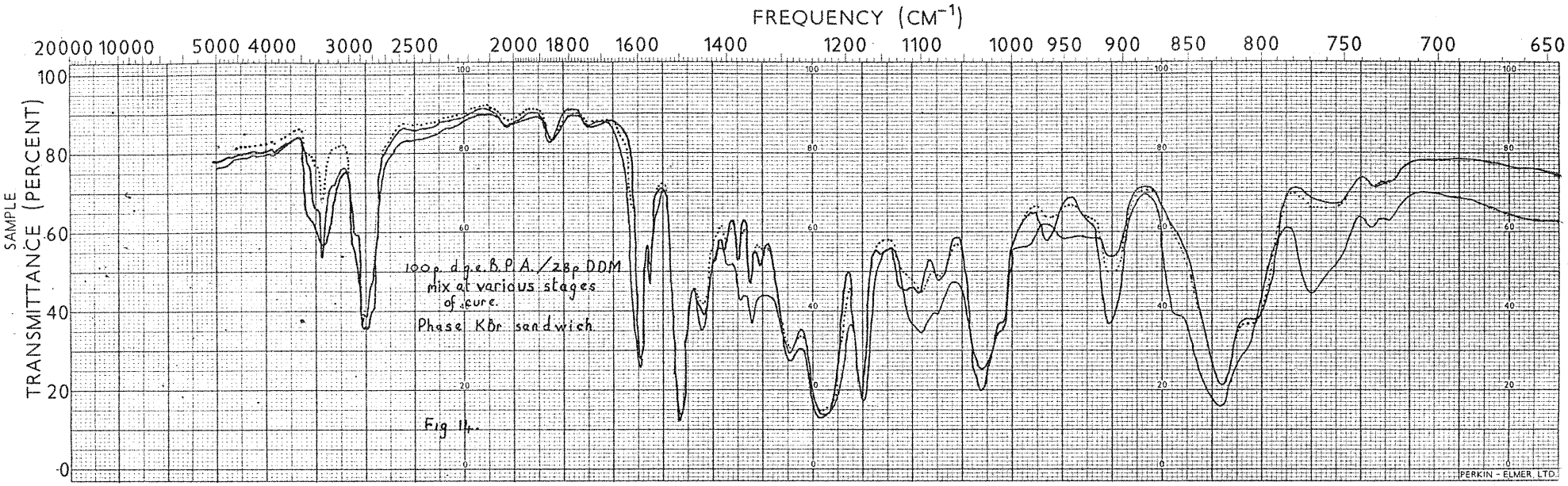

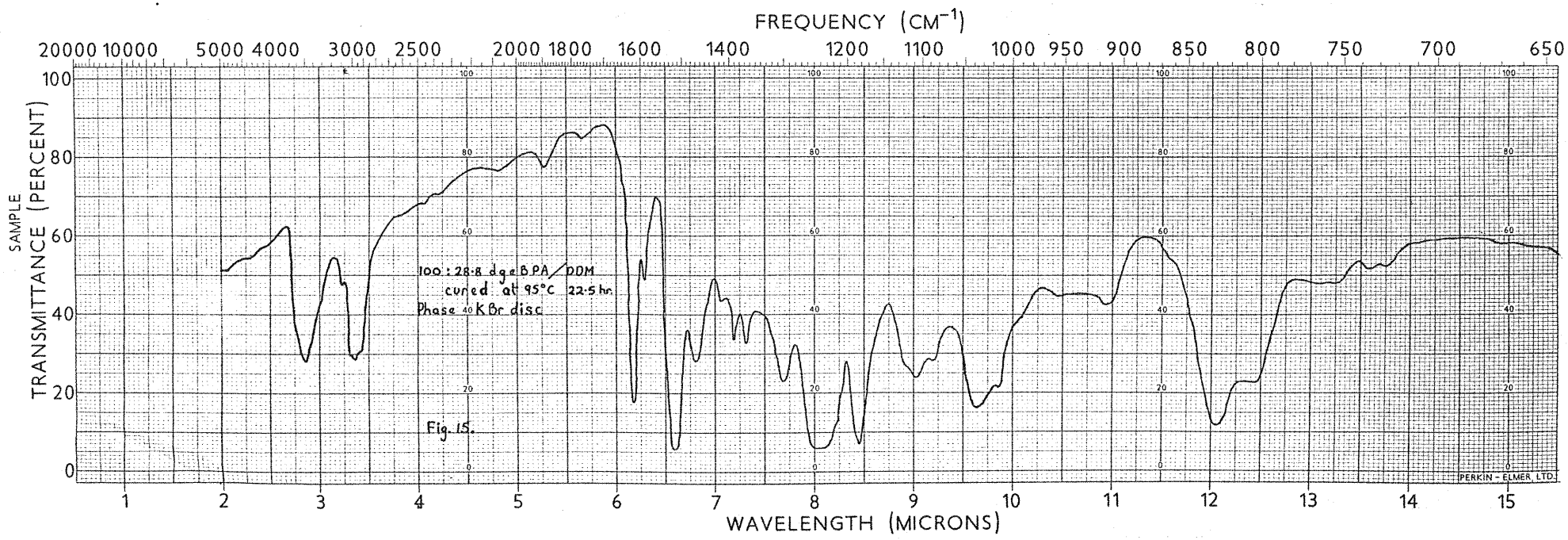

FIGURE 14 100p. d.g.e. B.P.A./ 28p DDM MIX AT VARIOUS STAGES OF CURE PHASE KBr SANDWICH

FIGURE 15 100:28·8 d g e B P A / DDM CURED AT 95°C 22·5 HR PHASE KBr DISC

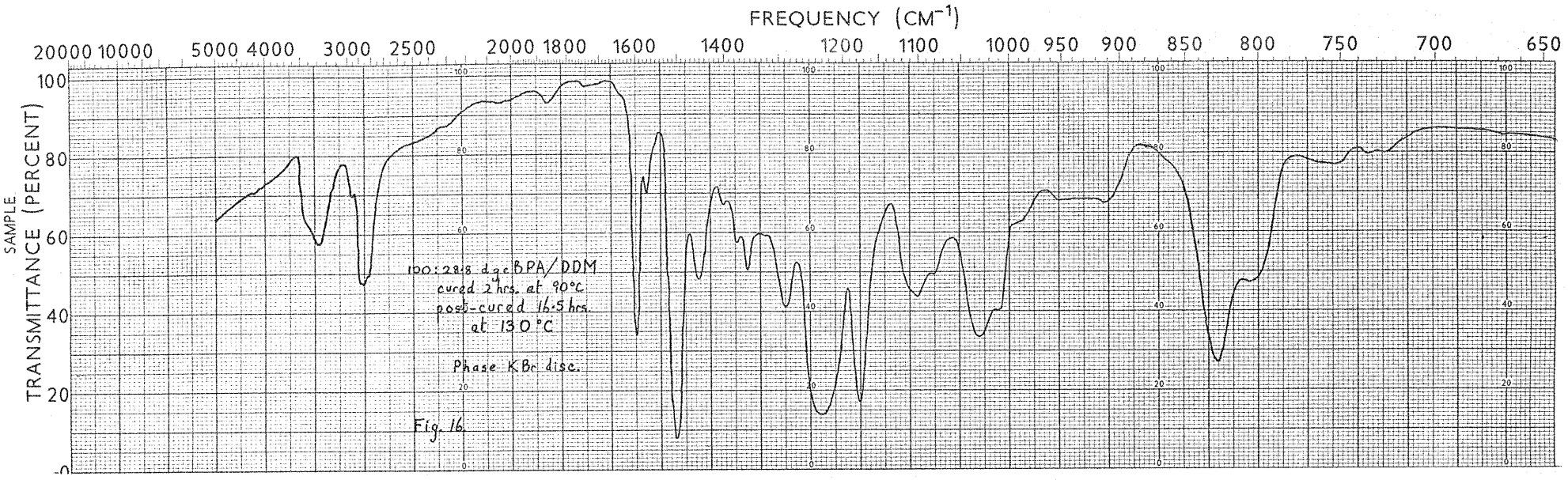

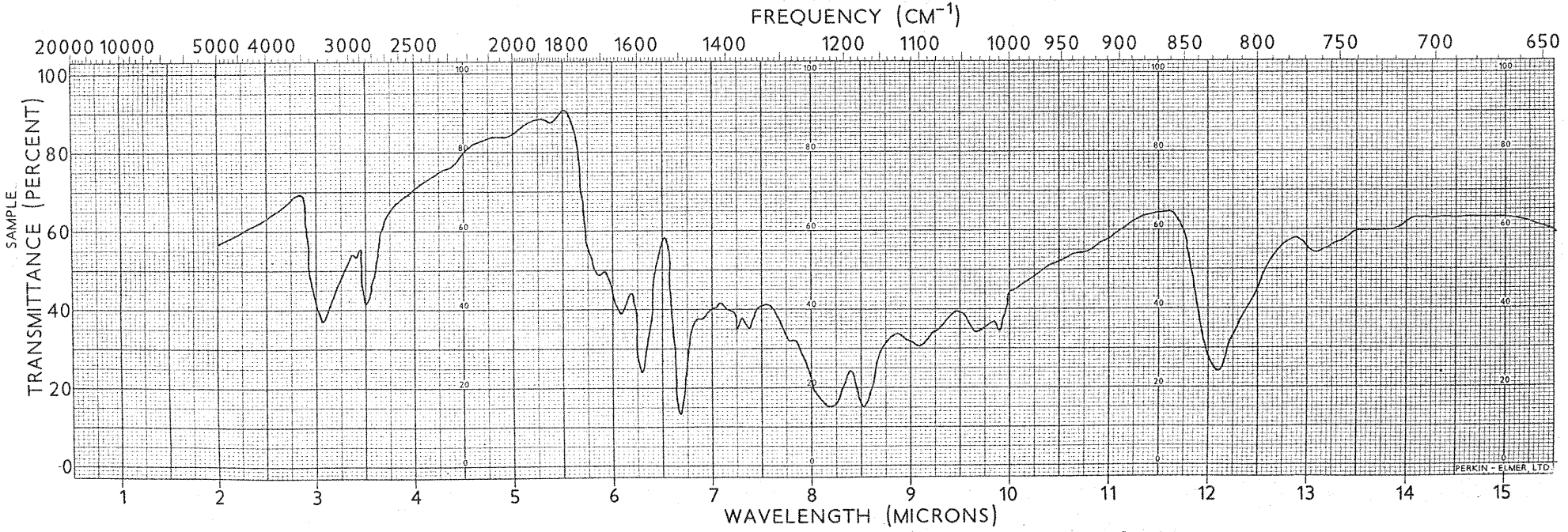

FIGURE 16 100:28·8 dge BPA/DDM CURED 2 HRS AT 90°C
POST-CURED 16·5 HRS AT 130°C
PHASE KBr DISC

FIGURE 17 EXTERIOR OF DISC CURED AT 180 C FOR 16 HRS IN AIR
PHASE KBr DISC

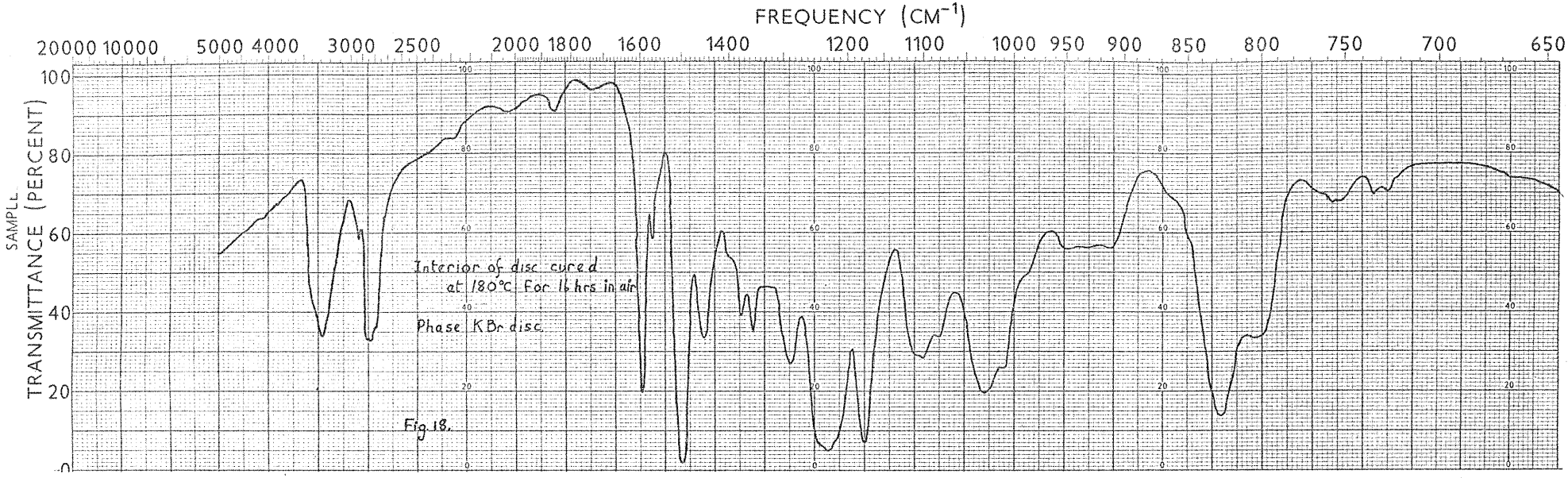

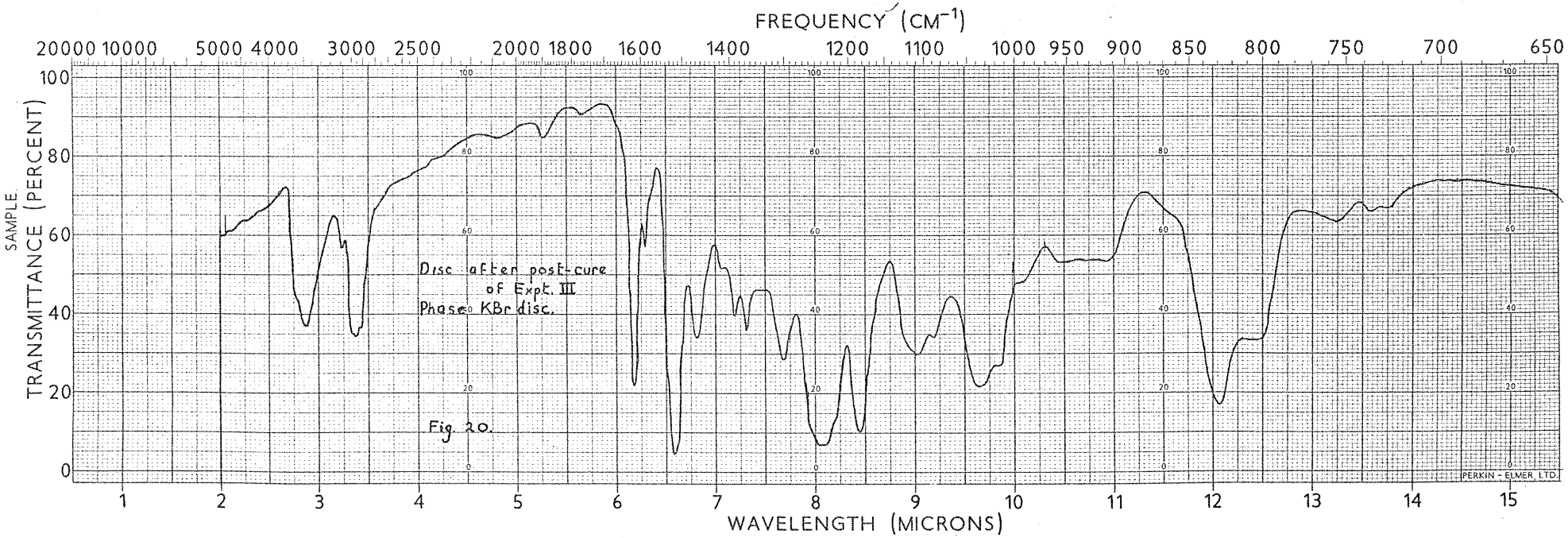

FIGURE 18 INTERIOR OF DISC CURED AT 180 C FOR 16 HRS IN AIR
PHASE K Br DISC

FIGURE 20 DISC AFTER POST-CURE OF EXPERIMENT III
PHASE K Br DISC

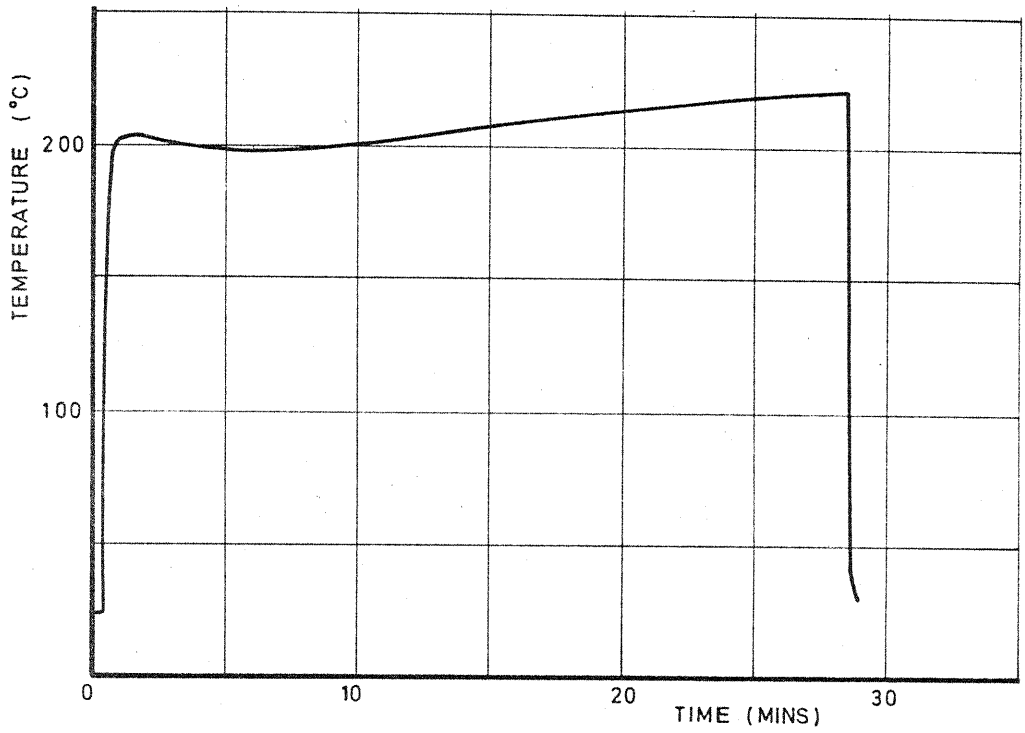

Figure 19 EXPERIMENT III

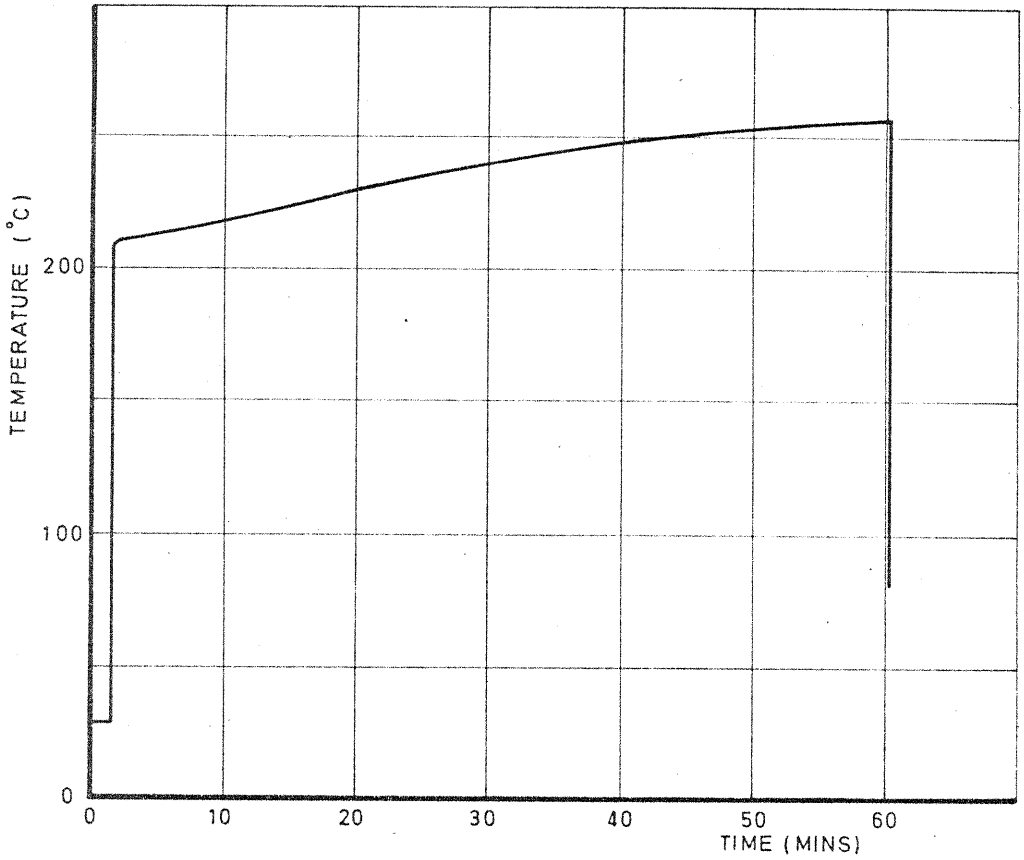

Figure 21 EXPERIMENT IV

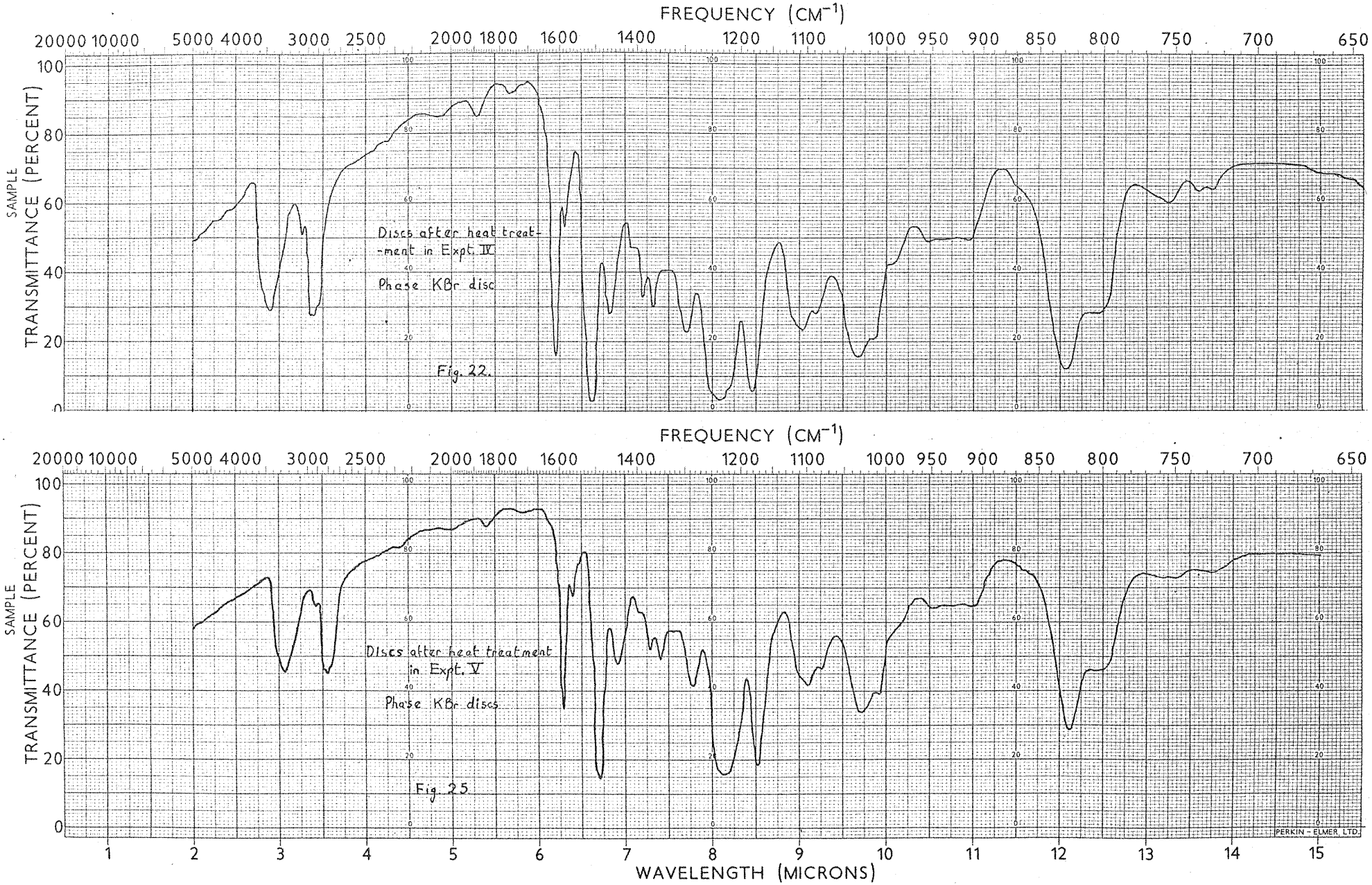

FIGURE 22 DISCS AFTER HEAT TREATMENT IN EXPERIMENT IV
PHASE KBr DISC

FIGURE 25 DISCS AFTER HEAT TREATMENT IN EXPERIMENT V
PHASE KBr DISCS

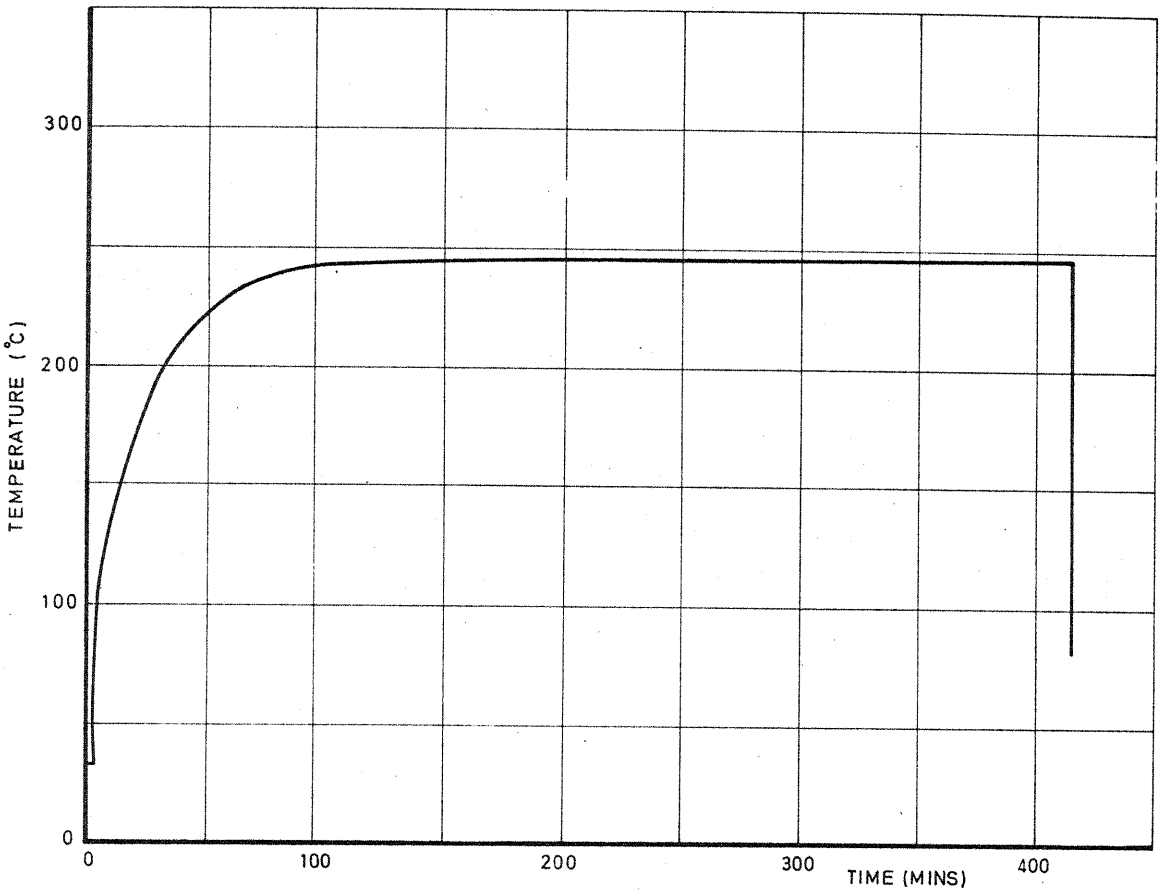

Figure 23 EXPERIMENT V

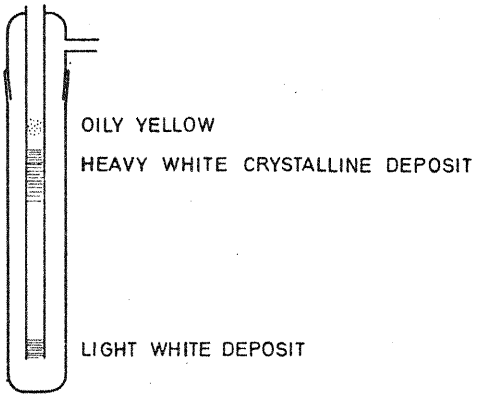

Figure 24 VACUUM LINE TRAP SHOWING CONDENSATES

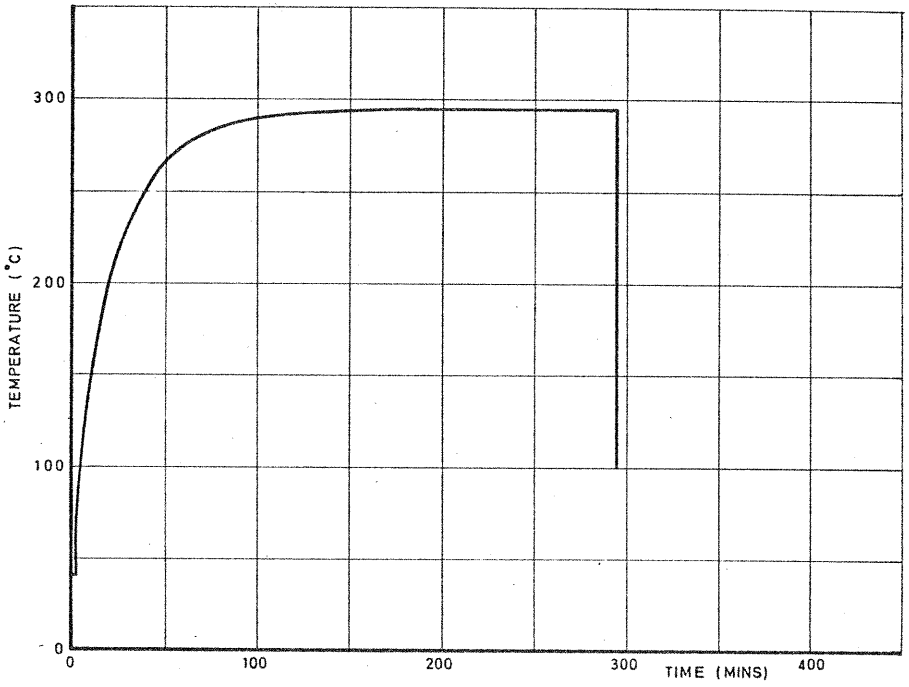

Figure 26 EXPERIMENT VI

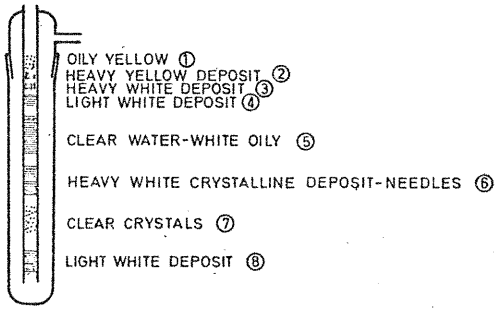

Figure 27 VACUUM LINE TRAP SHOWING CONDENSATES

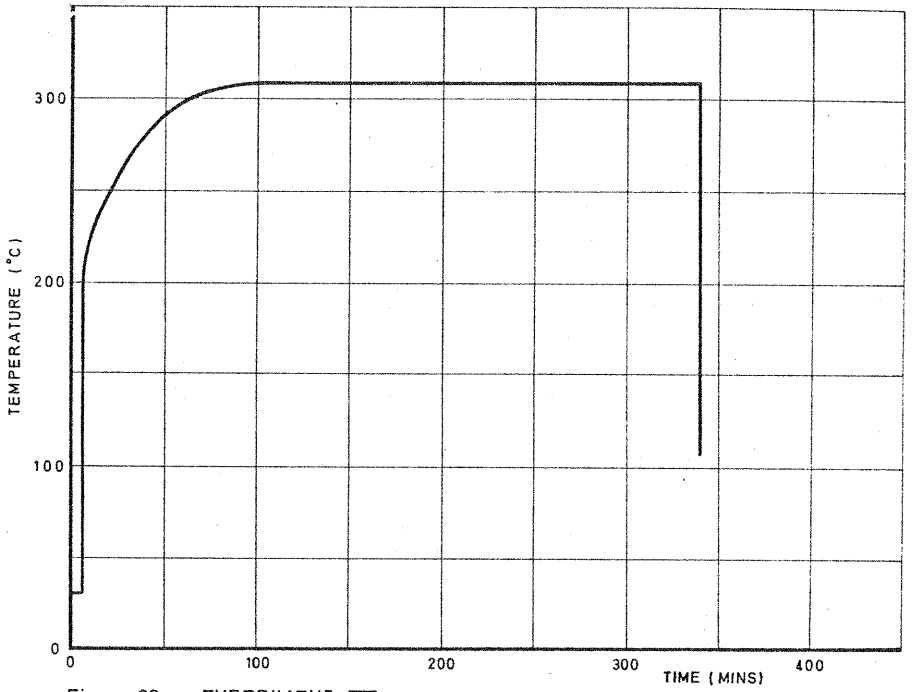

Figure 29 EXPERIMENT VII

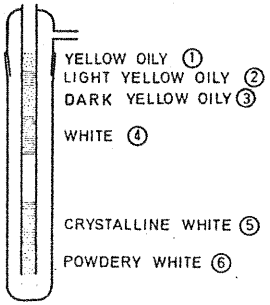

Figure 30 VACUUM LINE TRAP SHOWING CONDENSATES

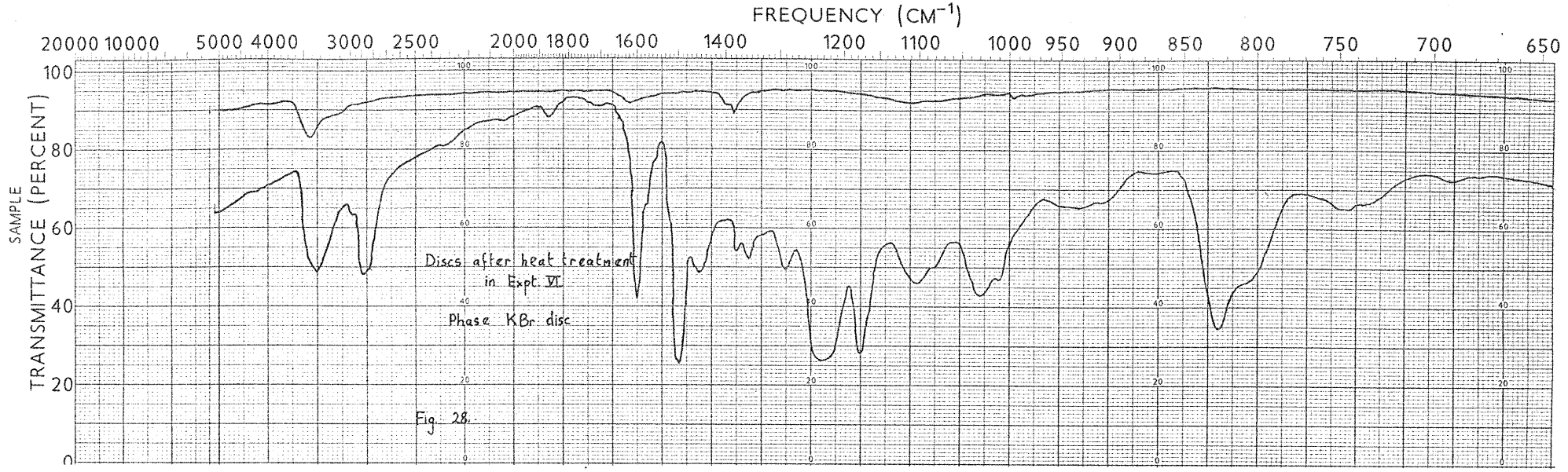

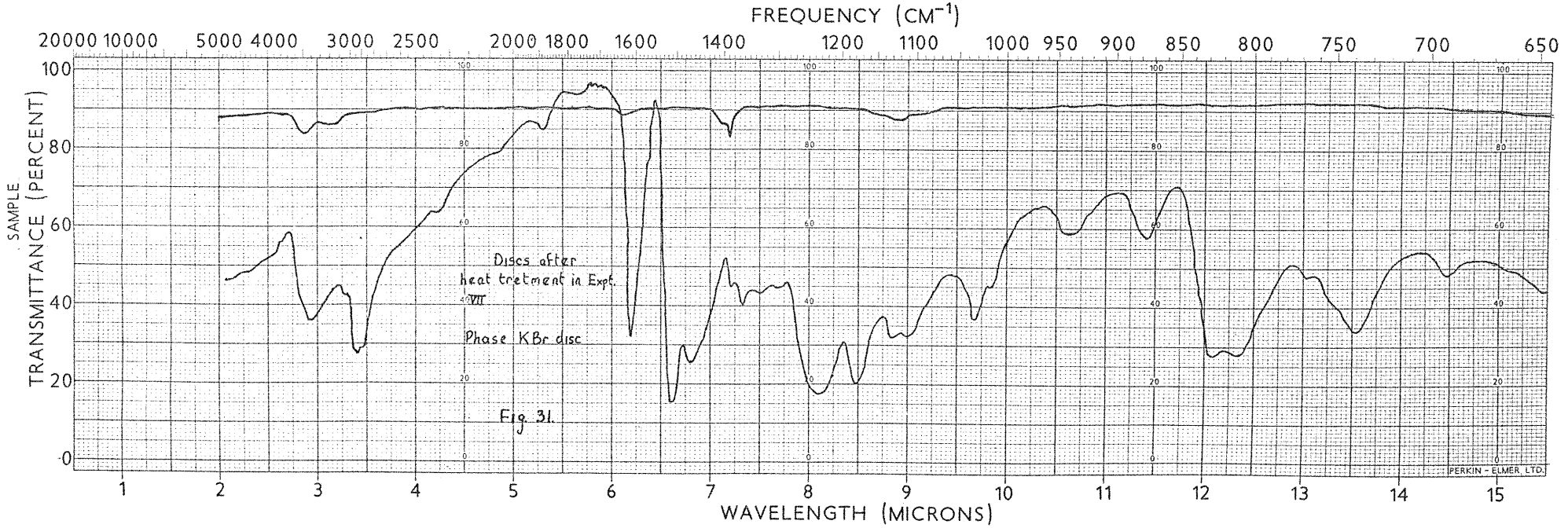

FIGURE 28 DISCS AFTER HEAT TREATMENT IN EXPERIMENT VI
PHASE KBr DISC

FIGURE 31 DISCS AFTER HEAT TREATMENT IN EXPERIMENT VII
PHASE KBr DISCS

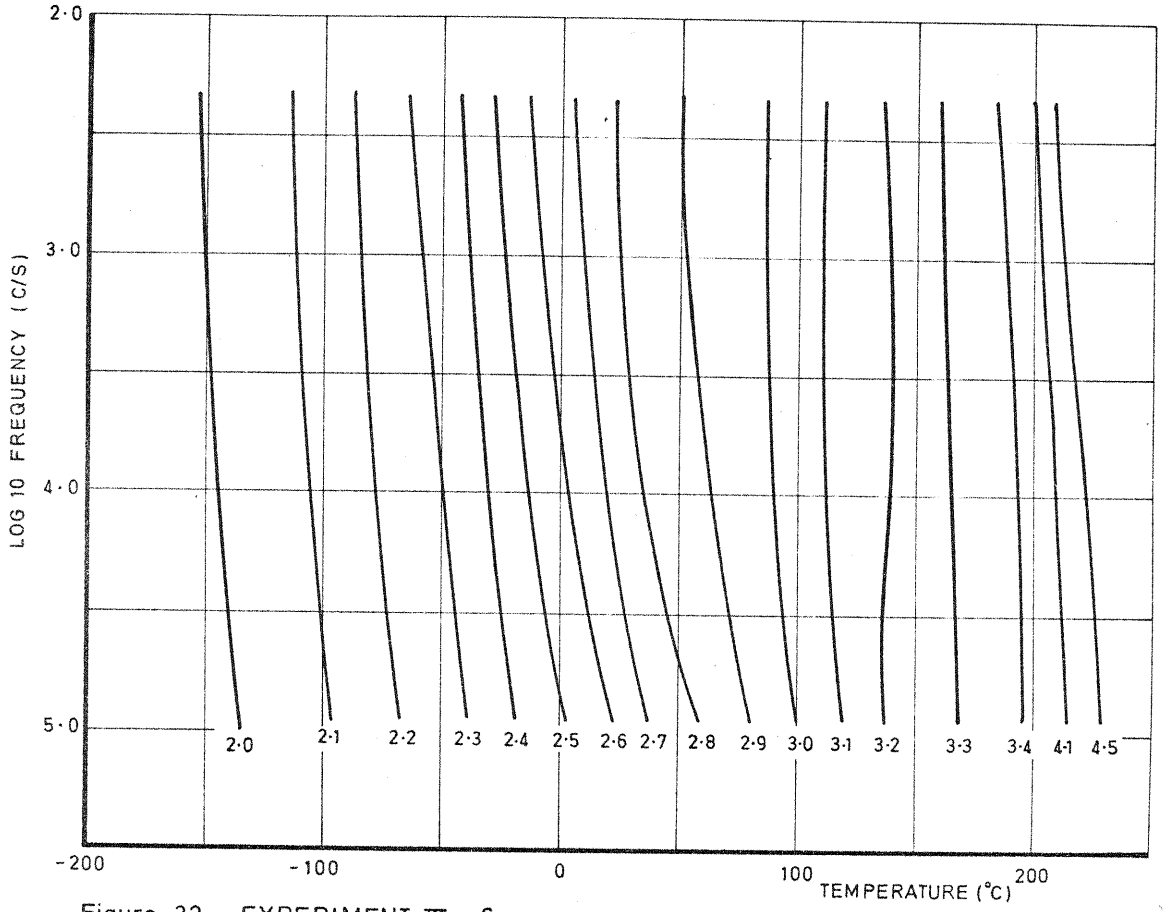

Figure 32 EXPERIMENT III ε

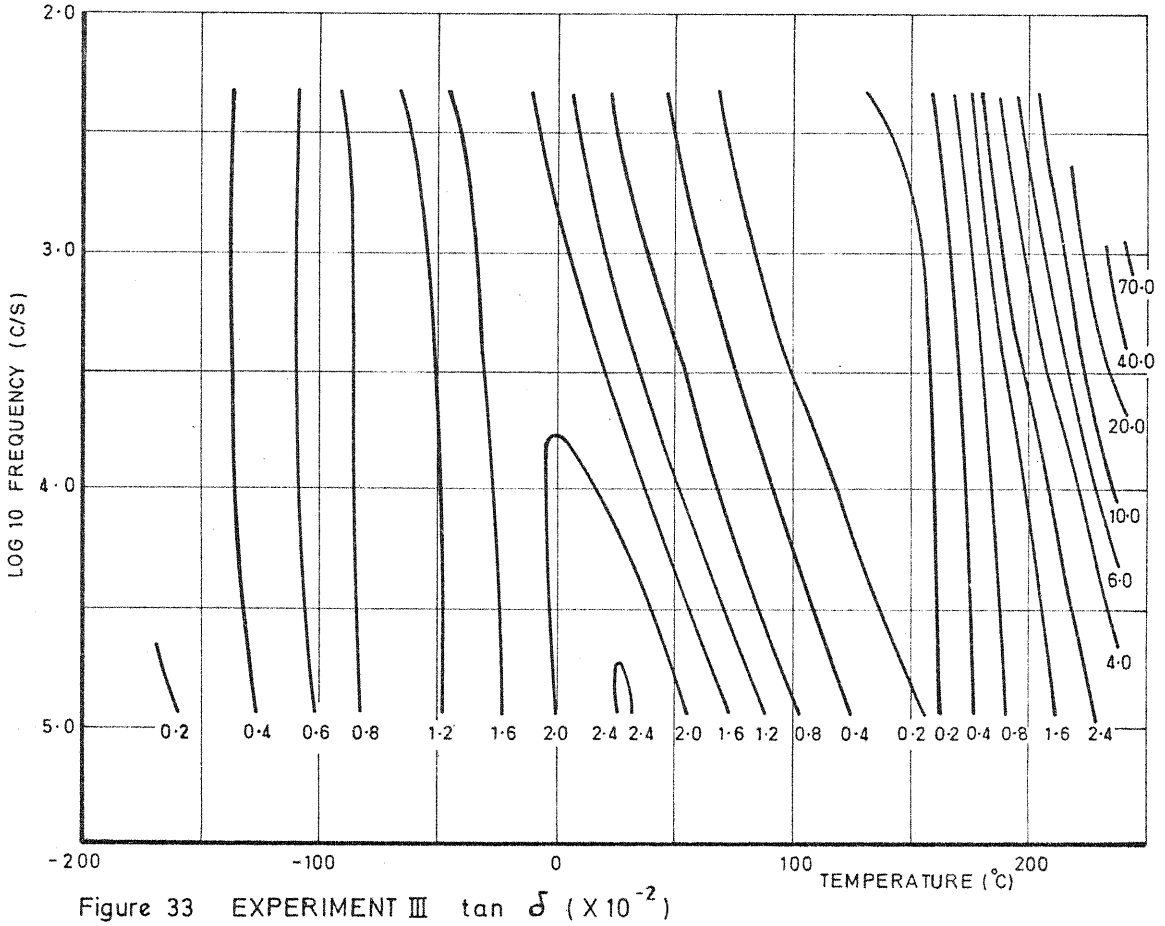

Figure 33 EXPERIMENT III $\tan \delta$ ($\times 10^{-2}$)

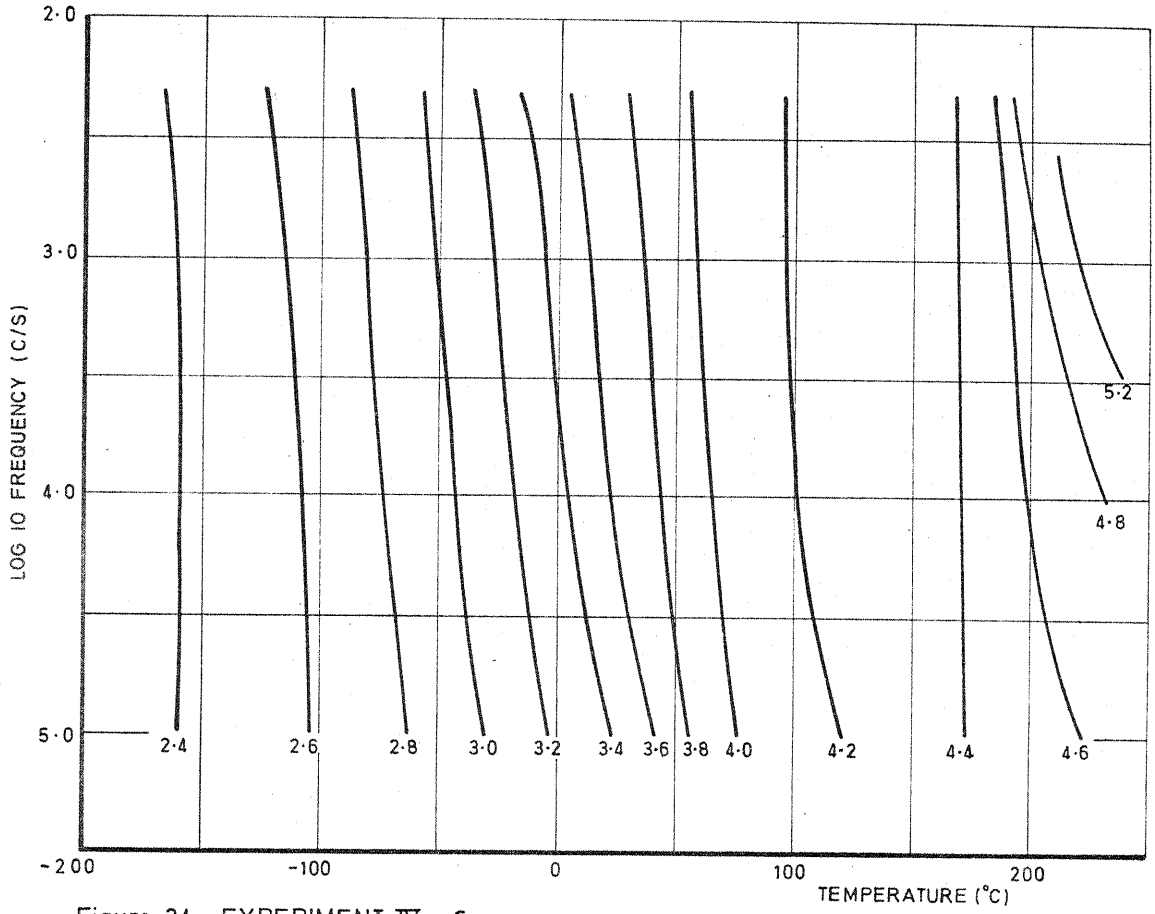

Figure 34 EXPERIMENT Ⅳ ε

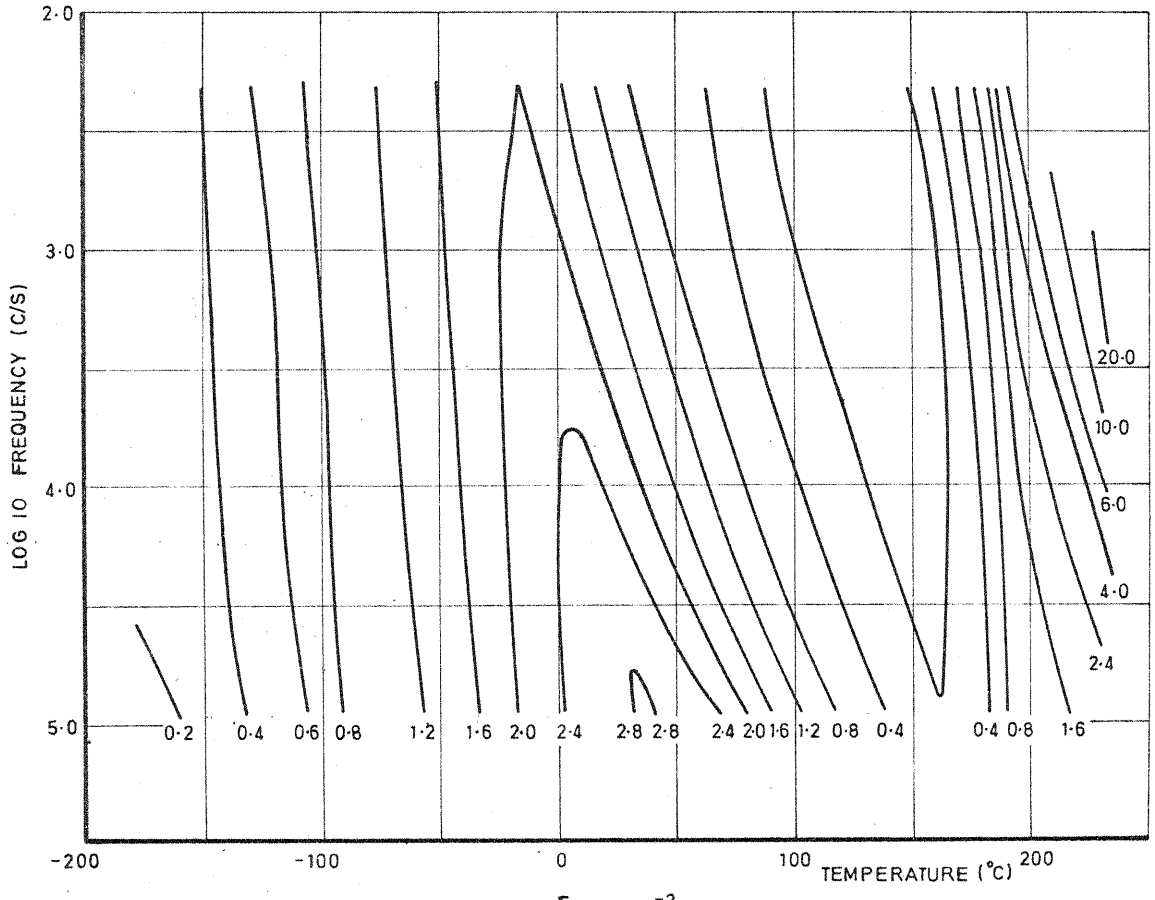

Figure 35 EXPERIMENT Ⅳ tan δ ($\times 10^{-2}$)

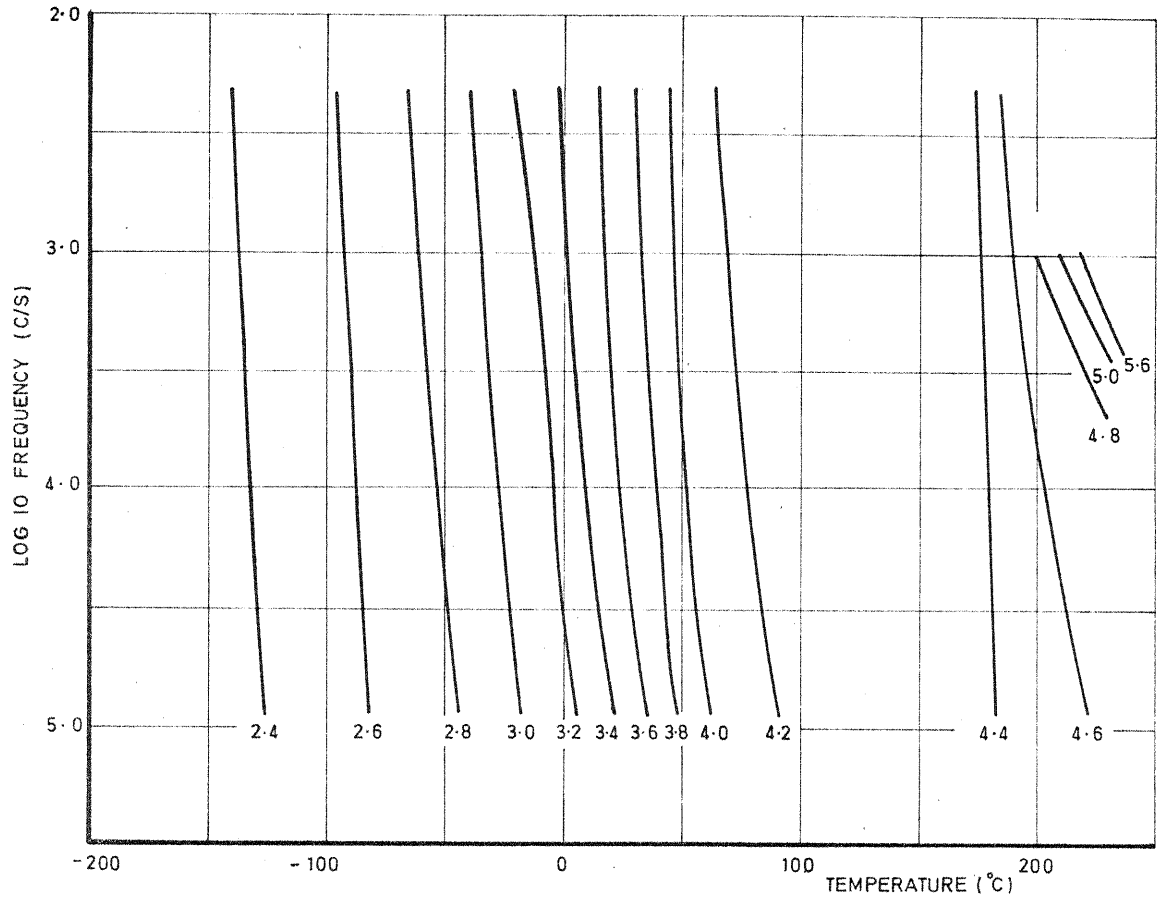

Figure 36 EXPERIMENT V ε

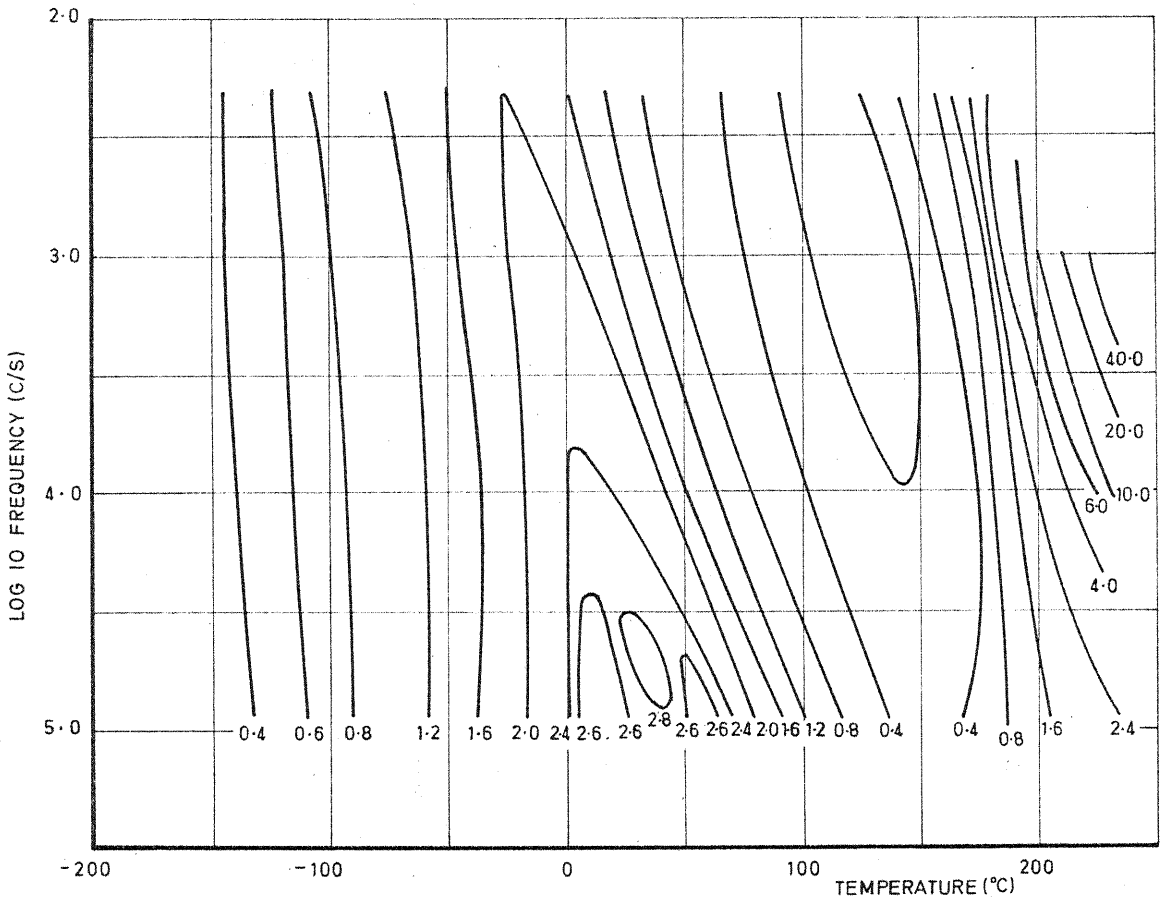

Figure 37 EXPERIMENT V tan δ ($\times 10^{-2}$)

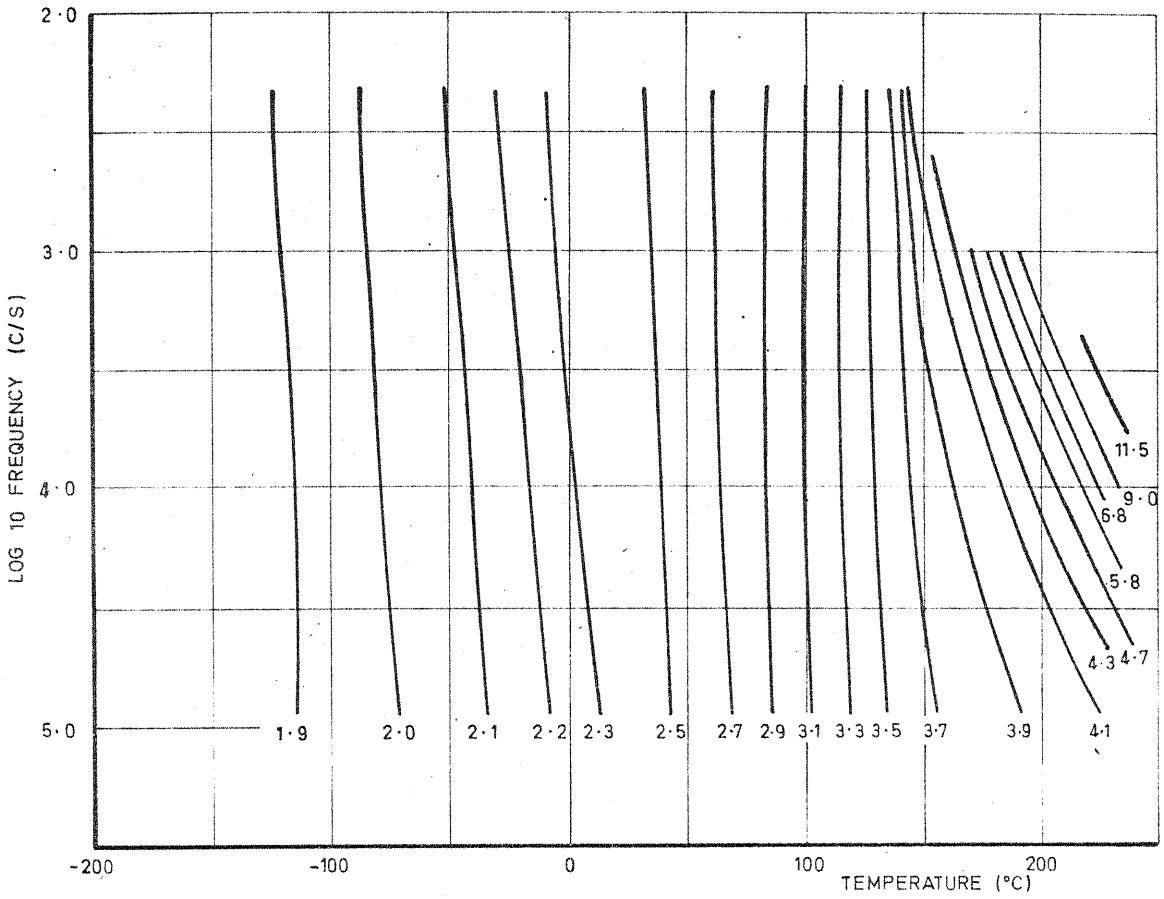

Figure. 38. EXPERIMENT Ⅵ ε.

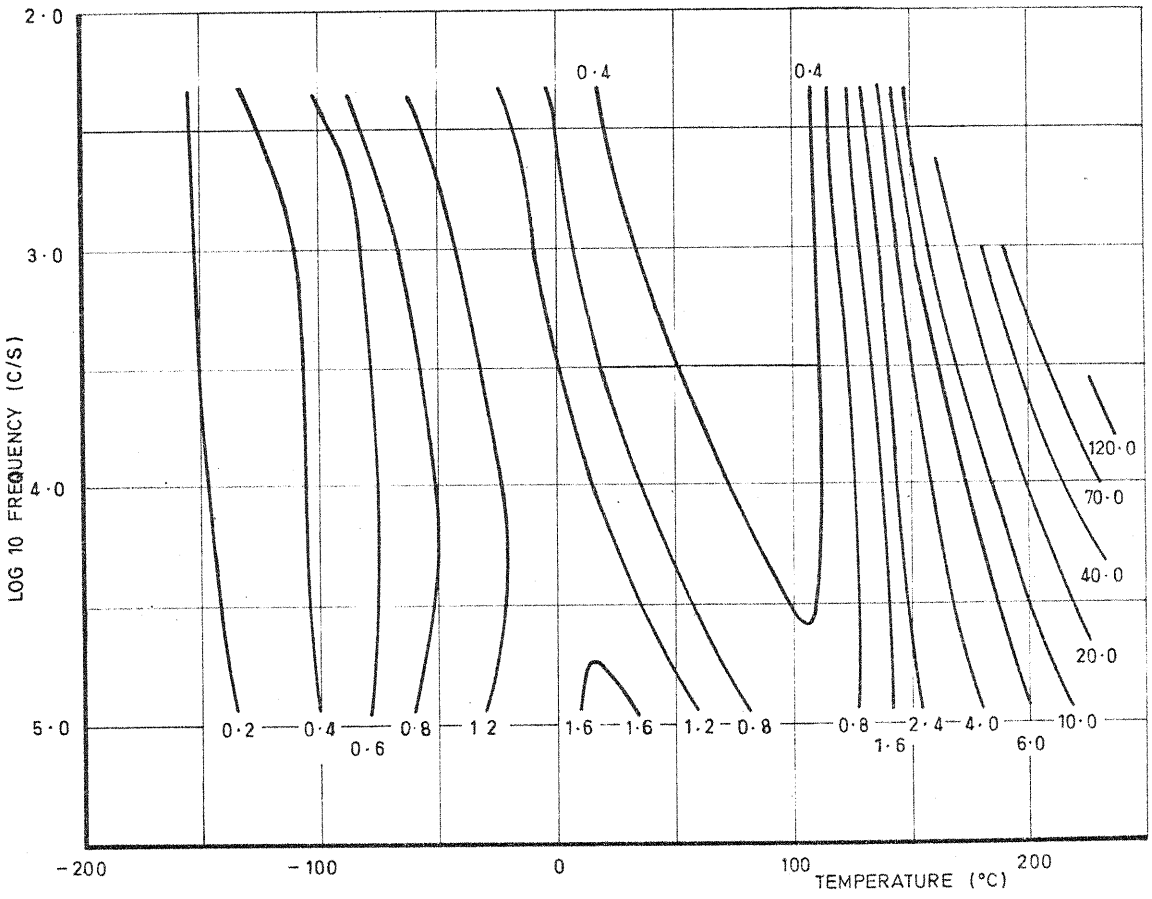

Figure. 39. EXPERIMENT Ⅵ tan δ (X 10^{-2})

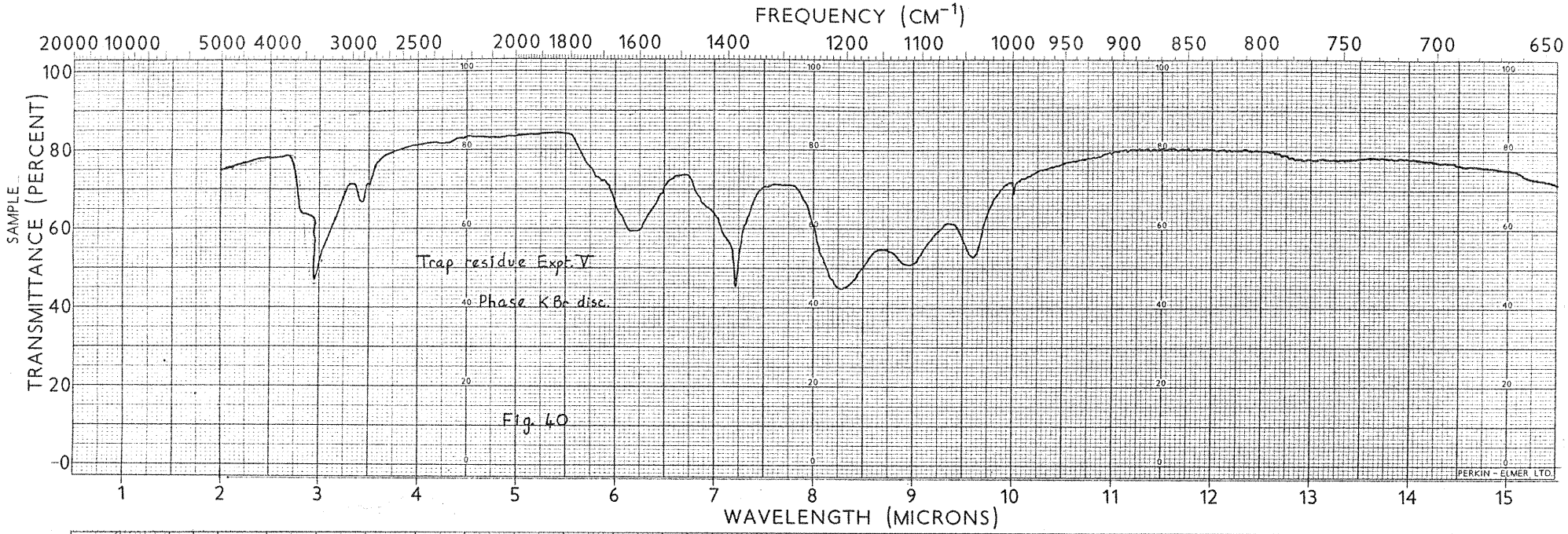

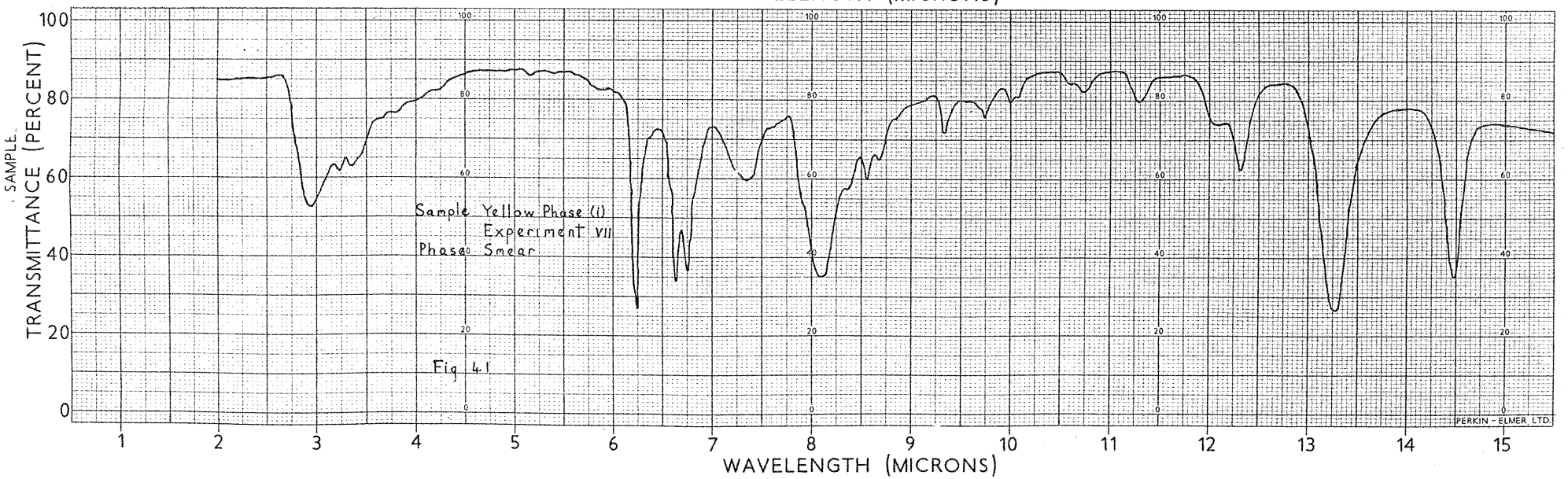

FIGURE 40 TRAP RESIDUE EXPERIMENT V PHASE K Br DISC

FIGURE 41 SAMPLE YELLOW PHASE (i) EXPERIMENT VII
PHASE SMEAR

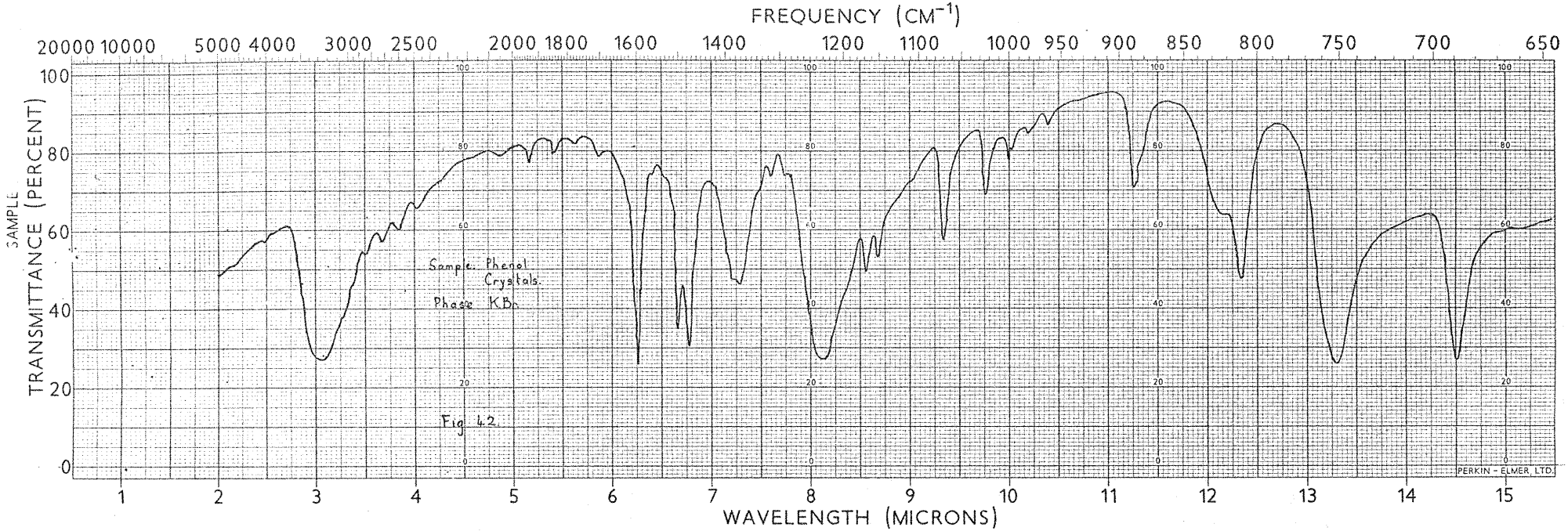

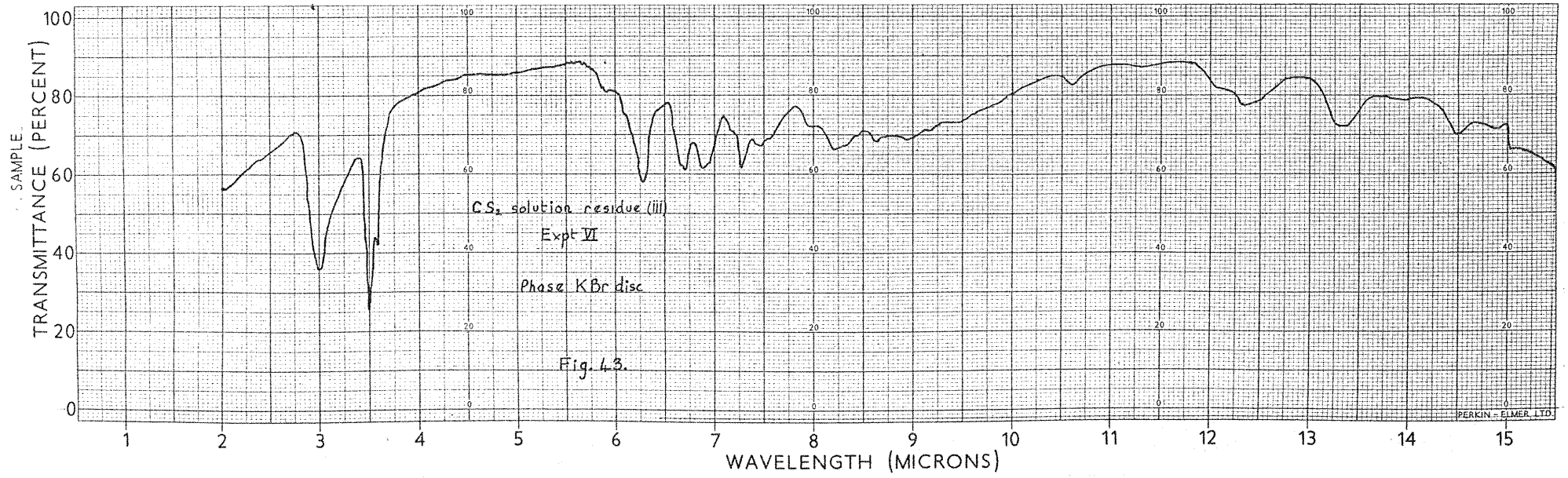

FIGURE 42 SAMPLE PHENOL CRYSTALS PHASE K Br

FIGURE 43 CS_2 SOLUTION RESIDUE (iii) EXPERIMENT VI
PHASE K Br DISC

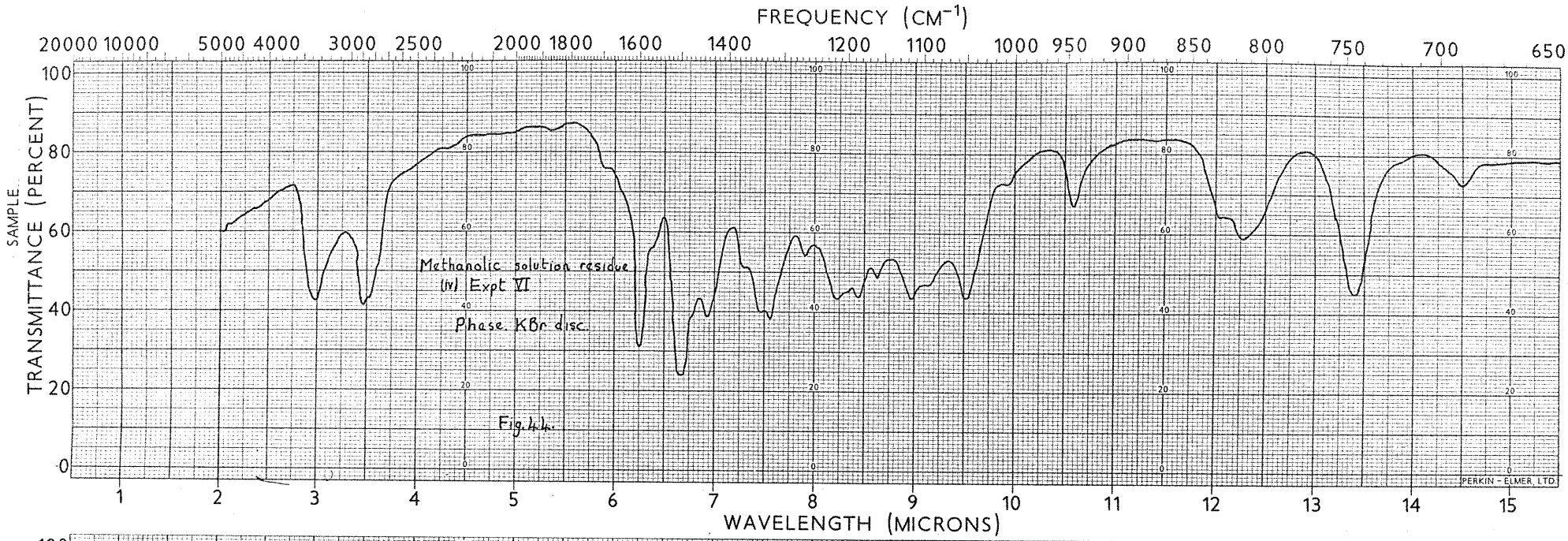

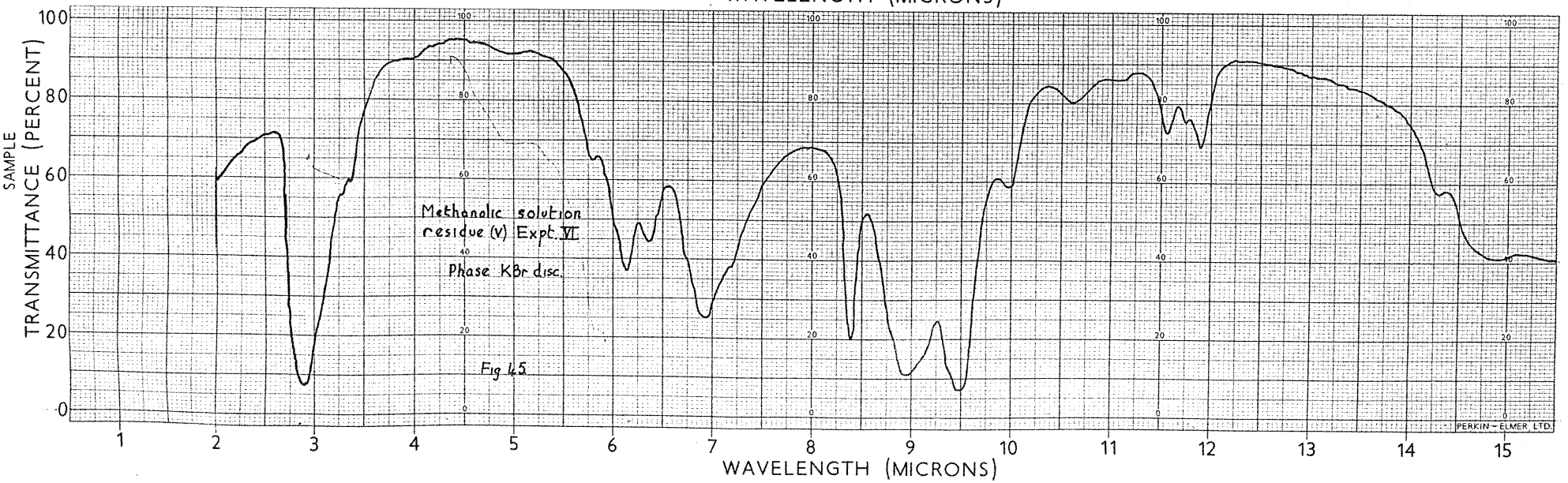

FIGURE 44 METHANOLIC SOLUTION RESIDUE (iv) EXPERIMENT VI
PHASE K Br DISC

FIGURE 45 METHANOLIC SOLUTION RESIDUE (V) EXPERIMENT VI
PHASE K Br DISC

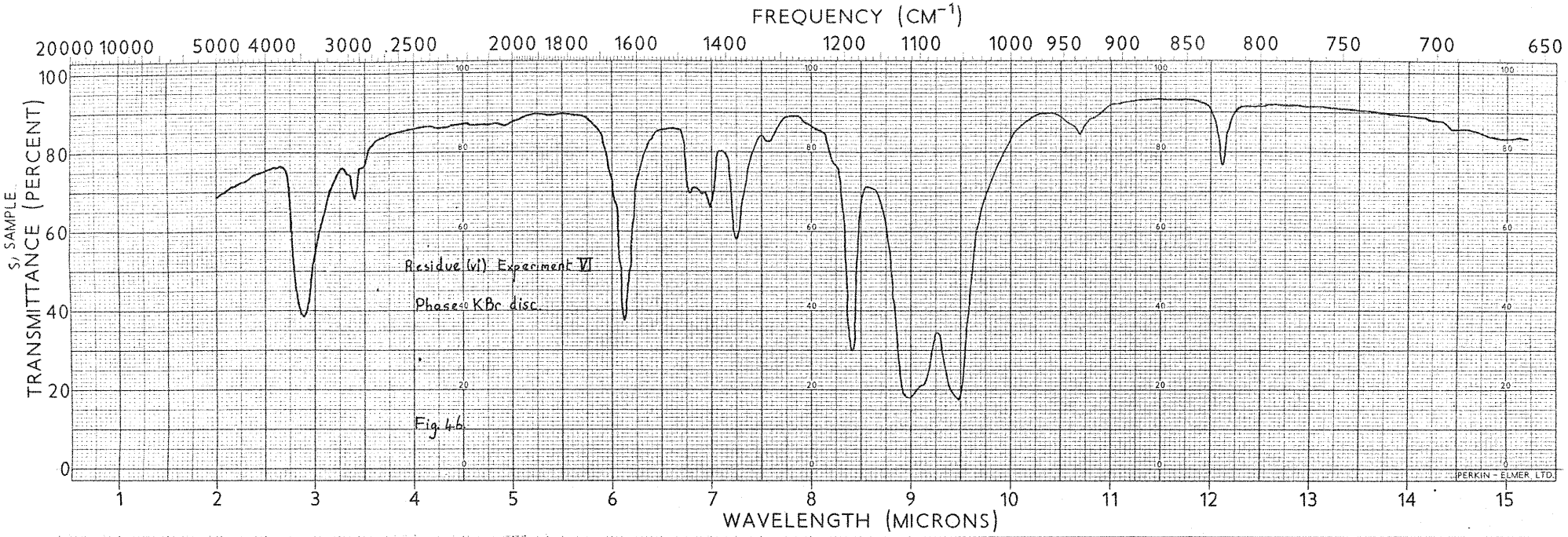

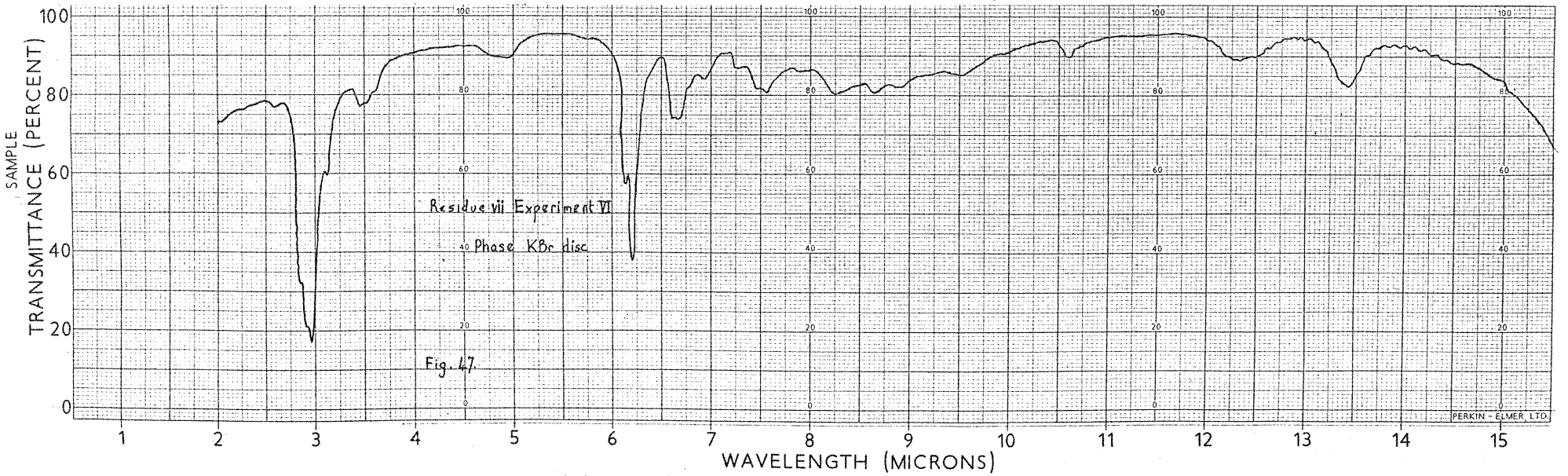

FIGURE 46 RESIDUE (vi) EXPERIMENT VI PHASE K Br DISC

FIGURE 47 RESIDUE (vii) EXPERIMENT VI PHASE K Br DISC

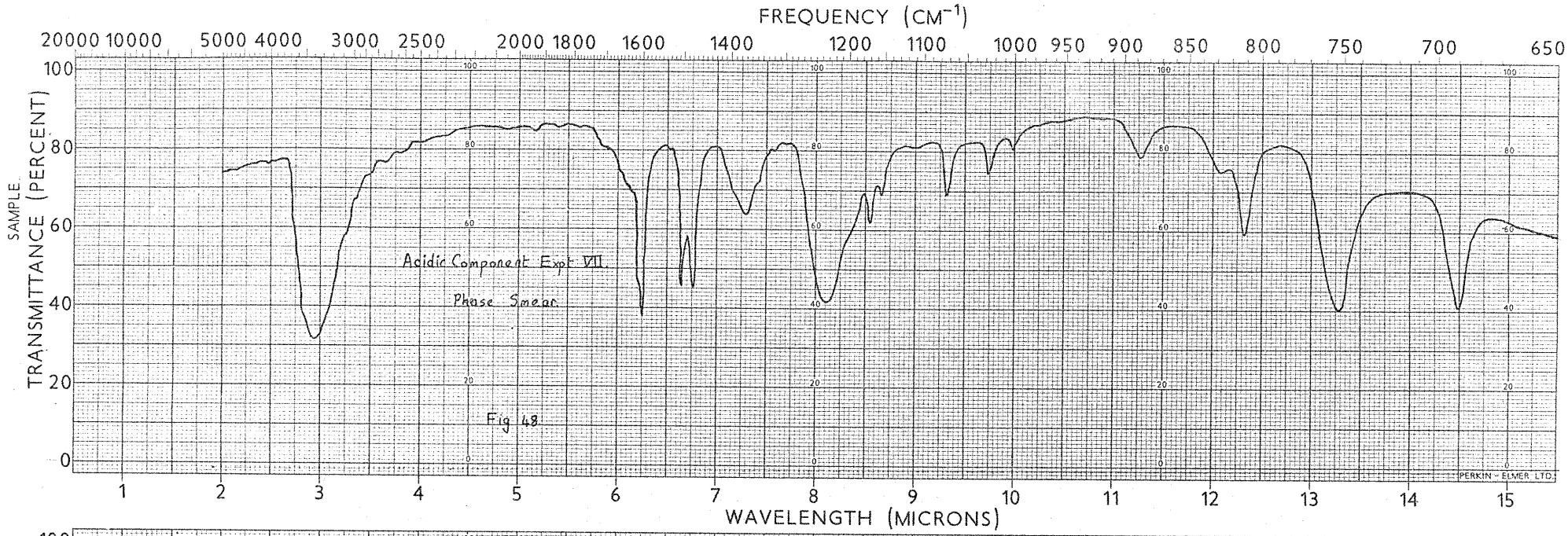

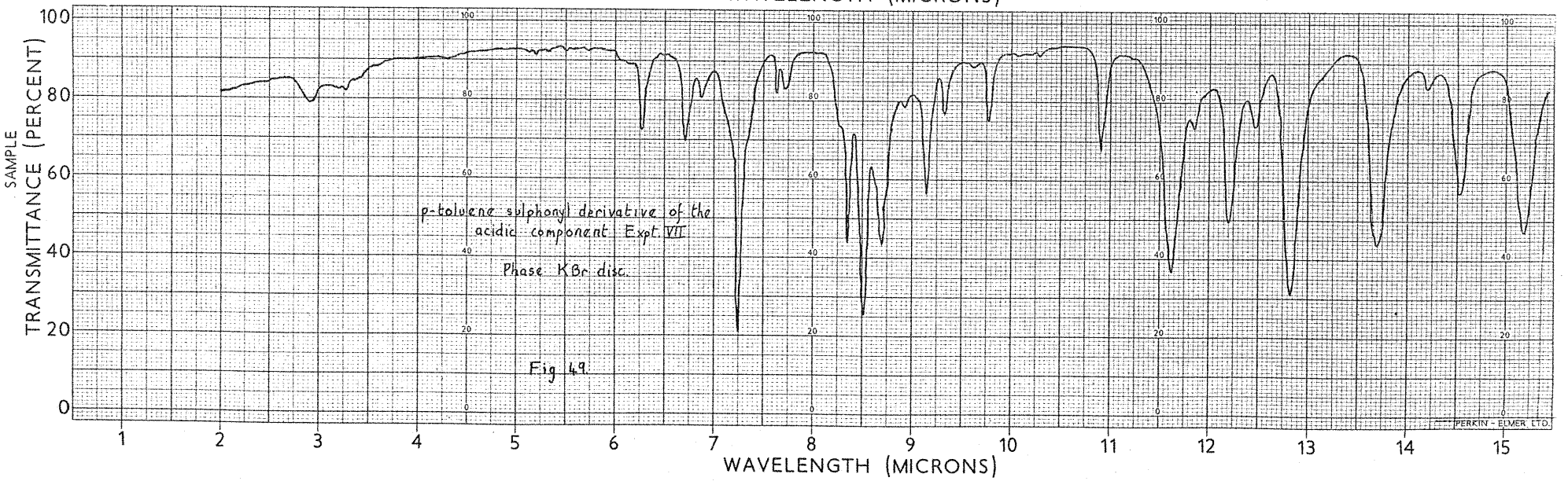

FIGURE 48 ACIDIC COMPONENT EXPERIMENT VII PHASE SMEAR

FIGURE 49 p-TOLUENE SULPHONYL DERIVATIVE OF THE ACIDIC COMPONENT EXPERIMENT VII

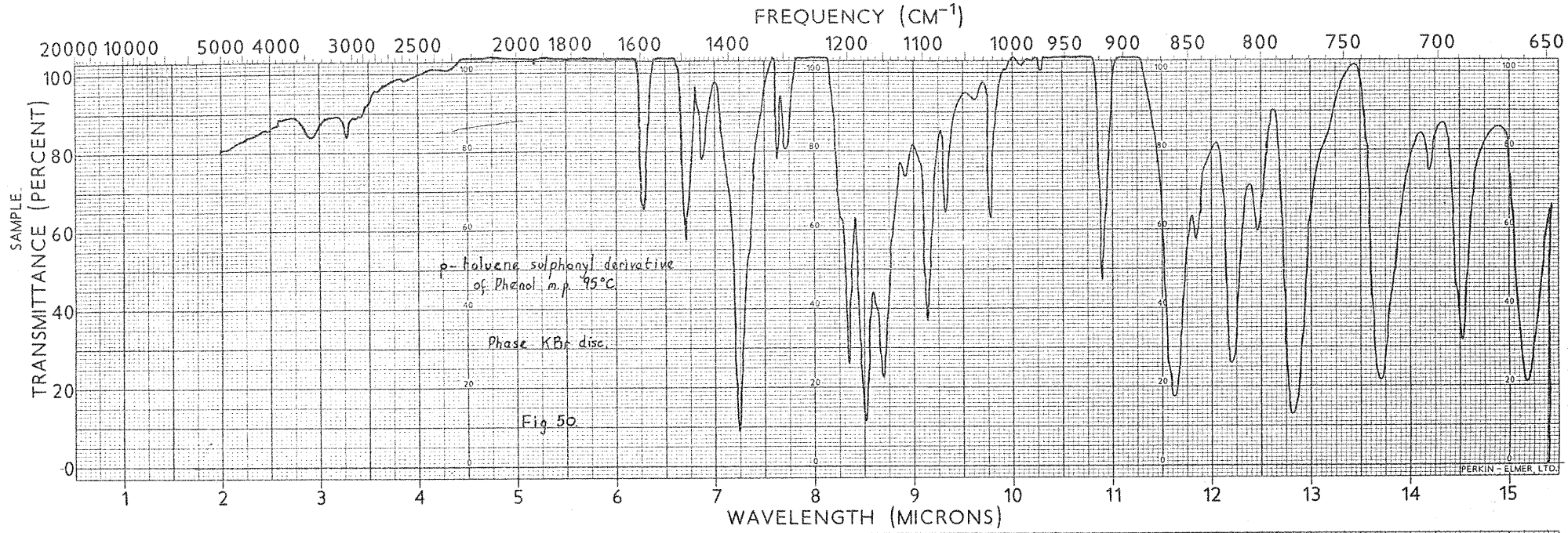

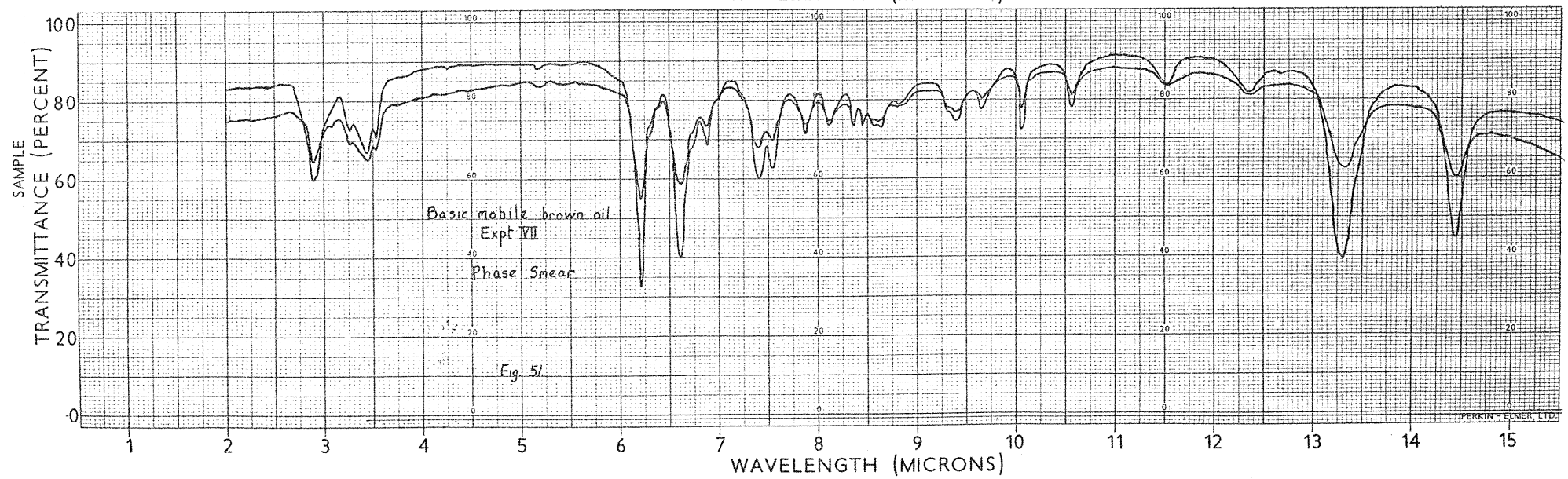

FIGURE 50 p - TOLUENE SULPHONYL DERIVATIVE OF PHENOL m.p. 95°C
PHASE K Br DISC

FIGURE 51 BASIC MOBILE BROWN OIL EXPERIMENT VII
PHASE SMEAR

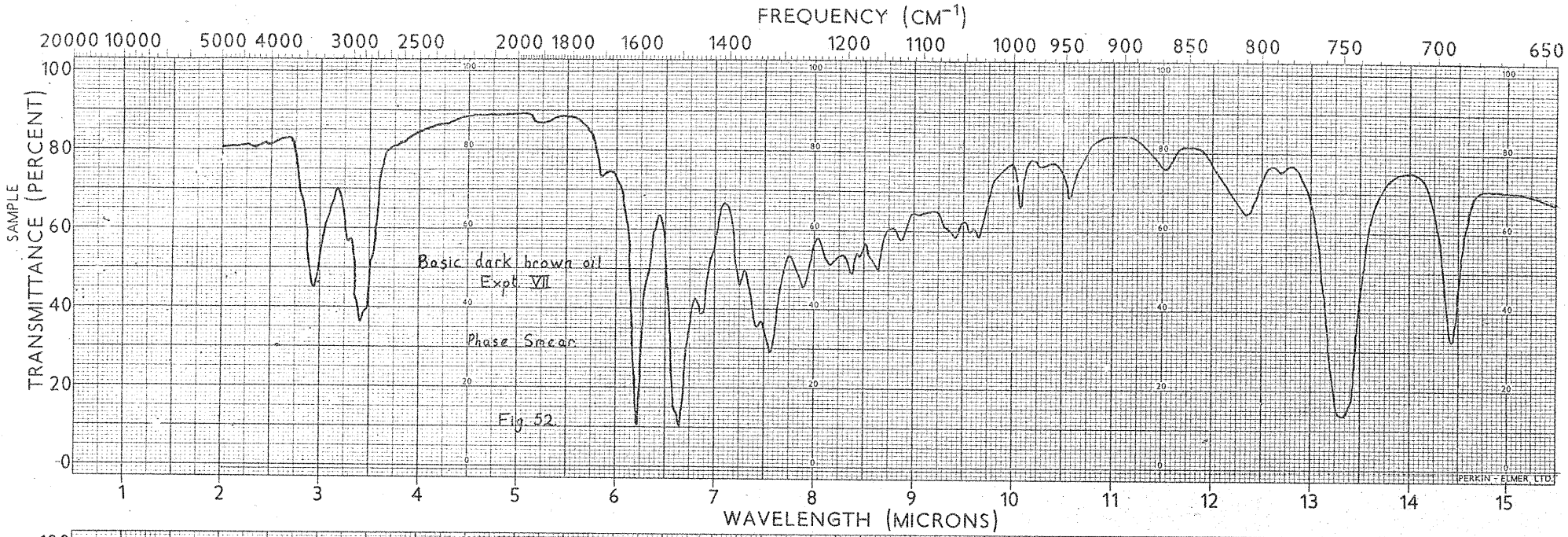

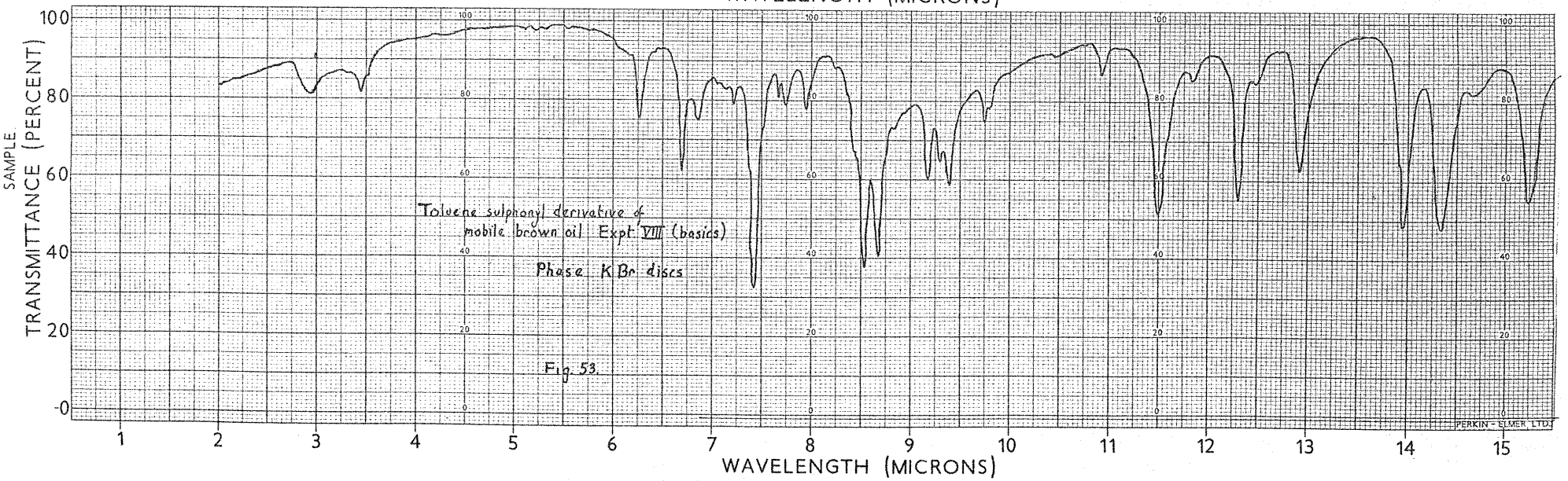

FIGURE 52 BASIC DARK BROWN OIL EXPERIMENT VII
PHASE SMEAR

FIGURE 53 TOLUENE SULPHONYL DERIVATIVE OF MOBILE BROWN OIL
EXPERIMENT VIII (BASICS) PHASE K Br DISCS

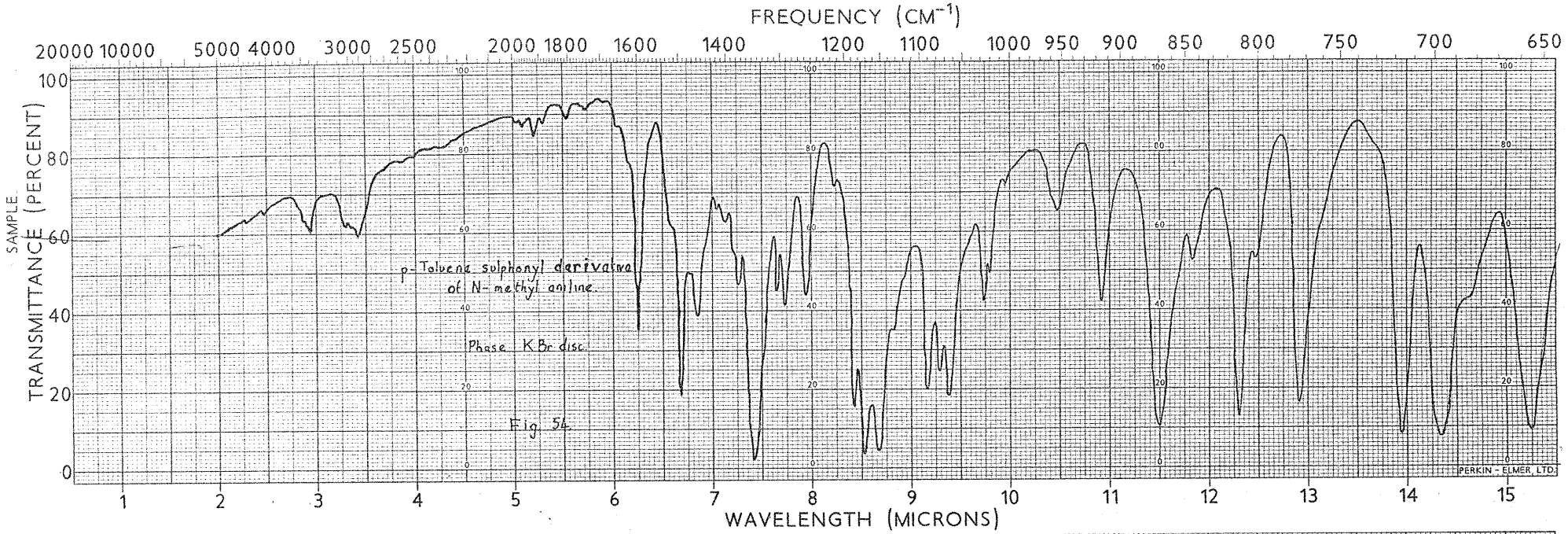

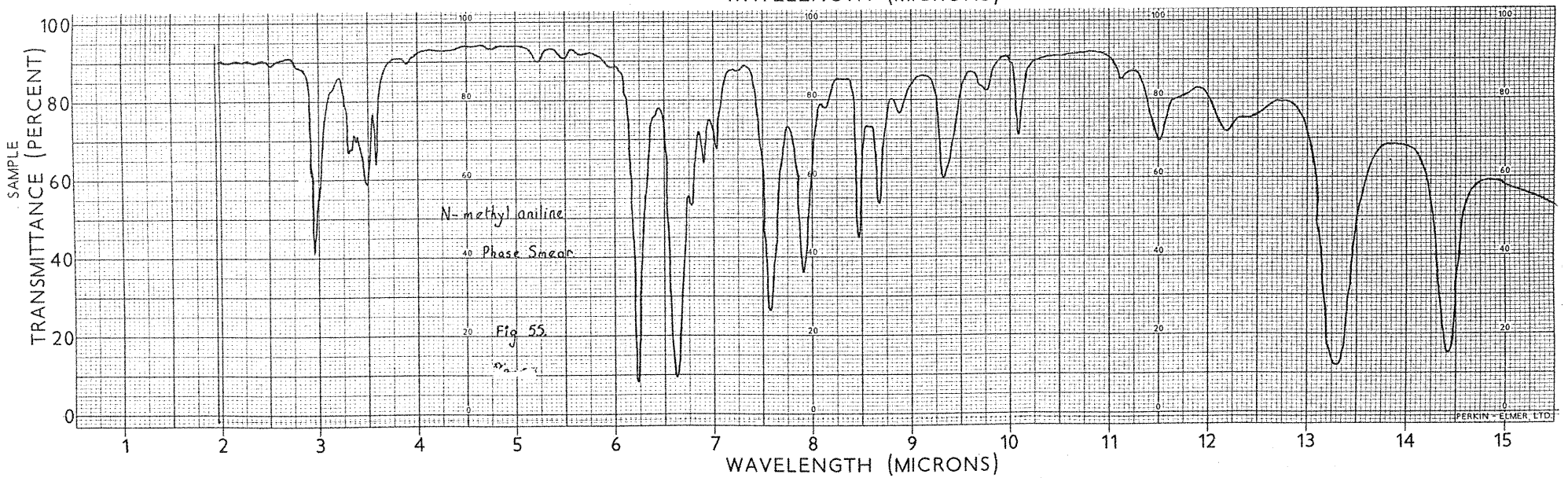

FIGURE 54 p-TOLUENE SOLPHONYL DERIVATIVE OF N-METHYL ANILINE PHASE K Br DISC

FIGURE 55 N-METHYL ANILINE PHASE SMEAR

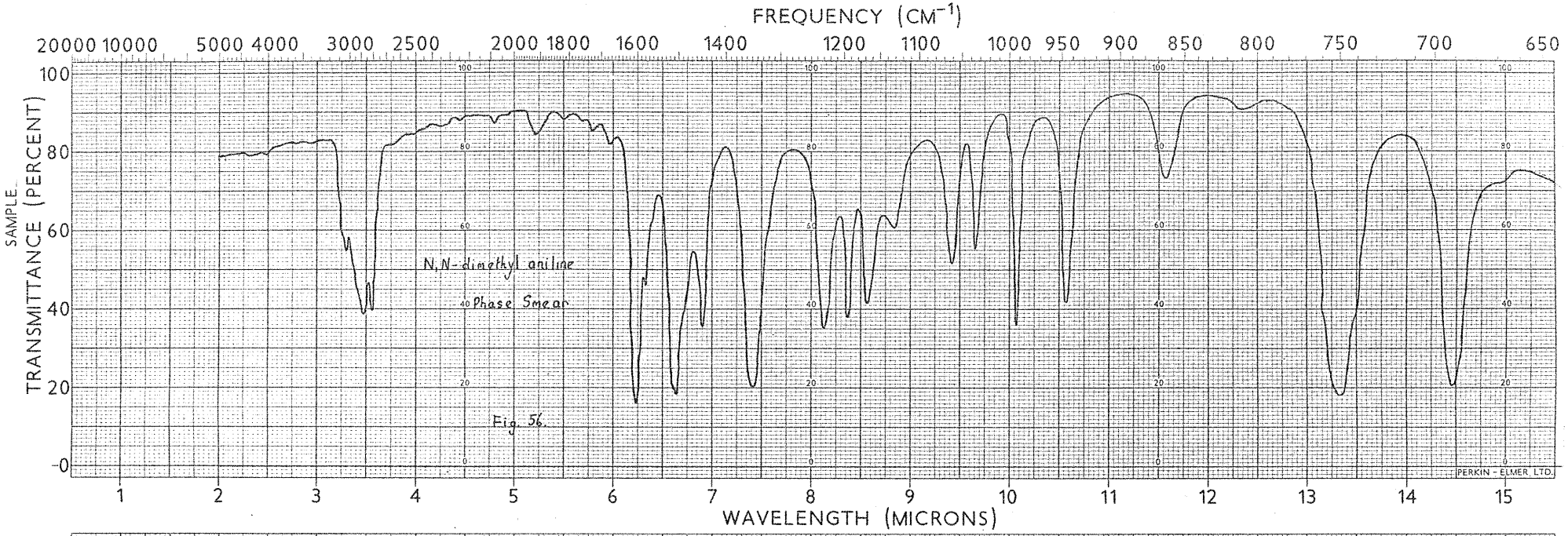

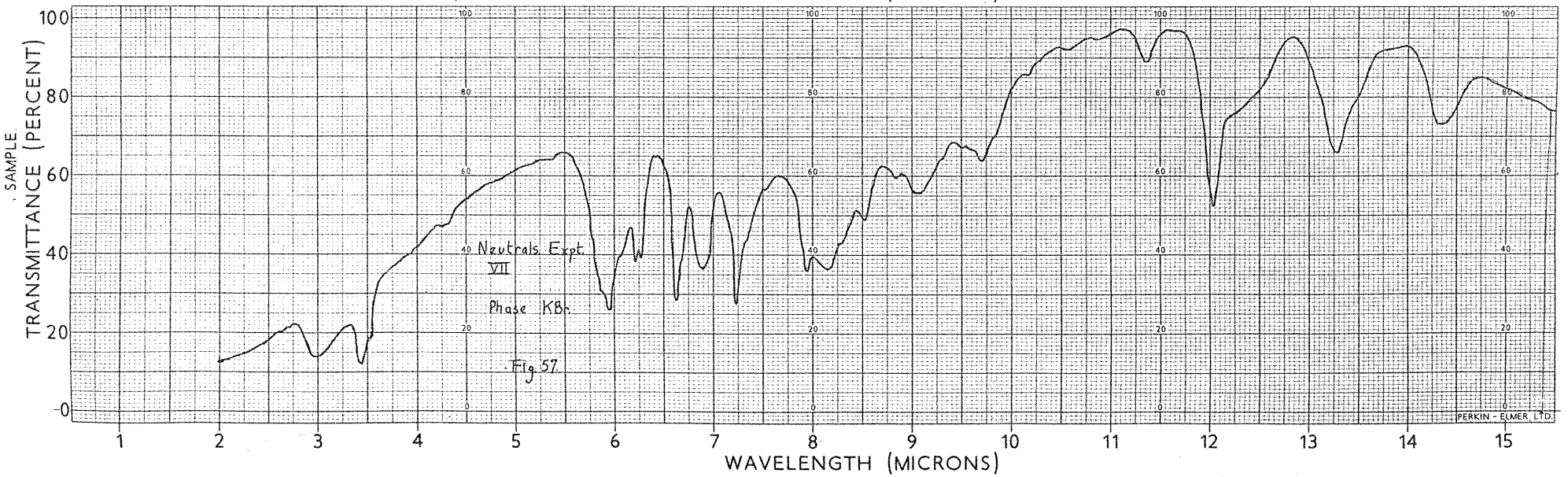

FIGURE 56 N,N - DIMETHYL ANILINE PHASE SMEAR

FIGURE 57 NEUTRALS EXPERIMENT VII PHASE K Br

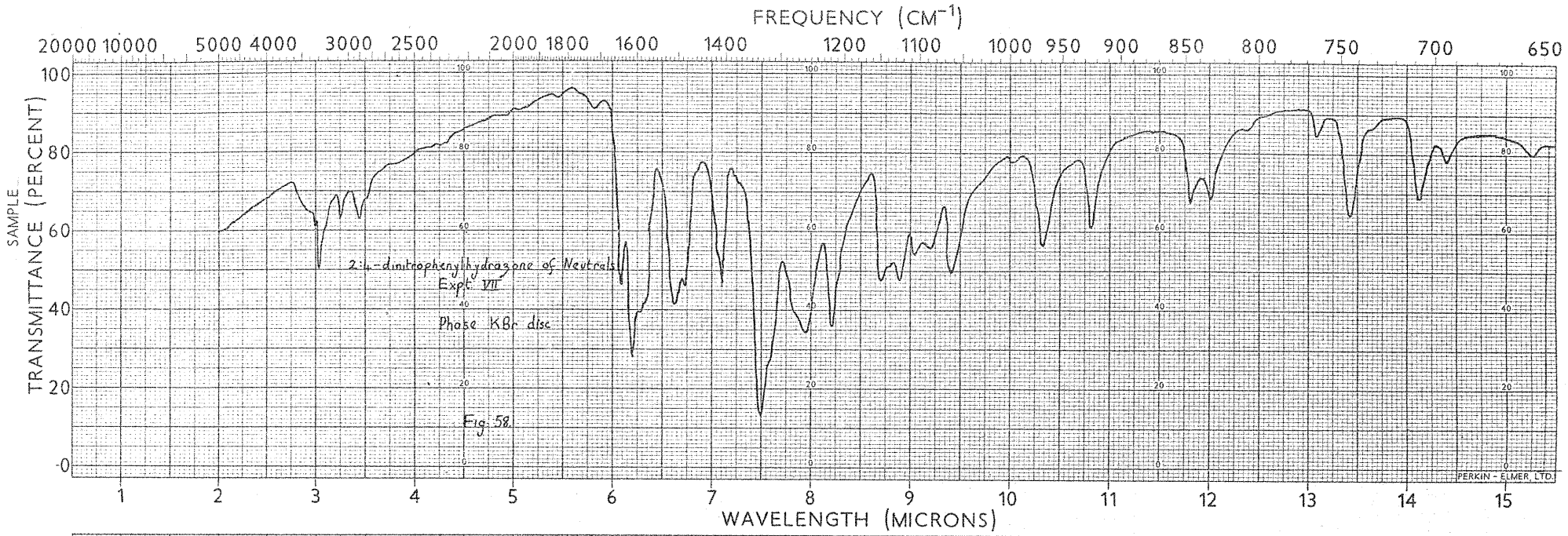

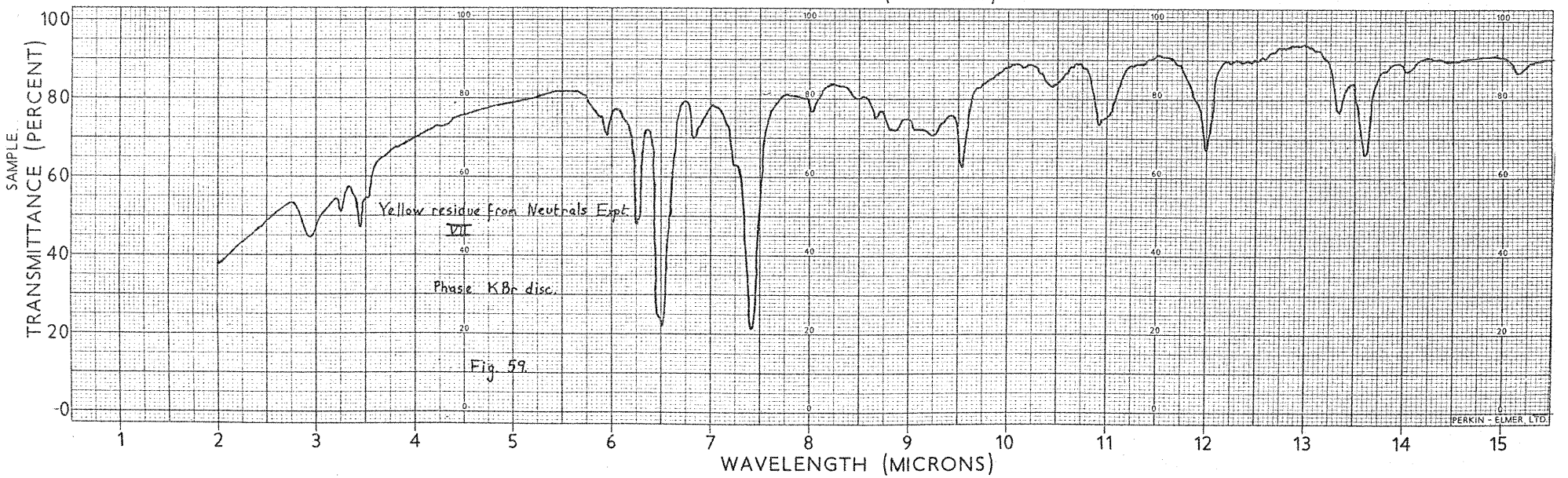

FIGURE 58 2:4- DINITROPHENYLHYDRAZONE OF NEUTRALS
EXPERIMENT VII PHASE K Br DISC

FIGURE 59 YELLOW RESIDUE FROM NEUTRALS EXPERIMENT VII
PHASE K Br DISC

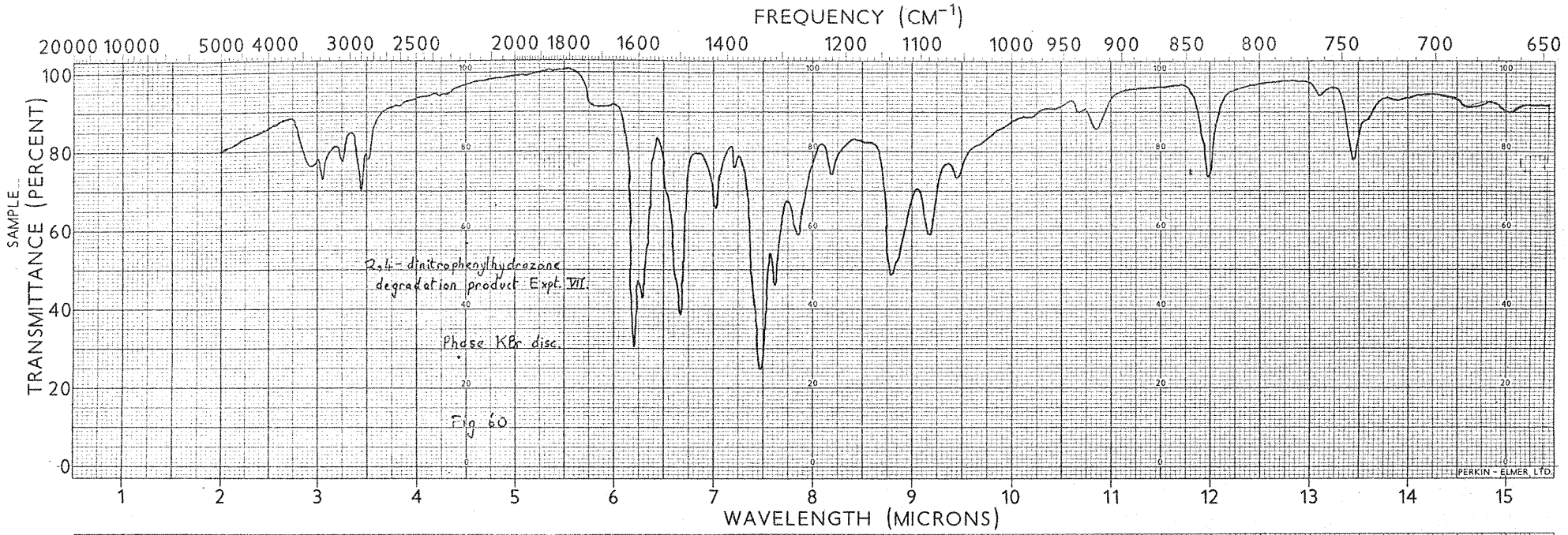

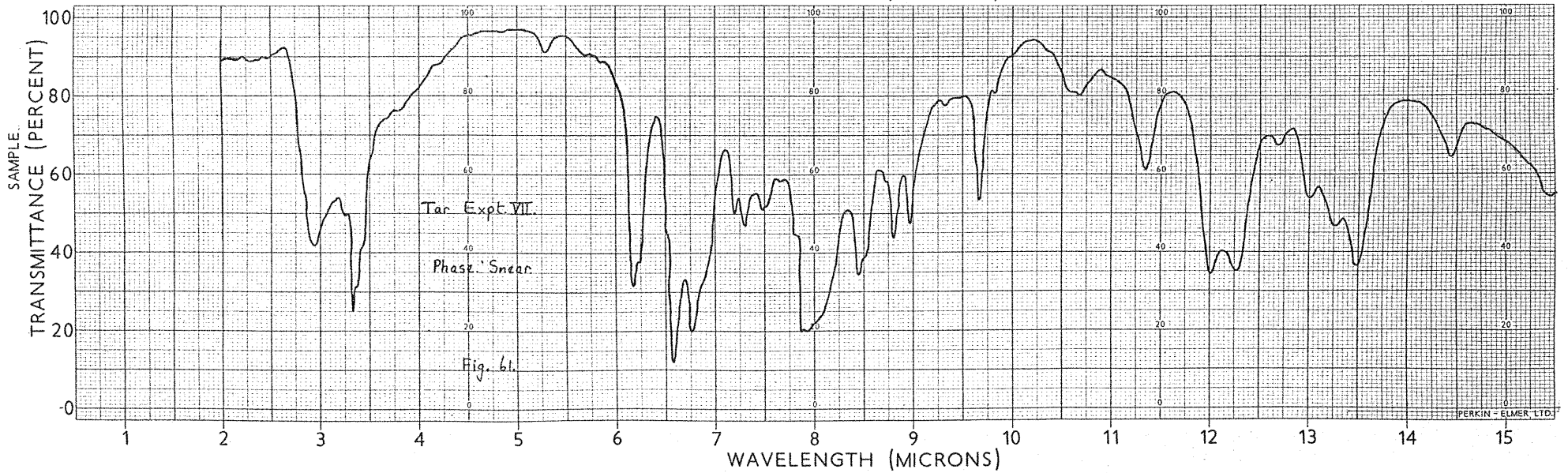

FIGURE 60 2,4-DINITROPHENYLHYDRAZONE DEGRADATION EXPERIMENT VII PHASE K Br DISC

FIGURE 61 TAR EXPERIMENT VII PHASE SMEAR

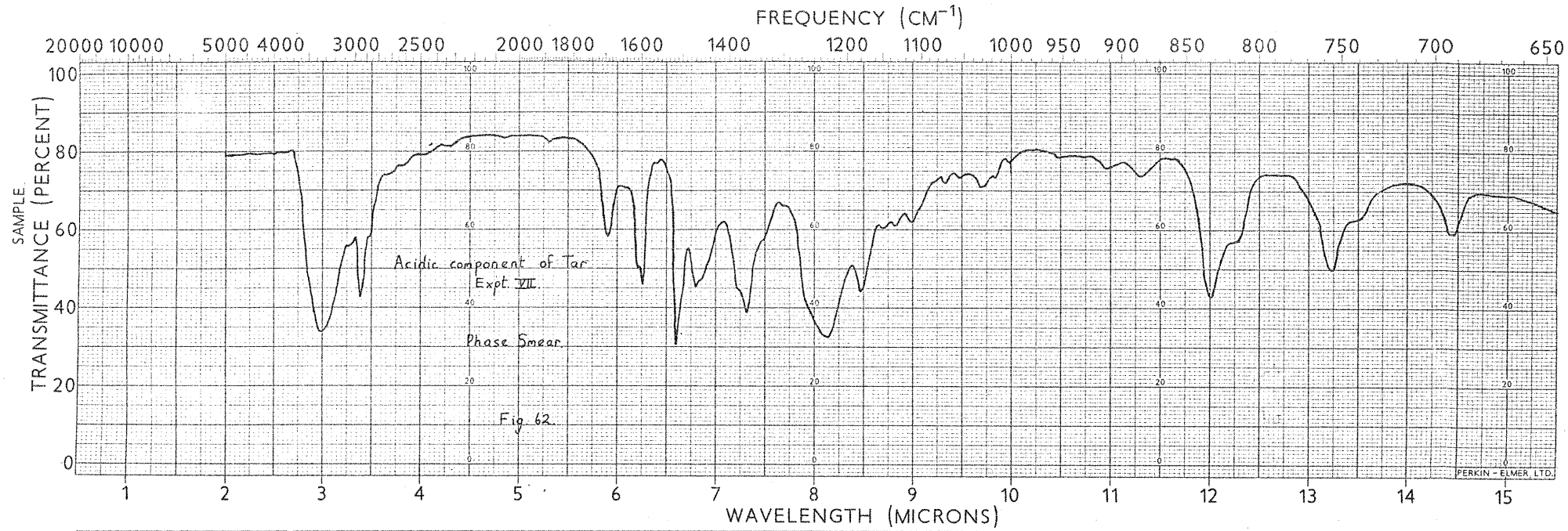

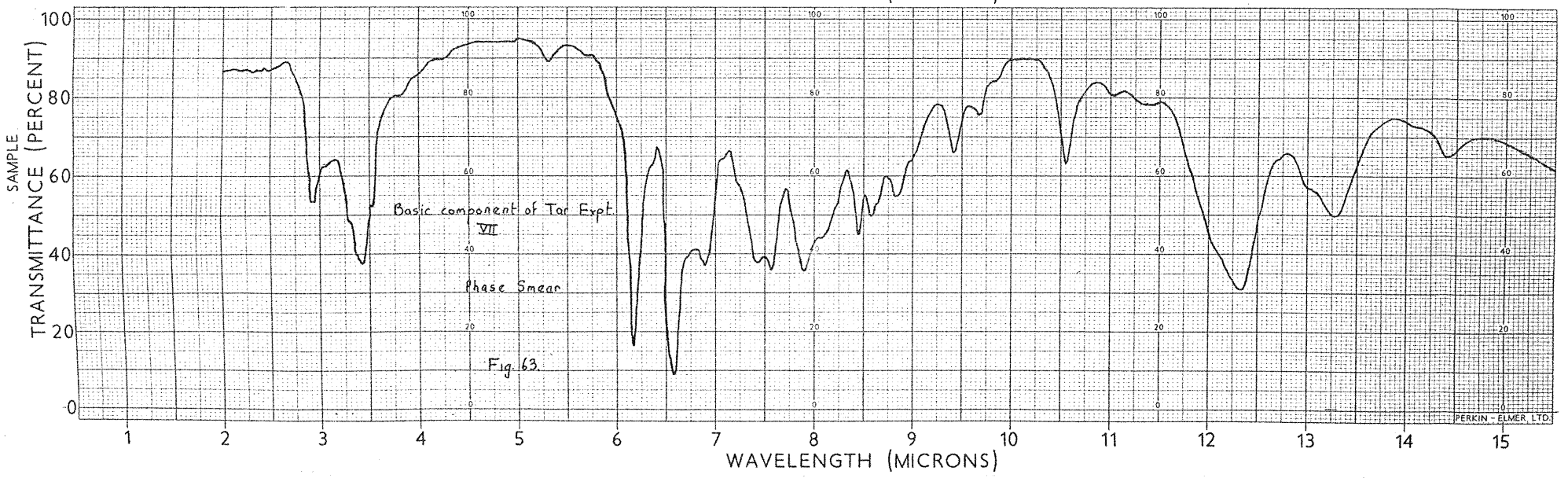

FIGURE 62 ACIDIC COMPONENT OF TAR EXPERIMENT VII
PHASE SMEAR

FIGURE 63 BASIC COMPONENT OF TAR EXPERIMENT VII
PHASE SMEAR

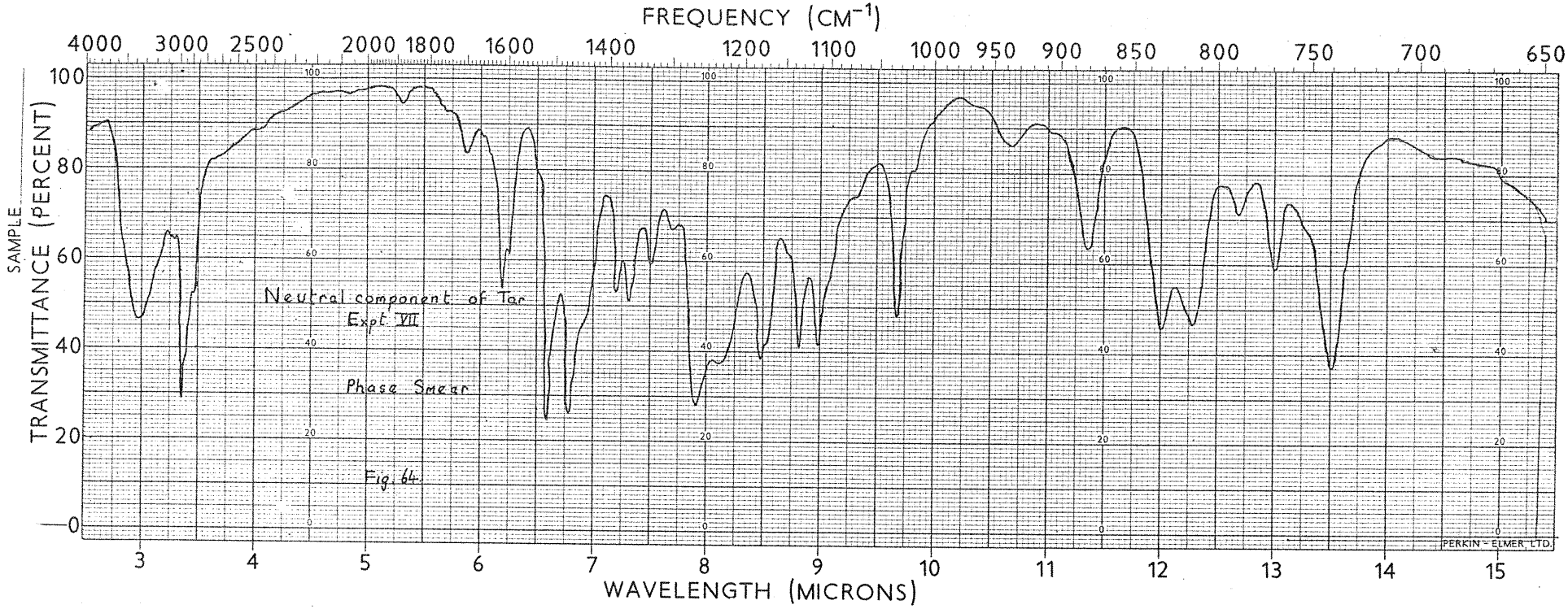

FIGURE 64 NEUTRAL COMPONENT OF TAR EXPERIMENT VII
PHASE SMEAR

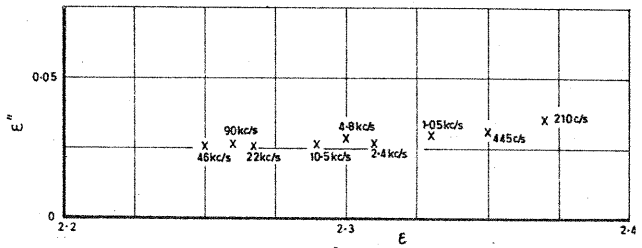

Figure 65 TEMPERATURE −50°C

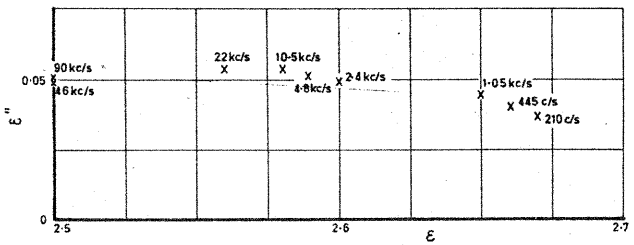

Figure 66 TEMPERATURE 0°C

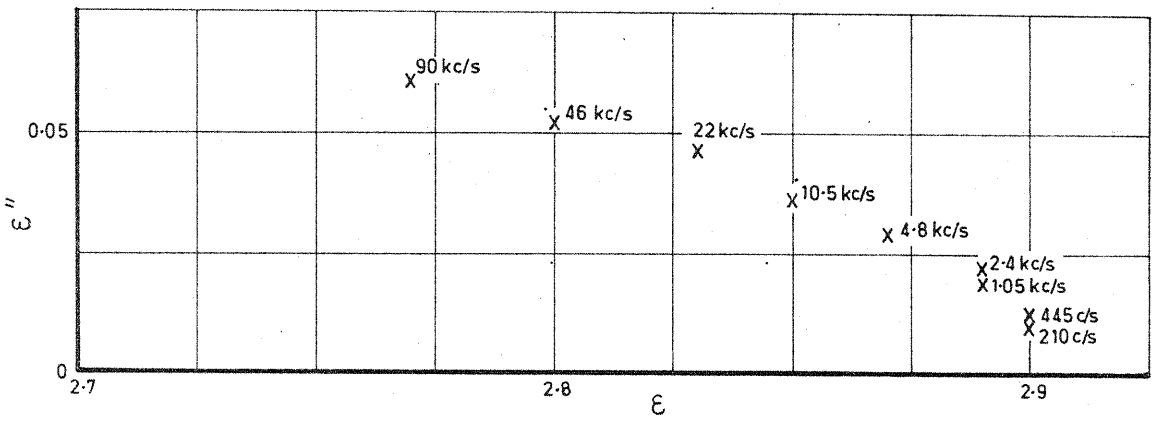

Figure 67 TEMPERATURE 50°C

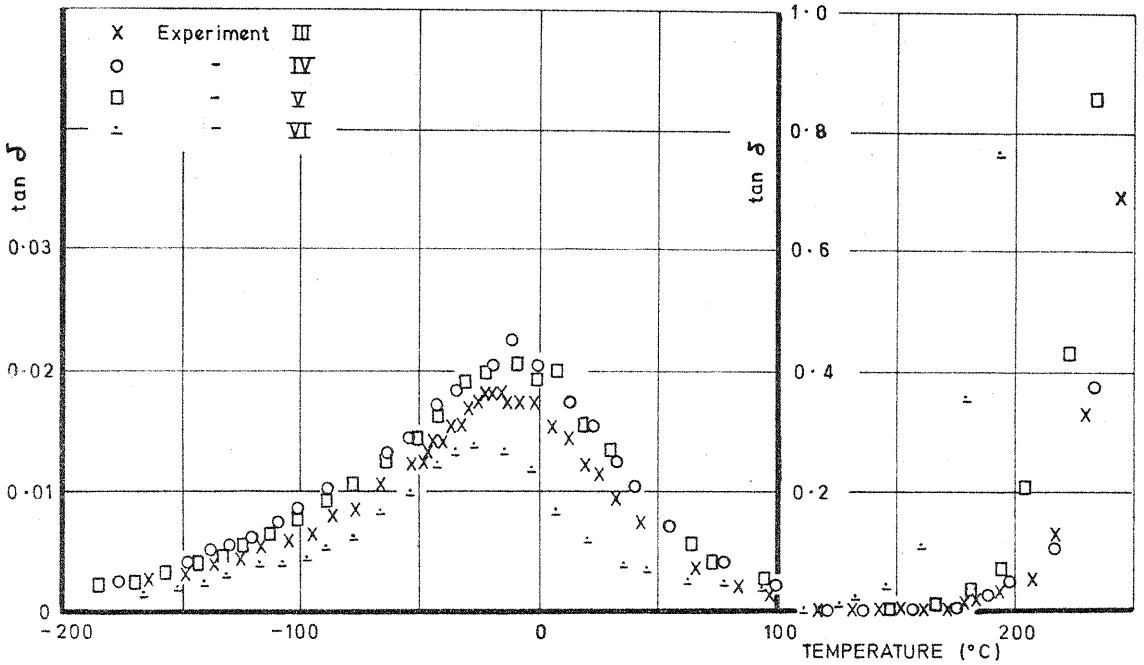

Figure. 68. EXPERIMENT III, IV, V and VI

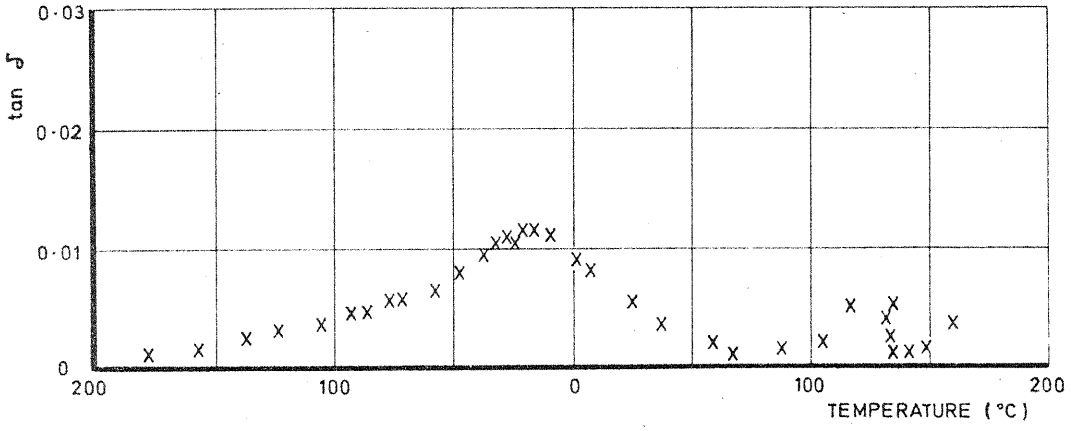

Figure. 69. EXPERIMENT 1.